

**DEVELOPMENT OF A THEORETICAL PACKING MODEL  
INCORPORATING THE EFFECT OF VIBRATION, SHAPE AND  
SURFACE TEXTURE**

Hetti Arachchige Chamod Kosala Hettiarachchi

(148048E)

Doctor of Philosophy

Department of Civil Engineering

University of Moratuwa

Sri Lanka

February 2018

**DEVELOPMENT OF A THEORETICAL PACKING MODEL  
INCORPORATING THE EFFECT OF VIBRATION, SHAPE AND  
SURFACE TEXTURE**

Hetti Arachchige Chamod Kosala Hettiarachchi

(148048E)

Thesis submitted in partial fulfilment of the requirements for the  
degree of Doctor of Philosophy in Civil Engineering

Department of Civil Engineering

University of Moratuwa  
Sri Lanka

February 2018

## **DECLARATION**

“I declare that this is my own work and this thesis does not incorporate without acknowledgement any material previously submitted for a Degree or Diploma in any other University or institute of higher learning and to the best of my knowledge and belief it does not contain any material previously published or written by another person except where the acknowledgement is made in the text.

Also, I hereby grant to University of Moratuwa the non-exclusive right to reproduce and distribute my thesis, in whole or in part in print, electronic or other medium. I retain the right to use this content in whole or part in future works (such as articles or books).”

Signature:

Date:

The above candidate has carried out research for the Doctoral thesis under my supervision.

Name of the supervisor: Prof. W.K. Mampearachchi

Signature of the supervisor:

Date:

## **Abstract**

Determination of packing density of a particulate mixture is still an open problem for researchers and scientists. The complex and random nature of particle behavior in a mixture and effect of various external factors have made it more and more complicated to develop theoretical and analytical models to predict the packing density. This study focused on the effect of vibration frequency, particle shape and surface texture on packing density. Initially, laboratory experiments were carried out to determine the use of packing concepts in concrete mixture design for interlocking concrete block pavers (ICBP). The approach found to be successful. However, determination of packing density of aggregate mixtures in laboratory was time consuming and difficult. Hence, the use of packing models to determine the packing density was studied. Validity of existing packing models for the aggregate mixtures was studied and as a result the 3-parameter model was found to be the only model that incorporates loosening effect, wall effect and wedging effect and the percentage error of 3-parameter model found to be lesser than that of Toufar model and compressible packing model. Hence, the 3-parameter model was selected for the modification. The results obtained from experiments were then analyzed and relationships were developed isolating the effect of vibration, surface texture and particle shape. Three effects were combined, and the packing density variations were obtained to incorporate the effects and modify the 3-parameter model. The packing density and vibration shows a 3<sup>rd</sup> order polynomial behavior while shape and surface texture shows a linear relationship with packing density. The developed model was validated for more than 300 independent data. The behavior of loosening effect, wall effect and wedging effect with vibration, surface texture and shape were also analyzed. The wall effect is affected by both surface texture and vibration frequency. The loosening effect is affected only by particle shape and the wedging effect does not affect by any of these factors.

Key words: Packing density, Vibration, Shape, Surface texture, Packing model

## **DEDICATION**

*To my mother who could not get a better sleep for the last 28 years.*

*To my father who went through all the trouble to made me who I am today.*

*To my wife who encouraged and supported me through thick and thin.*

*To my supervisor who believed in me and empowered me to achieve this dream.*

*To people of Sri Lanka whom I owe a debt of gratitude for paying for my education.*

## **ACKNOWLEDGEMENT**

First and foremost, I would like to express my sincere gratitude to my supervisor Prof. W.K. Mampearachchi for the continuous support, patience and motivation not only in academic field but also in difficult life situations. His guidance helped me in all the time of research and writing of this thesis. I could not have imagined having a better supervisor and a mentor for my Ph.D. study.

Besides my supervisor, I would like to thank my progress review committee: Prof. S.M.A. Nanayakkara, Dr. Nihal Somarathna, and Prof. Ashoka Perera, for their insightful comments and encouragement, but also for the hard questions which incited me to widen my research from various perspectives.

I wish to express my sincere thanks to the laboratory staff of Highway Engineering Laboratory and Materials Testing Laboratory of Department of Civil of Engineering, University of Moratuwa. I also express my sincere gratitude to the academic and non-academic staff of Department of Civil Engineering, University of Moratuwa for the continuous support and guidance throughout my undergraduate and postgraduate life.

I would like to thank the staff of SMS holdings (Pvt.) Ltd. for giving me the opportunity to use their factory premises and machines to carry out my research work.

I thank my fellow research colleagues for the stimulating discussions, for all the support they have given me to successfully complete my experimental work, and for all the fun we have had in the last four years.

Finally, I must thank my parents for their love and support throughout my life. Thank you both for giving me strength to reach for the stars and chase my dreams. My brothers deserve my wholehearted thanks as well. Also, I would like to thank my loving life partner Shankani for her understanding and support through thick and thin of my journey.

# TABLE OF CONTENTS

DECLARATION .....	i
Abstract .....	ii
DEDICATION .....	iii
ACKNOWLEDGEMENT .....	iv
LIST OF FIGURES .....	x
LIST OF TABLES .....	xiv
LIST OF ABBREVIATIONS .....	xv
CHAPTER 1 .....	1
1 INTRODUCTION .....	1
1.1 General .....	1
1.2 Objectives.....	2
1.3 Significance of the research .....	2
1.4 Thesis overview .....	3
CHAPTER 2 .....	5
2 LITERATURE REVIEW .....	5
2.1 Introduction.....	5
2.2 Particle optimization methods.....	5
2.2.1 Optimization curves .....	6
2.2.2 Discrete element models .....	9
2.2.3 Particle packing models .....	11
2.3 Overview of packing optimization in concrete mixture design .....	14
2.4 Particle packing and its influence on concrete properties.....	16

2.4.1	Particle packing density and water demand .....	17
2.4.2	Packing density and cement spacing .....	18
2.5	A summary of existing packing models .....	21
2.6	Applicability of existing packing models for ICBP .....	21
2.7	Development of 3-parameter model .....	26
2.7.1	Conventional model with 2 parameters .....	26
2.7.2	The wedging effect .....	30
2.7.3	3-parameter model .....	31
2.8	Effect of vibration, shape and surface texture on packing density .....	33
2.8.1	Effect of vibration on packing density .....	33
2.8.2	Effect of shape on packing density .....	36
2.8.3	Effect of surface texture on packing density .....	46
2.9	Summary of findings .....	51
CHAPTER 3 .....		52
3	METHODOLOGY .....	52
3.1	Introduction .....	52
3.2	Measurement of solid volume of particles ( $V_s$ ) .....	52
3.3	Measurement of total volume of the mixture ( $V_T$ ) .....	53
3.4	Application of vibration frequency .....	54
3.5	Measurement of shape factor .....	55
3.6	Measurement of surface texture of particles using British pendulum test .....	57
CHAPTER 4 .....		60
4	VALIDITY OF PACKING MODELS .....	60



4.1	Introduction.....	60
4.2	ICBP Manufacturing process and characteristics .....	61
4.3	Determination of mix design characteristics.....	62
4.3.1	Optimum Compression and Vibration .....	63
4.3.2	Coarse aggregate to fine aggregate ratio.....	64
4.3.3	Natural sand to manufactured sand proportion .....	64
4.3.4	Water/Cement Ratio.....	65
4.3.5	Effect of cement paste on strength .....	66
4.4	Estimation of field packing density in laboratory (Laboratory packing).....	67
4.5	Comparison of packing densities from models and experiments .....	67
4.6	Determination of compressive strength of ICBP .....	68
4.7	Summary of findings.....	72
4.8	Recommendations.....	73
CHAPTER 5 .....		74
5	COMBINED EFFECT OF VIBRATION FREQUENCY, SIZE RATIO AND LARGE PARTICLE VOLUME FRACTION.....	74
5.1	Introduction.....	74
5.2	Vibration time .....	75
5.3	Container wall effect.....	76
5.4	Analysis and development of model.....	78
5.4.1	Validation of the model.....	89
5.4.2	Cross check of the model .....	89
5.4.3	Limitations of the model.....	90

5.5	Design graphs.....	90
5.6	Summary of findings and recommendations.....	93
CHAPTER 6 .....		95
6	COMBINED EFFECT OF SHAPE, SURFACE TEXTURE AND VIBRATION ON PACKING DENSITY.....	95
6.1	Introduction.....	95
6.2	Development of particle packing models.....	96
6.3	Effect of particle shape on packing density .....	96
6.4	Effect of surface texture on packing density.....	100
6.5	Combined effect of vibration, shape and surface texture on packing density ...	101
6.6	Modification of 3-parameter model .....	102
6.6.1	Behavior of wall effect.....	110
6.6.2	Behavior of loosening effect .....	112
6.6.3	Behavior of wedging effect.....	113
CHAPTER 7 .....		115
7	CONCLUSIONS AND RECOMMENDATIONS .....	115
7.1	Conclusions.....	115
7.2	Limitations of the model and recommendations.....	116
REFERENCES.....		117
APPENDICES .....		126
Appendix A.....		126
Packing density results with respect to vibration.....		126
Vibration model correlation analysis .....		128

Design chart tables (Vibration analysis) .....	134
Appendix B .....	137
Packing density results with respect to particle shape .....	137
Shape factor model correlation analysis .....	137
Appendix C .....	140
Packing density results with respect to Surface texture (BPN).....	140
Surface texture model correlation analysis .....	141
Appendix D .....	144
Modified 3-parameter model correlation analysis .....	144
Appendix E .....	161
Mix design sample calculation.....	161

## LIST OF FIGURES

Figure 2.1: Ideal packing curves (Fennis & Walraven, 2012) .....	8
Figure 2.2: Discrete element models creating a particle structure without particles contact. ....	10
Figure 2.3: The volume of a flowable mixture compared to the volume occupied by a stable particle structure containing the same particles (Fennis, 2011).....	17
Figure 2.4: The flow value as a function of $\phi_{mix}/\alpha_t$ for mortar mixtures (Fennis, 2011)	18
Figure 2.5: Cube compressive strength of mortars in relation to CSF ( Fennis, 2011) ...	20
Figure 2.6: The volume occupied by a stable particle structure with coarse and fine fillers (F- Filler, C- Cement)( Fennis, 2011).....	20
Figure 2.7: Summary of packing models .....	22
Figure 2.8: Loosening effect .....	27
Figure 2.9: Wall effect .....	27
Figure 2.10: Packing density against volumetric fraction of fine particles (Kwan et al., 2013) .....	30
Figure 2.11: Wedging effect .....	32
Figure 2.12: Visual assessment of particle shape (a) Derived from Measurements of sphericity and roundness, (b) Based upon visual observations.....	38
Figure 2.13: Form triangle of Sneed and Folk (1958) .....	41
Figure 2.14: Particle Shape as defined by Wadell sphericity ( $\psi$ ) and Aschenbrenner shape factor (F) (Ozol, 1978).....	42
Figure 2.15: Convexity of a particle .....	45
Figure 2.16: Particle packing volume and macro-surface voids and micro-surface voids enclosed by packing volume membrane (Lamond & Pielert, 2006).....	47

Figure 2.17: Measurement method for characterizing the surface texture of an aggregate (Wright, 1955).....	49
Figure 3.1: Measurement of total volume.....	53
Figure 3.2: Schematic diagram of experimental setup.....	54
Figure 3.3: Dimensions of a particle.....	57
Figure 3.4: Selected aggregates for the experiment (a) Shape factor 0.15 (b) Shape factor 0.3 (c) Shape factor 0.45 (d) Shape factor 0.75 (e) Shape factor 0.9.....	57
Figure 3.5: British pendulum test apparatus.....	59
Figure 3.6: Samples prepared for different surface textures.....	59
Figure 3.7: The coated spherical beads.....	59
Figure 4.1: Hydraulic machine used in industry.....	61
Figure 4.2: 0.45 Power curve and aggregate size distribution at an industrial block manufacturer.....	62
Figure 4.3: Packing density vs. Vibration.....	63
Figure 4.4: Packing density vs. Compression.....	63
Figure 4.5: Packing density vs. Fine aggregate percentage (%) in the mix.....	64
Figure 4.6: Results of box test for different Water/Cement ratios.....	65
Figure 4.7: Comparison of packing models.....	68
Figure 4.8: Sample ICBP using optimized concrete mixture.....	71
Figure 4.9: Gradation of aggregates used in the study and optimized blend.....	72
Figure 5.2: Packing density variation with respect to the large particle diameter to container diameter ratio ( $d/D$ ).....	78
Figure 5.3: Effect of vibration frequency on packing density for various large particle fractions at size ratio of 0.15.....	79



Figure 6.16: The wall effect variation with respect to size ratio for various surface textures.....111

Figure 6.17: The wall effect variation with respect to size ratio for various vibration frequencies.....112

Figure 6.18: The loosening effect variation with respect to size ratio for various shape factors .....113

Figure 6.19: The wedging effect variation with respect to size ratio.....114

## LIST OF TABLES

Table 2.1: Computer applications and packing models used in the industry.....	13
Table 2.2: Shape factor variation with particle shape.....	42
Table 3.1: Vibration analysis data.....	55
Table 3.2: Shape analysis data .....	56
Table 3.3: Surface texture analysis data.....	58
Table 4.1: Effect of cement paste on strength.....	66
Table 4.2: Comparison of packing models with experimental results .....	69
Table 4.3: Concrete mix proportions and strengths .....	70
Table 4.4: Results obtained from field experiments .....	71
Table 5.1: Time for maximum packing with vibration for various large particle volume fractions. ....	76
Table 5.2: Packing density values with respect to the large particle diameter to container diameter ratio ( $d/D$ ) .....	77
Table 5.3: Particle arrangement before and after vibration.....	80
Table 5.4: A, B, C and D Parameters (110 Rad/s) .....	82
Table 5.5: Variation of A, B, C and D sub-parameters ( $A_1, A_2, A_3, B_1, B_2, \dots, D_1, D_3$ ) .....	84
Table 6.1: Variation of m and c value with large particle fraction .....	97
Table 6.2: Values of sub-parameters.....	102
Table 6.3: Values and equations for each sub parameter.....	105
Table 6.4: Percentage error of each model at optimum packing.....	110
Table 6.5: Percentage error of each model at various fine particle volume fractions....	110



## LIST OF ABBREVIATIONS

<b>Abbreviation</b>	<b>Description</b>
ICBP	Interlocking concrete block pavers
DEM	Discrete element models
3D	Three dimensional
UHPC	Ultra high-performance concrete
W/C	Water/Cement
CSF	Cement spacing factor
LPDM	Linear packing density model
SSM	Solid suspension model
CPM	Compressible packing model
3PM	Three parameter model
SA	South Africa
IS	Indian Standards
SLS	Sri Lanka Standards
FHWA	Federal highway administration
BPN	British pendulum number
SN	Skid number
MTD	Mean texture depth

# CHAPTER 1

## 1 INTRODUCTION

### 1.1 General

Densification of particulate mixtures to obtain desired characteristics is a main requirement and a challenge in materials engineering and science. The packing density of a mixture is an indication of how well the packing is occurred. It is measured as the solid volume of a mixture over total volume. Higher the packing density, higher the solid volume of the mixture, which indicates that the density of the mixture is higher as well. Higher packing densities are often desired in material industry to achieve both high strength materials and impermeable materials. (i.e.: high strength concrete, impermeable concrete, aggregate base course etc.). However, sometimes it is required to obtain mixtures that has the lowest packing density which may carry higher volume of voids (i.e. open graded friction course, permeable concrete, porous asphalt etc.). Thus, it is important to determine the packing density of a mixture beforehand in-order to achieve required properties of a mixture.

Determination of packing density of a mixture is practically a tedious process. The process gets more and more complicated when the particles are of various shapes and textures. The compaction process also affects the packing density. Hence, simulating or replicating similar conditions in a laboratory is difficult. To overcome such difficulties and predict the packing density of a particulate mixture, researchers have been trying to develop theoretical packing models over the past few decades. However, most of these models are based on basic assumptions like spherical, smooth particles with random or loose packing. Therefore, applicability and reliability of such models are limited for more advanced applications.

Hence, development of a theoretical model that can accurately predict packing density of a given complex mixture accommodating shape, texture and packing method (vibration)

is a need of the industry and scientific community. This study focusses on developing a theoretical packing model incorporating shape, texture and vibration frequency.

## **1.2 Objectives**

The objective of this study is to develop a theoretical packing model incorporating vibration frequency, surface texture and particle shape. It is proposed to,

1. Determine the validity of existing theoretical packing models
2. Determine the effect of vibration frequency on packing density
3. Determine the effect of surface texture on packing density
4. Determine the effect of particle shape factor on packing density
5. Develop a theoretical packing model incorporating vibration frequency, surface texture and shape factor

## **1.3 Significance of the research**

Particulate mixtures and materials are widely used in many industries. Concrete technology, mining and mineral processing industries, ceramics processing, powder metallurgy, asphalt mix design etc. have shown an interest in packing of solid particles for the advancement of respective field. Most of these industries try to achieve highest packing density for better performance while some try to achieve lowest packing density for certain applications. Either case, prediction of packing density of solid mixtures without going through rigorous trial and error process is preferable to save time, money and effort. However, determination of packing density of a particulate mixture is a challenge due to complexness. The task becomes more challenging when number of factors such as particle shape, packing method, particle surface texture etc. affect the packing.

Several attempts have been made to develop theoretical packing models to accurately predict the packing density of a particulate mixture. Still, most of these packing models are not accurate enough for complex mixtures such as optimization of concrete aggregate

packing, determination of asphalt aggregate blend etc. The main reason for this limited reliability is because these models are based on several basic assumptions such as spherical smooth particles with random loose packing. Nevertheless, the real conditions of a particulate mixture are different. For example, aggregates used in concrete are of different shapes, different textures and vibration is used for better compaction. Hence, the basic packing models that do not incorporate these factors, thus may not provide the best packing density values. Several attempts have been taken to develop packing models by taking these realistic conditions into account. These attempts are successful to a certain extent. However, majority of these models consider only one factor at a time into account and they do not consider the combined effect to predict the packing density of a mixture. Thus, they cannot be used for more complex situations.

This study identifies the significance of developing a new theoretical packing model. The study incorporates three most critical parameters; shape, texture and vibration in a new packing model. By accounting these three factors in to the model, this study will significantly improve the understanding of packing of particulate mixtures.

#### **1.4 Thesis overview**

Chapter 1 presents an introduction of the study with importance of determination of packing density of particulate mixtures. Also, this chapter explains the thesis structure and overview.

Chapter 2 reveals the findings of literature review. Literature review presents particle optimization methods, influence of packing on concrete properties, applicability of packing models on mixture designing of interlocking concrete block pavers (ICBP), effect of vibration, shape and texture on packing density.

Chapter 3 presents the methodology of the research. It includes the method followed to measure the packing density, apparatus and the techniques used for applying the vibration, method of measuring shape and surface properties etc.

Chapter 4 describes the validity of particle packing models in mixture design for the application of ICBP. The chapter evaluates the existing particle packing models and selects the 3-parameter model for further modification.

Chapter 5 reveals the effect of vibration frequency, size ratio and large particle volume fraction on packing density of binary spherical mixtures. The chapter further explains the development of an analytical model to predict the packing density of binary spherical mixtures subjected to vibration.

Chapter 6 explains the combined effect of shape, surface texture and vibration on packing density of binary particulate mixtures. This chapter explains the individual effect of shape and surface texture on packing density and develops analytical equations. Further the 3-parameter model is modified to account the combined effect of vibration, surface texture and shape factor.

Chapter 7 contains the conclusions, limitations and recommendations of the study.

## **CHAPTER 2**

### **2 LITERATURE REVIEW**

#### **2.1 Introduction**

Particle packing optimization is of paramount importance in the field of materials engineering and science. The ultimate objective of the study is to develop a theoretical packing model that incorporates the effect of vibration, surface texture and shape parameters of particles on packing density of a mixture. To develop the model, a systematic approach was adopted, and this chapter presents the literature published under the subject.

The section 2.2 presents the particle optimization methods available and analyses the most suitable method to incorporate vibration, shape and texture. The section 2.3, 2.4 and 2.5 studies the influence of particle packing on concrete properties and applicability of existing packing models for ICBP mixture design. The section 2.5 reveals the shortcoming and loopholes of existing packing models and provides an idea to improve the packing models to predict more realistic values by incorporating shape, texture and vibration. The section 2.6 describes the basic theory behind conventional two parameter model and development of 3-parameter model incorporating wedging effect. The section 2.7 explains the effect of vibration, shape and surface texture on packing density and how to measure each parameter. The final section concludes the literature review.

#### **2.2 Particle optimization methods**

Packing optimization in concrete mixture design is the process of selecting suitable sizes and proportions of different aggregates to achieve desired properties in concrete. Simply, smaller particles should be selected in a way that the size and proportion of the smaller particles can fill up the gaps in between larger particles to obtain the maximum packing density. Higher the packing density, lesser the voids in the mixture.

Optimization of particle packing can be divided into three categories:

- Optimization curves.

Optimization curves use particle size distribution curves of group of particles (continuous gradation of particles) and provide an optimum curve to achieve the maximum packing mixtures from the available group of particles.

- Discrete element models.

These models use numerical analysis and produce virtual packing structure using advanced computer applications to predict the packing density and packing arrangement of a given particulate mixture.

- Particle packing models.

Particle packing models are analytical models which calculate the final packing density of discrete or continuous particle groups by analyzing the geometry, packing characteristics and inter particle effects.

### **2.2.1 Optimization curves**

Feret (1892) studied the influence of aggregates on concrete strength in early 1892. Based on his studies, researchers experimented ways to determine the ideal grading curve that provides the best packing. One of the most prolific finding in this area is the Fuller curve which was found by Fuller and Thompson (1907). This curve is still in use for the calculation of concrete mix designs. The Fuller curve is given in Equation 2.1 ( $q = 0.5$ ). Various researchers modified the equation for the value of  $q$  (Talbot & Richart, 1923). Andreasen and Andersen (1930) proposed a  $q$  value in the range of 0.3-0.5. Further, they proposed that this factor may vary with the particular aggregate characteristics such as angularity, surface texture etc. and the precise value needs to be determined experimentally for the given aggregate group. For angular particles  $q$  becomes lower (0.3)

and for ideal spherical particles q becomes 0.5 and the equation gets identical to the Fuller curve (Kumar & Santhanam, 2003).

$$P(d) = \left(\frac{d}{d_{max}}\right)^q \dots\dots\dots \text{Equation 2.1}$$

P(d) - Size cumulative distribution function

d - Particle diameter in meters

d<sub>max</sub> - Maximum particle diameter in the mixture in meters

q - Parameter (0.3-0.5) which adjusts the curve for fineness or coarseness

Funk et al. (1980) documented that every particle size distribution should have a finite minimum size d<sub>min</sub>. Hence, they modified the equation to accommodate the minimum particle size and the equation is given by:

$$P(d) = \frac{d^q - d_{min}^q}{d_{max}^q - d_{min}^q} \dots\dots\dots \text{Equation 2.2}$$

The value of q = 0.37 for optimum packing according to their studies.

Both Equation 2.1 and Equation 2.2 provide mixtures with highest packing density. These curves do not address the effect of particle shape, packing method or surface texture etc. However, the particle shape influences the packing of a mixture (Walker Jr, 2003; Zheng, Johnson, & Reed, 1990). Also, Zheng et al. (1990) has studied the effect of shape on packing and tried to modify the equation to accommodate shape effects. They have documented various q values for various particle shapes. Figure 2.1 shows the ideal packing curves according to Fuller, Andreasen and Funk and Dinger for a maximum



particle diameter of 32 mm and a minimum particle diameter of 63 $\mu$ m (Fennis & Walraven, 2012).

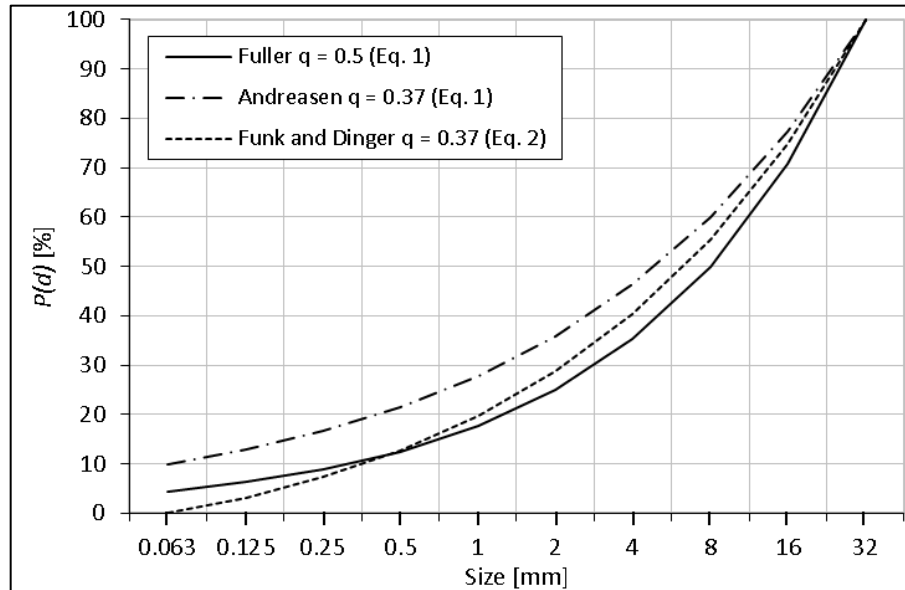


Figure 2.1: Ideal packing curves (Fennis & Walraven, 2012)

High porosity means less packing density and vice versa. Peronius and Sweeting (1985) developed an equation to calculate the porosity of mixtures accommodating the roundness of particles and Fuller curve. Many researchers used the Funk and Dinger model to optimize concrete mixtures and used various  $q$  values according to the requirement (Brouwers & Radix, 2005; Garas & Kurtis, 2008; Hunger, 2010; Kumar & Santhanam, 2003; Lagerblad & Vogt, 2004).

By using the equations for optimization curves, commercial computer programs have been developed to optimize the aggregate mixtures. EMMA [concrete.elkem.com] is such computer application which produces optimized aggregate mixtures for a fixed  $q$  value. COMPASS is another program which uses several packing equations to produce either aggregate mixtures or concrete mixtures with further input of particle size distribution data and required concrete properties.

However, these programs do not accommodate particle shape effects when performing the optimization process. Hence, the results obtained from these programs would not yield the mixture with the maximum packing density. The optimization curves do not have the capacity to accommodate such variations in particle packing process to produce a more realistic output.

Furthermore, Palm and Wolter (2009) and Stroeven and Stroeven (1999) have shown that instead of continuous mixtures, gap graded mixtures may lead to a higher packing density. However, optimization curves produce continuous mixtures which might produce lower packing density mixtures where use of selected mixtures with binary or ternary particle classes may yield more packing density.

Andreasen and Andersen (1930) assumed that the particle packing characteristics must remain similar when the particles and the container scaled in size. Based on this assumption Funk and Dinger (2013) studied the relationship between packing density of several single sized particulate mixture and the packing density of continuous particle size distributions presented by Furnas (1928). Even though their research did not confirm a mathematical relationship between the packing of discrete and continuous size distributions Brouwers (2006) found a mathematical correlation between the packing of discrete and continuous size distributions.

### **2.2.2 Discrete element models**

Discrete element models (DEM) produce a computer aided virtual particle matrix using the particle size distribution. Initially DEM models were developed as a static model where once the particle was placed, it would not move. Particles were placed randomly in the order of largest particles to the smallest. The simulation output is a three-dimensional (3D) model with a particulate mixture of different particle sizes. Hymosrtuc model which was developed by Technical university of Delft and the model developed by Zheng and Stroeven (1999) are commonly used to produce high quality concrete mixtures. Figure 2.2 shows the output of such models.

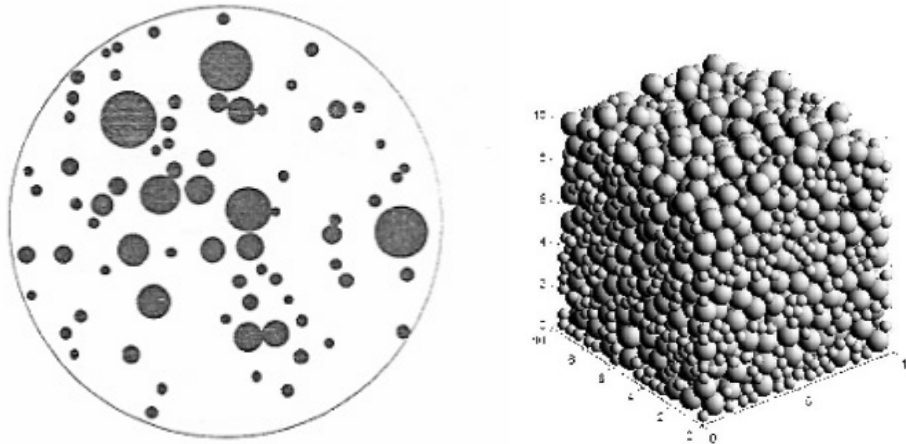


Figure 2.2(a): Model by Zheng and Stroeven (1999) Figure 2.2(b): Model by Fu and Dekelbab (2003)

Figure 2.2: Discrete element models creating a particle structure without particles contact.

Figure 2.2(a) shows the output of a 2D model by Zheng and Stroeven (1999) and Figure 2.2(b) shows the output of a 3D model by Fu and Dekelbab (2003). With the advancement of technology, computers were able to solve more complicated problems rapidly. This led to the development of dynamic models which are more complicated in nature. Dynamic models placed particles in the confined space randomly allowing them to move freely and achieve the maximum packing status by iterative process. These simulations run millions of different arrangements and calculate the maximum packing arrangement. The particles were subjected to gravity and interparticle collision to create forces that move particles. These models create mixtures with random loose packing and according to Fu and Dekelbab (2003). One of the main disadvantages of these models is that they do not generate the mixtures with the highest possible packing for a given particle size distribution. To overcome this problem, some models produce particles in a container and decrease the container size (Stroeven & Stroeven, 1999) and certain models leave particles to overlap and increase the container so that particles rearrange until particles do not overlap (Kolonko et al., 2008). These models will produce a virtual packing mixture with known particle locations, shapes and sizes. Figure 2.2(b) shows a simulation model produced by Fu and Dekelbab (2003). The mixture will be analysed to produce results

such as maximum packing, porosity, interconnected voids and lengths etc once the container volume is defined. The packing models can also be used to collect more information about particle packing such as determining the resistance to external loads (Snoeijer et al., 2004), calculating the number of connected points between particles etc. Further, these models can be used to measure the rheology and flowing properties of concrete mixtures (Gram & Silfwerbrand, 2007; Roussel et al., 2007). When the particle size distribution is continuous or the number of particle size classes is higher, determination of the suitable composition to achieve the maximum packing density becomes more complex. Also the number of inputs to the system increases and the simulation time increases as the number of particles to be analyzed is higher. Hence, the time taken to simulate a single mixture is very high. To overcome such issues, researchers adapted to a stepwise approach where small particle mixtures are first packed and put them in the voids between large particles (Kolonko et al., 2008).

### 2.2.3 Particle packing models

Analytical packing models calculate the theoretical packing density of a particulate mixture. These models predict the packing density based on geometrical principal and mathematical relationships. The mathematical relationships are developed to determine the inter particle interactions (which will be explained in detail in section 2.6.1 and 2.6.2) within different size classes. Usually packing models have two equations for two cases where large particle dominant case and smaller particle dominant case. The minimum value of the two equations will provide the packing density of the mixture.

The two basic mathematical equations of almost all particle packing models are the same and purely based on the geometry of the particles, Equations 2.3 and 2.4.

$$\alpha_t = \frac{\alpha_1}{1-r_2} = \frac{\alpha_1}{r_1} \dots\dots\dots \text{Equation 2.3}$$

$$\alpha_t = \frac{1}{1+\frac{r_2}{\alpha_2}} \dots\dots\dots \text{Equation 2.4}$$

- $\alpha_t$  - Calculated packing density of a mixture
- $\alpha_1$  - Packing density of the large size class 1
- $\alpha_2$  - Packing density of the small size class 2
- $r_1$  - Volume fraction of size class 1
- $r_2$  - Volume fraction of size class 2

For two size classes, by definition  $r_1 + r_2 = 1$

The basic equations given above were introduced by Furnas (1928). The basic equations were developed based on number of assumptions and can only be valid for binary mono sized spherical particulate mixtures with no interaction between particles (small particle diameter to large particle diameter is close to 0). The two different equations resemble the two different cases. Case 1 is when volumetric fraction of large particles is greater and dominates the mixture while small particles freely fit into the voids in between large particles without disturbing the packing structure. Case 2 is when the volumetric fraction of smaller particles is greater and dominates the mixture while larger particles are embedded in a sea of smaller particles without disturbing the matrix of smaller particles.

Westman and Hugill (1930) developed an algorithm using the discrete packing theory. This model can also be used for mixtures with more than two particle classes which do not have inter particle interaction. Furnas (1931) proposed a model to predict the packing density of multiparticle mixtures and supporting equations to derive interparticle interactions.

Aim and Le Goff (1968) incorporated the interaction effects, the wall effect (which occurs when introducing a large particle to a small particle dominant mixture) into the Furnas model and Schwanda (1966) presented a model incorporating both interaction effects, wall effect and loosening effect (which occurs when introducing a small particle into the matrix of larger particles) (Reschke, 2001).

Modeling of multiparticle mixtures from binary mixtures was initially studied by Toufar et al. (1976). Following the studies of Toufar et al. (1976), Stovall et al. (1986) and Yu and Standish (1987) modified the basic Furnas equation. Dewar (2002) developed an equation in a systematic method to incorporate multiple particles.

Following these models, more sophisticated models have been developed. Most of the models try to achieve a reliable packing density prediction through more and more realistic assumptions. For many of these models need to be fed the packing density of mono sized particle mixtures, compaction method and energy input, shape characteristics and texture characteristics of particles involved etc. The 3-parameter model proposed by Kwan et al. (2013) introduces a new interaction effect called wedging effect to produce more reliable output. The 3-parameter model will be analyzed in great detail in Chapter 2, section 2.7, hence will not be explained in this section. Furthermore, several packing models based on the basic models have been developed and each model addresses a different application. Hence those models will not be explained, and the most relevant models will be presented in this chapter under the section 2.6 (Fennis, 2011; Goltermann et al., 1997b; Johansen, 1991; Kumar & Santhanam, 2003). Following computer applications and packing models given in Table 2.1 are also used in industry for various applications.

Table 2.1: Computer applications and packing models used in the industry

Model / Application	Source
Europack	(Toufar et al., 1976)
MixSim	(Dewar, 2002; Jones, Zheng, & Newlands, 2002)
4C- Packing	(Mette Glavind, Olsen, & Munch, 1993)
Compressible packing model - CPM	(Francois De Larrard, 1999)
Schwanda model	(Geisenhanslüke, 2009; Reschke, 2001)
Linear mixture packing model	(Yu & Standish, 1987)
Compaction interaction packing model	(S. Fennis, 2011)

### **2.3 Overview of packing optimization in concrete mixture design**

One of the earliest information on particle packing for concrete production was published by Féret in 1892 (Goltermann et al., 1997; Johansen, 1991). Packing methods in mixing of concrete have been used in Scandinavia as early as 1896 for providing concrete resilience in marine environment. Plethora of literature on packing was published in the 1930s explaining the optimization of packing followed by Furnas (1928) and by Westman and Hugill (1930). Powers (1969) in his studies on aggregate mixtures presented that the voids ratio of a binary particulate system would be minimum at a specific combination. In 1981, Petersen showed the use of packing concepts in relation to the mechanical and the rheological properties. Petersen (1981) found that the model by Aim and Le Goff (1968) gave the best fit of the theoretical to the experimental packing densities for small particle diameter ratios and that the model defined by Toufar et al. (1976) gave the best fit for larger diameter ratios. Goltermann et al. (1997) used three models (Aim model, Toufar model and the modified Toufar model) in their tests, (Johansen, 1991; Kumar & Santhanam, 2003). A large variety in particle size and size distribution of natural and crushed aggregates were considered in his study and the results showed that the Toufar model, and especially the modified Toufar model, agrees very well with the measured packing degrees. The Aim model did not fit the test results and could not be used for the aggregates. Glavind and Pedersen (1999) studied that when choosing a concrete mix design, it is always desirable to combine the aggregates as densely as possible. That reduces the required quantity of binder which should fill the voids between the aggregates for a constant concrete workability. Apart from an evident economic benefit, a minimum of binder in concrete results in less shrinkage and creep and a denser and consequently a more robust and strong concrete mix.

De Larrard and Sedran (2002) have established a method that uses a new technique for concrete mixing. Their software, Bétonlab, was reliable with their mathematical models. In addition to evaluating the packing degree by use of the models, the authors presented that one can determine the fresh concrete properties and also the compressive strength.

Wong and Kwan (2008) measured the packing densities of cementitious materials comprising ordinary Portland cement, pulverized fly ash and condensed silica fume. The results for non-blended materials exposed that the accumulation of a superplasticizer would always improve the packing densities of ordinary Portland cement and pulverized fly ash, the addition of a polycarboxylate based superplasticizers could reduce the packing density of condensed silica fume. Fennis and Walraven (2012) studied determination of the packing density to lower the cement content in concrete. The study explains how centrifugal consolidation can be used to determine the packing density of powders. The process is evaluated based on experimental data, calculations and polarization and fluorescence microscopy of the samples.

Wong and Kwan (2014) proposed the three-tier system design. The mix design would be separated into three stages. At the initial stage, the packing density of the cementitious materials would determine the water demand, and at the second stage the aggregate particles smaller than 1.2 mm would determine the paste demand and at third stage the aggregate particles larger than 1.2 mm would determine the mortar demand. Rao and Krishnamoorthy (1993) studied the quantities required for minimum void content followed a linear trend fairly similar to what one would obtain from the theoretical gradings of Fuller and Thompson (1907). An empirical equation has been fitted for this linear trend so that it can be used to determine the proportions of coarse and fine aggregate of minimum void contents.

The perfect mixture proportion to gain the maximum packing depends on the properties of concrete. For example, the maximum/optimum packing density can vary with the aggregate shape, aggregate size ratios, aggregate surface texture and the compaction method. Further rounded aggregate will provide a better packing density and workability while angular aggregates will provide a better green strength and low workability. Hence, required properties of the concrete needs to be investigated to select the optimal packing density and suitable aggregate types.



Typically, high packing density is an essential characteristic in concrete mixture design procedure to produce ultra high performance concrete (UHPC) and ecological concrete. High packing density reduces the water demand and increase the strength of the concrete. Analytical packing models and discrete element models can be successfully used to calculate the maximum packing density of concrete mixtures. However, scientists do not use discrete element models due to limitations in computational speeds and tools. Thus, analytical packing models are the ideal tool for the design of concrete mixtures using packing density approach.

#### **2.4 Particle packing and its influence on concrete properties**

Optimization of aggregate packing of concrete mixtures has many advantages during both fresh and hardened state. Maximum packing state is having the minimum voids content, thus the space for water requirement is minimal. Therefore, fine particle addition to minimize the voids will reduce the water demand of the concrete (De Larrard, 1999; Kronlöf, 1997; Wong & Kwan, 2008). Reschke (2001) reported that increase of packing density of the mixture improves the strength of concrete if all the porous spaces in between aggregates are filled with cement paste.

High packing density creates a very strong aggregate skeleton and restrain the shrinkage and creep within the concrete. Moreover, low water demand reduces the shrinkage effects due to the presence of low evaporable water in the cement paste (Neville, 1995). Kwan and Mora (2002) also reported that reduction of voids in the mixture due to higher packing density leads to a reduction of cement paste. Lower cement paste produces low heat during the hydration process. Hence the drying shrinkage is reduced.

Dhir et al. (2005) presented the performance of several properties of concrete. According to his studies particle packing techniques influence the compressive strength of concrete. This section emphasizes the importance and influence of particle packing density on two main concrete properties; water demand and cement spacing.

### 2.4.1 Particle packing density and water demand

Particle packing density is an important factor on the water demand of concrete. Packing density is the amount of solid volume of particles in a unit bulk volume of a mixture. Though, the packing density of a stable particle mixture and a real concrete mixture is different. As shown in Figure 2.3 particles in a stable mixture are in contact with each other while in a real concrete mixture, particles are dispersed all over the volume. Hence, the packing density is lower. Part of the water used in a real concrete mixture will fill the voids in between particles and the excess water will improve the workability of the mixture.

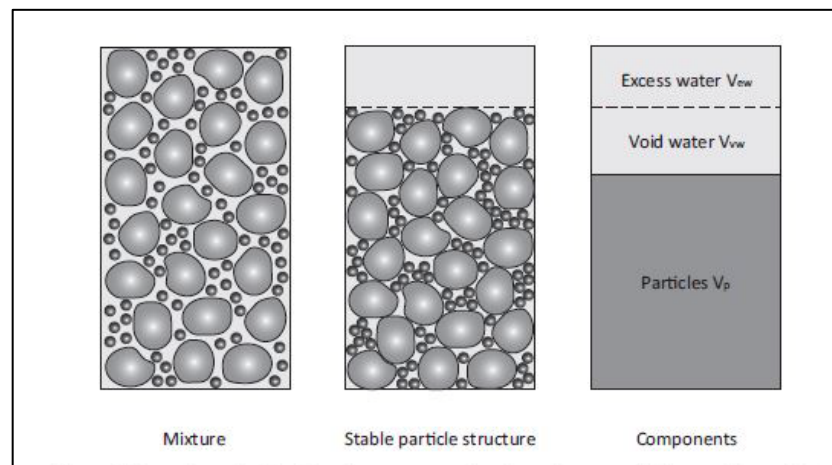


Figure 2.3: The volume of a flowable mixture compared to the volume occupied by a stable particle structure containing the same particles (Fennis, 2011)

If optimization is done to the mixture, packing density will increase and the voids volume will decrease. Hence, the water requirement to fill the voids will reduce. So, the excess water which can be maintained at required level to achieve the desired workability. Hence, the overall water demand of an optimized concrete will be lesser than that of normal concrete. Fennis (2011) has studied the relationship between flowability and packing density of mixtures and Figure 2.4 shows the results extracted from his study.

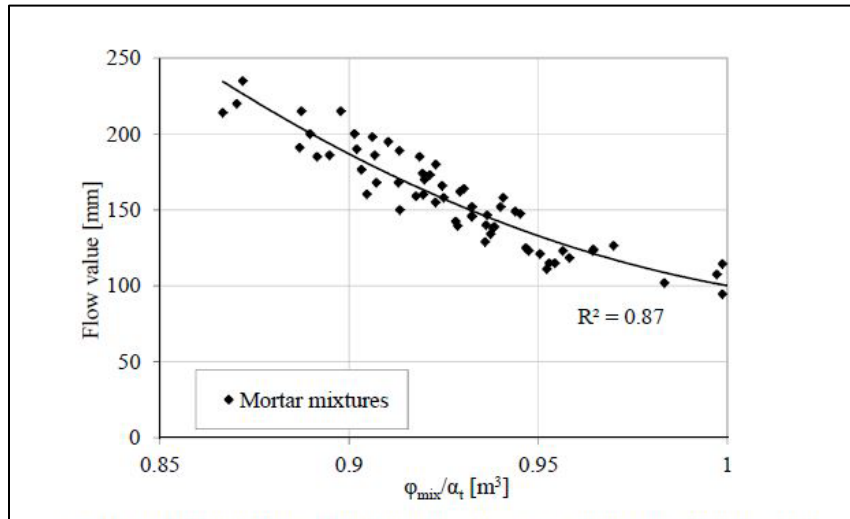


Figure 2.4: The flow value as a function of  $\phi_{mix}/\alpha_t$  for mortar mixtures (Fennis, 2011)

X axis represents the ratio between solid volume of the mixtures  $\phi_{mix}$  and the maximum packing density  $\alpha_t$ . This relationship can be effectively used to design high performance concrete (Using low water/cement ratio while maintaining the same workability) or ecological and economical concrete with low amount of cement.

#### 2.4.2 Packing density and cement spacing

The packing optimization can also help to decrease the space between cement particles. The space between cement particles depends mainly on the water content and aggregate structure of the mixture. Dense packing allows particles to pack close to each other. Hence, the cement particles are forced to pack closer to each other. This helps the hydration products to effectively be utilized in bonding process resulting in high strengths rather than filling up the voids. If the aggregate particles and cement particles are not close to each other the hydration products will have to bridge a larger gap. This leads to a weak bonding strength and ultimately the concrete strength will be low.

Typically, most of the equations developed to predict the strength of concrete is based on the water/cement ratio (Abrams, 1919; Bolomey, 1935; De Larrard, 1999; Feret, 1892;

Garas & Kurtis, 2008; Mechling et al., 2007; Mikulic et al., 2008; Neville, 1995; Popovics, 1998; Powers, 1969; Souwerbren, 1998). However, use of packing models allows to predict the concrete characteristics better by calculating the particle packing structure and void spaces. As explained earlier, use of a DEM or analytical model is helpful to calculate the space available for cement paste. The direct and indirect information available from these models can be effectively used to produce more advanced, specific concrete mixtures.

Cement spacing factor (CSF) given in Equation 2.5 can be used to calculate the space between cement particles (Fennis, 2011).

$$CSF = \frac{\varphi_{cem}}{\varphi_{cem}^* \frac{\alpha_t}{\varphi_{mix}}} = \frac{\varphi_{cem} \times \varphi_{mix}}{\varphi_{cem}^* \times \alpha_t} \dots\dots\dots \text{Equation 2.5}$$

- $\varphi_{cem}$  - Partial volume by the cement in a stable particle structure
- $\varphi_{cem}^*$  - Maximum partial volume that the cement occupies under the presence of other particles
- $\varphi_{mix}$  - Partial volume of all particles in a mixture in a unit volume
- $\alpha_t$  - Calculated packing density of a mixture

$\varphi_{cem}$  is the volume of the cement in the mixture while  $\varphi_{cem}^*$  is the maximum volume that cement can be occupied in the mixture when other particles are present. Hence the term  $\varphi_{cem}/\varphi_{cem}^*$  expresses the free voids around cement particles. increase of  $\varphi_{cem}$  will lead to less amount of voids due to closer packing of cement particles. similarly, fine fillers can be used to fill the voids and improve the packing density by reducing the  $\varphi_{cem}^*$ .

Actual concrete mixture has water in the voids in between stable particle structure and also excess water improves the workability as explained in a previous section. Addition of water forces particles to move away from each other and this factor is represented by the term  $\alpha_t/\varphi_{mix}$ . Hence, addition of more water increases the space between cement

particles and reduces the strength of the concrete. Figure 2.5 shows the relationship of CSF and the compressive strength of mixtures (Fennis, 2011).

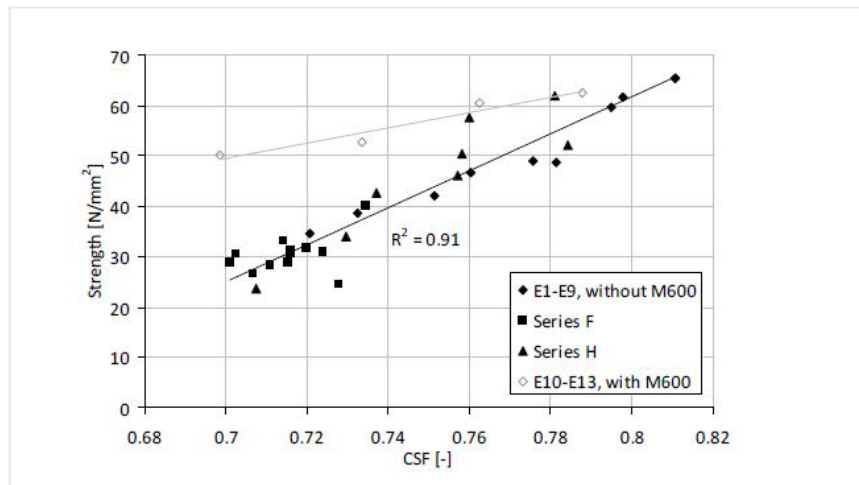


Figure 2.5: Cube compressive strength of mortars in relation to CSF ( Fennis, 2011)

Figure 2.6 shows the influence of packing density on the spacing between cement particles. The spacing between cement particles increases due to the introduction of coarse fillers with similar dimensions to cement particles (Figure 2.6 (a)). However, if smaller filler materials are used, the spacing between cement particles will not affect largely and the packing density of the mixture will increase as shown in Figure 2.6 (b) ( Fennis, 2011).

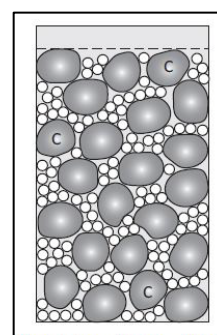
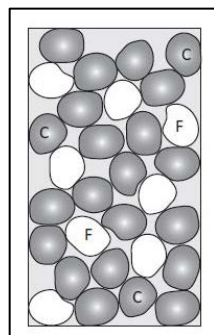


Figure 2.6 (a): Coarse particles

Figure 2.6(b): Fine particles

Figure 2.6: The volume occupied by a stable particle structure with coarse and fine fillers (F- Filler, C- Cement)( Fennis, 2011)

## **2.5 A summary of existing packing models**

Packing of particles and densification of particle mixtures is an important subject in scientific studies and industrial applications. A number of different approaches and studies have been performed to understand the behavior of particulate mixtures in confined containers. Involvement of many different factors has made the prediction of packing density a complex problem thus the development of packing models to predict the packing densities accurately is one of the main challenges faced by scientists. However, many attempts have been made throughout the last few decades and number of packing models are developed incorporating various factors to accurately predict the packing density of discrete and continuous mixtures. Due to the simplicity and easiness, most of these models have been developed under basic assumptions such as spherical, smooth particles, loose packing etc. According to these studies, there are three main effects that affect the packing density; wall effect, loosening effect and wedging effect. Wall effect and loosening effect occur with the dominance of large particle fraction and small particle fraction respectively while wedging effect can occur at any time (Kwan et al., 2013). Figure 2.7 shows the summary of widely used packing models developed thus far (Aim & Le Goff, 1968; Andreasen & Andersen, 1930; De Larrard & Sedran, 1994; Dewar, 2002; Fuller and Thompson, 1907; Funk & Dinger, 1994; Furnas, 1928; Goltermann et al., 1997a; Kwan et al., 2013; Kwan et al., 2015; Powers, 1969; Roquier, 2017; Sedran & De Larrard, 1999; Stovall et al., 1986; Toufar et al., 1976; Vesilind, 1980; Wong & Kwan, 2014; Yu et al., 1996).

## **2.6 Applicability of existing packing models for ICBP**

Several theoretical packing models were studied to determine the applicability for ICBP. Compressible Packing Model (CPM) ( De Larrard, 2000), 3-parameter model (Wong & Kwan, 2014), modified Toufar model (Goltermann et al., 1997) were selected for the optimization. Toufar model was selected because it is widely used for generalized concrete applications on high performance concrete. wedging effect.

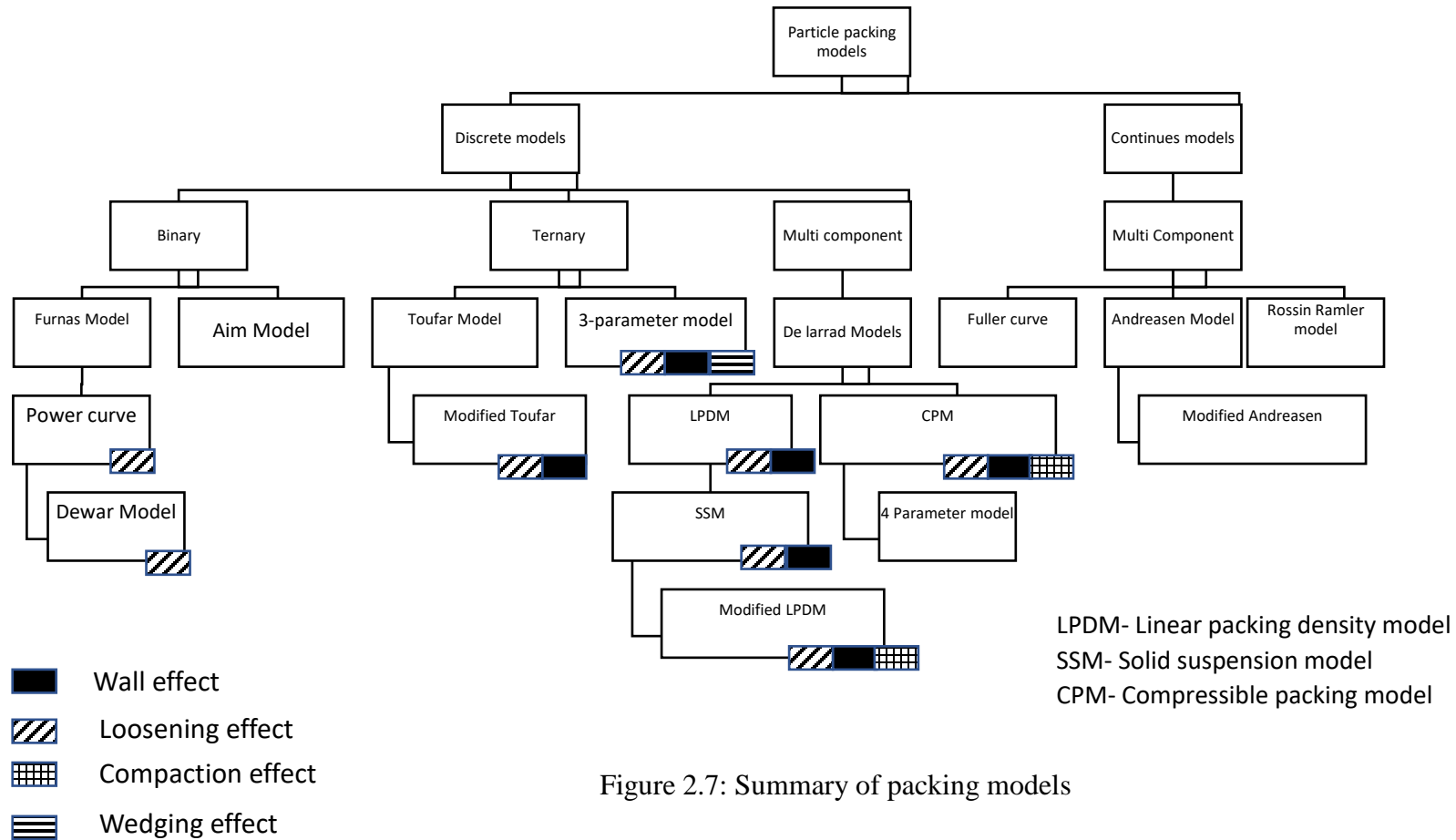


Figure 2.7: Summary of packing models

The compressible packing model which incorporates vibration was selected since the ICBP is cast specially applying vibro-compression. 3-parameter was selected because it considers a new interaction effect called . The model proposed by Goltermann et al. (1997), based on the Toufar’s model (Toufar et al. , 1976) has been validated by comparing around 800 test results from multiple sources. The packing density predicted by this model is expressed as in equation 2.6.

$$\varphi = \frac{1}{\left(\frac{y_1}{\varphi_1} + \frac{y_2}{\varphi_2} - y_2 \left(\frac{1}{\varphi_2} - 1\right) k_d k_s\right)} \dots\dots\dots \text{Equation 2.6}$$

Where:

- $\varphi$  - Packing density of the mixture
- $y_1$  - Volumetric proportion of fine particles in the mix
- $\varphi_1$  - Packing density of fine particles alone
- $y_2$  - Volumetric proportion of coarse particles in the mix
- $\varphi_2$  - Packing density of coarse particles alone
- $k_d$  - A factor that determines the influence of the diameter ratio
- $k_s$  - A statistical factor

Wong & Kwan (2014) three parameter model has considered three interaction effects. Loosening effect, wall effect and wedging effect. This is a semi empirical model where experimental data and regression analysis are used to determine the a, b and c parameters given in equations 2.7 to 2.13.

$$\frac{1}{\varphi_1^*} = \left(\frac{r_1}{\varphi_1} + \frac{r_2}{\varphi_2}\right) - (1 - a) \cdot \frac{r_1}{\varphi_1} \cdot \left[1 - c \cdot \left(\frac{r_1}{r_1^*}\right)^2\right] \dots\dots\dots \text{Equation 2.7}$$

$$\frac{1}{\varphi_2^*} = \left(\frac{r_1}{\varphi_1} + \frac{r_2}{\varphi_2}\right) - (1 - b) \cdot (1 - \varphi_2) \cdot \frac{r_2}{\varphi_2} \cdot \left[1 - c \cdot \left(\frac{r_2}{r_2^*}\right)^2\right] \dots\dots\dots \text{Equation 2.8}$$

$$r_1^* = \frac{(1-b)(1-\varphi_2)/\varphi_2}{\frac{1-a}{\varphi_1} + (1-b)(1-\varphi_2)/\varphi_2} \dots\dots\dots \text{Equation 2.9}$$



$$r_2^* = \frac{(1-a)/\phi_1}{\frac{1-a}{\phi_1} + (1-b)(1-\phi_2)/\phi_2} \quad \dots\dots\dots \text{Equation 2.10}$$

$$a = 1 - (1 - s_{12})^{3.3} - 2.6 \cdot s_{12} \cdot (1 - s_{12})^{3.6} \quad \dots\dots\dots \text{Equation 2.11}$$

$$b = 1 - (1 - s_{12})^{1.9} - 2 \cdot s_{12} \cdot (1 - s_{12})^6 \quad \dots\dots\dots \text{Equation 2.12}$$

$$c = 0.322 \tanh(11.9 \cdot s_{12}) \quad \dots\dots\dots \text{Equation 2.13}$$

Where,

- $r_1$  - Volumetric proportion of fine particles in the mix
- $r_1^*$  - Optimum volumetric proportion of fine particles
- $\phi_1$  - Packing density of fine particles alone
- $r_2$  - volumetric proportion of coarse particles in the mix
- $\phi_2$  - Packing density of coarse particles alone
- $r_2^*$  - Optimum volumetric proportion of coarse particles
- $a$  - The loosening effect parameter
- $b$  - The wall effect parameter
- $c$  - The wedging effect parameter
- $d_1$  - Diameter of fine particles
- $d_2$  - Diameter of coarse particles
- $s$  - Size ratio of two particle sizes ( $d_1/d_2$ )

Out of these three models, only compressible packing model addressed the packing process. It uses a compaction index (K) a constant related to the method of packing. (i.e.: corresponding to vibration under 15 psi of pressure is equal to the value 9.0)

$$K = \frac{\frac{y_1}{\beta_1}}{\frac{1-\beta_1}{\phi^* \gamma_1}} + \frac{\frac{y_2}{\beta_2}}{\frac{1-\beta_2}{\phi^* \gamma_2}} \dots\dots\dots \text{Equation 2.14}$$

Where,

$$\gamma = \min \left[ \gamma_1 = \frac{\beta_1}{1 - \left(1 - \frac{\beta_1}{\beta_2} a_{12}\right) y_2}; \gamma_2 = \frac{\beta_2}{1 - \left(1 - \beta_2 + b_{12} \beta_2 \left(1 - \frac{1}{\beta_1}\right)\right) y_1} \right] \dots\dots\dots \text{Equation 2.15}$$

$$a_{12} = \sqrt{1 - \left(1 - \frac{d_2}{d_1}\right)^{1.02}} \dots\dots\dots \text{Equation 2.16}$$

$$b_{12} = 1 - \left(1 - \frac{d_1}{2}\right)^{1.5} \dots\dots\dots \text{Equation 2.17}$$

Where,

- K - The compaction index
- $y_1$  - Volumetric fraction of particle size 1
- $y_2$  - Volumetric fraction of particle size 2
- $\gamma_1$  - Packing density of the mix when particle size 1 is dominant
- $\gamma_2$  - Packing density of the mix when particle size 2 is dominant
- $\beta_1$  - Packing density of particle size 1 alone
- $\beta_2$  - Packing density of particle size 2 alone
- $a_{12}$  - The Loosening effect parameter
- $b_{12}$  - The Wall effect parameter

Results of the selected packing models were compared with experimental results. The results are presented in Chapter 4, section 4.5. The results and the literature review recommended that 3-parameter model is the most suitable packing model for further modification. Hence, 3-parameter model is further studied in next section 2.7.

## **2.7 Development of 3-parameter model**

The 3-parameter model was developed by Kwan et al. (2013) to accurately predict the packing density of a binary spherical particulate mixture. The model was developed based on the conventional two parameter model with loosening effect and wall effect. The 3-parameter model added a new effect called wedging effect to the conventional model and developed equations for particle interactions to make the model more accurate and reliable. The following subsections will explain the model in great details.

### **2.7.1 Conventional model with 2 parameters**

When the large particles are dominant (small particle amount is insufficient to fill the voids among large particles, thus large particles are closely packed against each other) the filling effect occurs where small particles filling the voids among large particles. And, when the small particles are dominant (small particle amount is higher than the large particle amount hence small particles are tightly packed against each other) the occupying effect occurs where large particles occupy the solid volume of porous bulk volume of small particle mixture. These effects can occur even when there is no particle interaction. These two effects would improve the packing density of the mixture. The conventional 2 parameter models accommodate another two effects in addition to occupying and filling effects.

The loosening effect occurs in a mixture of dominant large particles. When the small particles could not fit into the voids between large particles due to its size, the small particles try to fill the voids by intruding into the voids disturbing the already formed packing arrangement of large particles. Hence, this phenomenon would reduce the packing density of the mixture by creating additional voids in between large particles. Figure 2.8 shows the occurrence of loosening effect.

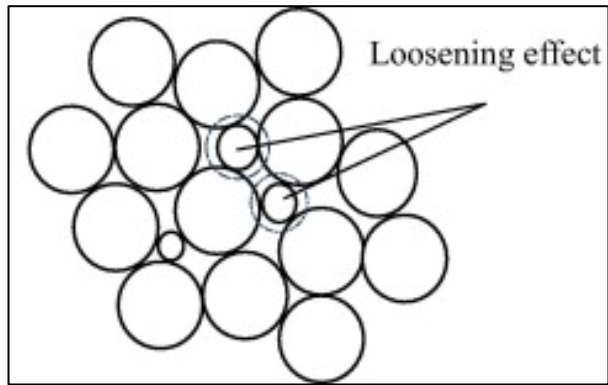


Figure 2.8: Loosening effect

The wall effect occurs when smaller particles are dominant. When a large particle is introduced into the already tightly packed small particle mixture, the packing is disturbed by solid surfaces of large particles. These surfaces act like walls and the arrangement of smaller particles against the wall becomes irregular creating void spaces along the wall. Figure 2.9 shows the occurrence of wall effect.

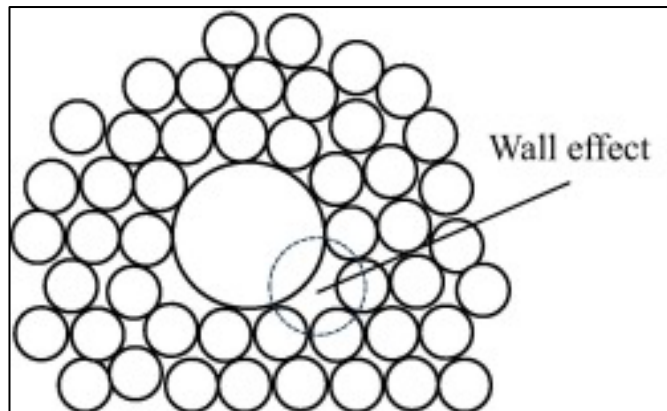


Figure 2.9: Wall effect

Both these effects reduce the packing density of the mixture by disturbing the proper packing arrangement. These effects are also called particle interactions and are small when the size ratio of small particles to large particles are small and vice versa. The effects are negligible when the size ratio is closer to 0. These mixtures have no particle interactions. When the size ratio is close to 1 (Both particle class sizes are similar) total interaction occurs and the contribution of the filling and occupying effect eliminates.

In between these two extreme ends, mixtures would have partial interactions and the level of interaction will depend on the size ratio.

Let's take a binary particulate mixture (A mixture of particles with only two size classes). The size class 1 is for small particles and size class 2 is for large particles. As explained when size class 2 is dominant both loosening effect and filling effect occurs. The packing density of the binary mixture ( $\phi_2^*$ ) in this case can be written as;

$$\frac{1}{\phi_2^*} = \frac{r_2}{\phi_2} + a \cdot \frac{r_1}{\phi_1} \dots\dots\dots \text{Equation 2.18}$$

- Size class 1 represents small particles
- Size class 2 represents large particles
- $r_1$  and  $r_2$  : volumetric fractions of solids in size classes 1 and 2; ( $r_1 + r_2 = 1$ )
- $\phi_1$  and  $\phi_2$ : packing densities of size class 1 and 2
- $a$  : loosening effect parameter ( $a=0$  for no interaction and  $a=1$  for total interaction)
- $\phi_2^*$ : Packing density of the mixture when size class 2 is dominant

The term  $\frac{r_2}{\phi_2}$  is the contribution to the bulk volume from size class 2 and the term  $a \cdot \frac{r_1}{\phi_1}$  is the contribution to the bulk volume from the loosening effect of the size class 1. For a clear understanding the equation can be rewritten as;

$$\frac{1}{\phi_2^*} = \left( \frac{r_1}{\phi_1} + \frac{r_2}{\phi_2} \right) - (1 - a) \cdot \frac{r_1}{\phi_1} \dots\dots\dots \text{Equation 2.19}$$

Similarly, when size class 1 is dominant, both wall effect and occupying effect would contribute to the packing density of the mixture. The packing density of the binary mixture when size class 1 is dominant can be written as;

$$\frac{1}{\phi_1^*} = \frac{r_1}{\phi_1} + r_2 + (b) \cdot (1 - \phi_2) \cdot \frac{r_2}{\phi_2} \dots\dots\dots \text{Equation 2.20}$$

- $b$  is the wall effect parameter ( $b=0$  for no interaction and  $b=1$  for total interaction)
- $\phi_1^*$ : Packing density of the mixture when size class 1 is dominant

The first term  $\frac{r_1}{\phi_1}$  is the contribution to the bulk volume from size class 1 and the second term  $r_2$  is the contribution to the bulk volume from size class 2. The last term  $(b) \cdot (1 - \phi_2) \cdot \frac{r_2}{\phi_2}$  is the contribution from wall effect to the bulk volume. For the simplicity, the equation can be rewritten as;

$$\frac{1}{\phi_1^*} = \left( \frac{r_1}{\phi_1} + \frac{r_2}{\phi_2} \right) - (1 - b) \cdot (1 - \phi_2) \cdot \frac{r_2}{\phi_2} \dots\dots\dots \text{Equation 2.21}$$

The loosening effect parameter  $a$  and the wall effect parameter  $b$  should be found using regression analysis of the experimental results. The values of both loosening effect and wall effect should fall within 0 and 1. When there are total interactions (both  $a$  and  $b$  equal to 1), both equations converge to the same equation. This is expected since total interaction means both particle size classes are similar hence the total mixture becomes a mixture of mono sized particles.

$$\frac{1}{\phi^*} = \left( \frac{r_1}{\phi_1} + \frac{r_2}{\phi_2} \right) \dots\dots\dots \text{Equation 2.22}$$

Instead of considering which size class is dominant, the packing density of the binary mix can be determined simply as:

$$\phi_{mix} = \min(\phi_1^*, \phi_2^*) \dots\dots\dots \text{Equation 2.23}$$

The 2-parameter model generates two packing density curves for the two equations. The curves will join at a mid-point creating a sharp peak at the point of intersection. Figure 2.10 shows the typical variation of 2 parameter model with experimental results made by Kwan et al. (2013). At the peak, the maximum packing density is achieved and the corresponding volumetric fractions of size class 1 and size class 2 can be obtained.

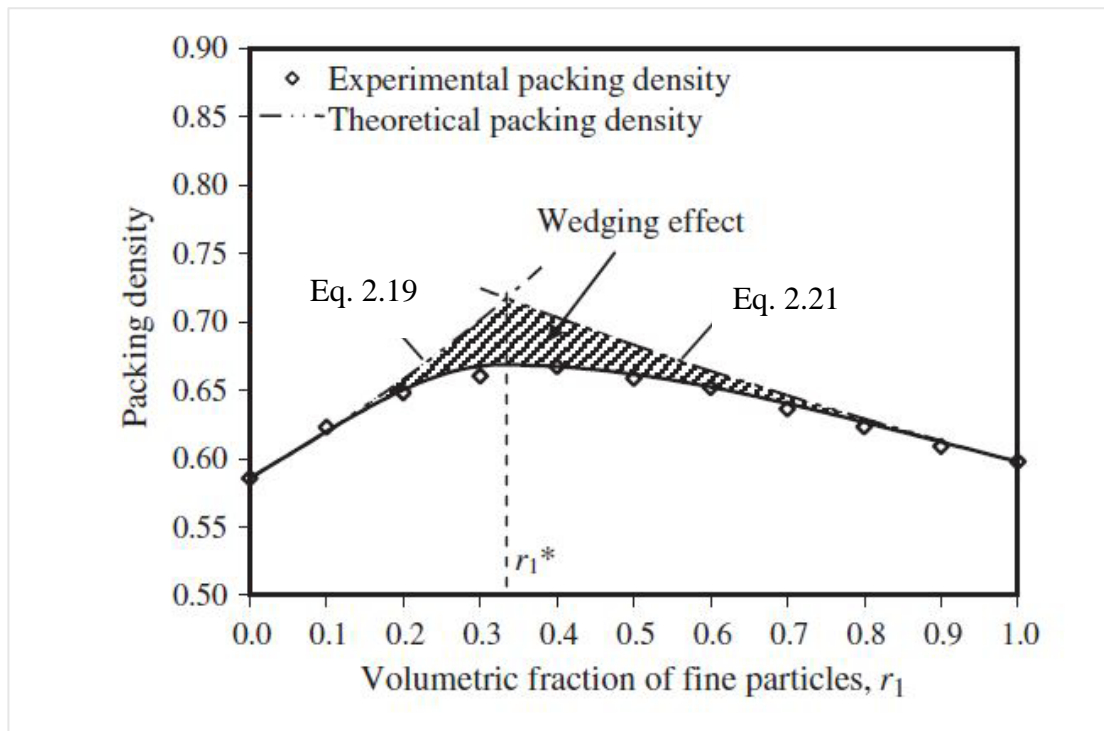


Figure 2.10: Packing density against volumetric fraction of fine particles (Kwan et al., 2013)

According to Figure 2.10, the sharp peak with steep curves denotes the sensitivity of packing density with volumetric fractions. Nevertheless, experimental results of Kwan et al. (2013) reveals that the variation does not create a sharp peak, in fact the variation produced a very smooth curve with a rounded peak. The sensitivity observed in experimental results were not that high as in 2-parameter model. The results also revealed that the 2-parameter model overestimated the packing density while experimental results are significantly lower than the predictions closer to the peak region. Further Kwan et al. (2013) suggested that the difference of the predictions and experimental values may be due to the wedging effect which will be explained in greater detail in a subsequent section.

### 2.7.2 The wedging effect

Consider a situation where all the small particles would fill the voids in large particles when the large particles are dominant. There may be some isolated small particles trapped in between walls of two large particles that may act as a wedge to create a small open space in between two large particles as shown in Figure 2.11(a). This effect

is quite similar to loosening effect but caused by isolated small particles in between the gap of two large particles. When small particles are introduced to the packing of large particles, first set of small particles will fill up the voids. When small particles are filling up the voids the number of particles trapped in between the gap will be higher. Hence, the wedging effect would be higher when the fine particles are close to filling up the voids closer to the peak of the curve.

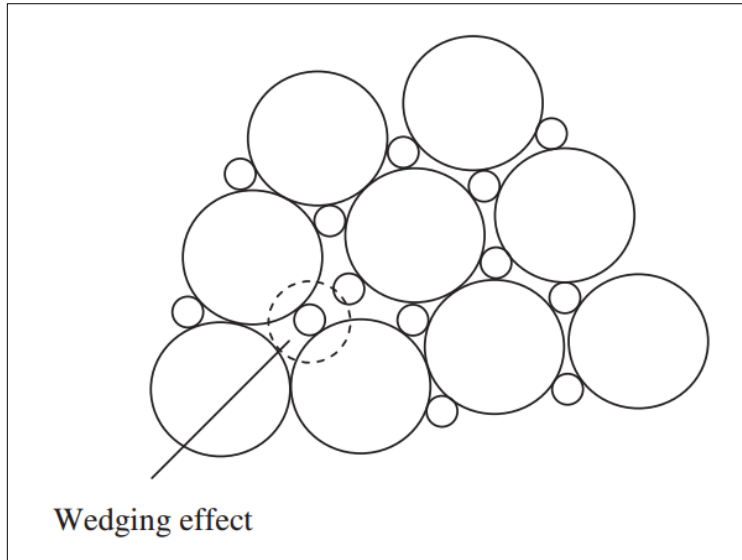
When small particles are dominant, large particles will be introduced to the sea of small particles and since small particles are dominant there will not be any large particle closer to another large particle. This gap between two large particles are not uniform and sometimes there may be two large particles with relatively narrow gap. These gaps can be wedged by fine particles as shown in Figure 2.11(b) and reduce the packing density of the mixture. In this case also, the wedging effect caused by isolated small particles in the mixture.

When compared to the wall effect, wedging effect occurs due to incomplete layers of small particles closer to the gaps between large particles. When the large particles are introduced to the mixture, the small particles will again loose the dominancy. When enough amount of larger particles are added, the fine particles would fill up the voids. When the voids are close to be filled small particles will again act as wedges creating voids. With the wedging effect incorporated by adding one more parameter, a 3-parameter model is developed.

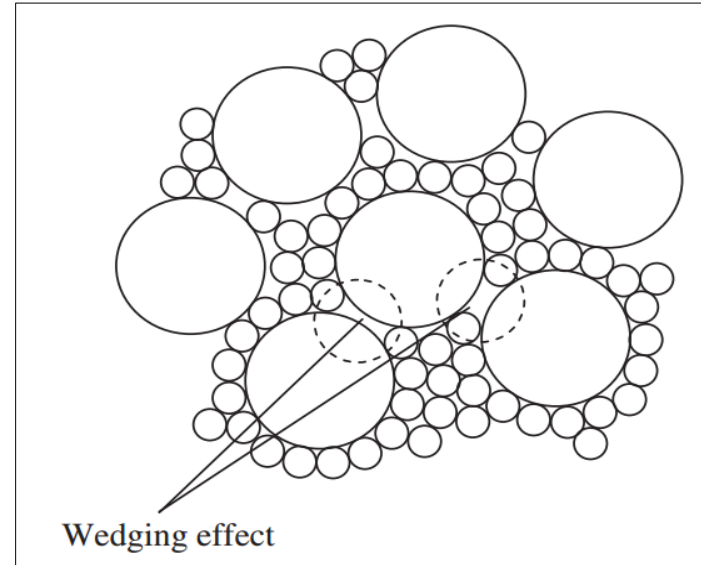
### **2.7.3 3-parameter model**

The 3-parameter model for binary spherical mixtures can be explained using Equation 2.24 and Equation 2.25. Equation 2.24 is to be used when small particles are dominant while Equation 2.25 is to be used when large particles are dominant. However, one can simply use both equations at the same time and final packing density of the mixture will be the minimum value of both equations.





(a) When large particles are dominant



(b) When small particles are dominant

Figure 2.11: Wedging effect

$$\frac{1}{\phi_i^*} = \left( \frac{r_i}{\phi_i} + \frac{r_j}{\phi_j} \right) - (1 - b_{ij})(1 - \phi_j) \frac{r_j}{\phi_j} [1 - c_{ij}(2.6^{r_j} - 1)] \dots\dots\dots \text{Equation 2.24}$$

$$\frac{1}{\phi_j^*} = \left( \frac{r_i}{\phi_i} + \frac{r_j}{\phi_j} \right) - (1 - a_{ij}) \frac{r_i}{\phi_i} [1 - c_{ij}(3.8^{r_i} - 1)] \dots\dots\dots \text{Equation 2.25}$$

Where,

$$a = 1 - (1 - s)^{3.3} - 2.6 \times s \times (1 - s)^{3.6} \dots\dots\dots \text{Equation 2.26}$$

$$b = 1 - (1 - s)^{1.9} - 2.0 \times s \times (1 - s)^{6.0} \dots\dots\dots \text{Equation 2.27}$$

$$c = 0.322 \cdot \tanh(11.9s) \dots\dots\dots \text{Equation 2.28}$$

The parameters a, b and c respectively the loosening effect, wall effect and wedging effect are derived using back calculation of experimental data through curve fitting. Hence, the equations can be modified to incorporate vibration, surface texture and shape factor.

## **2.8 Effect of vibration, shape and surface texture on packing density**

Since most of the packing models are developed based on the assumption of spherical smooth particles under random loose packing, it is necessary to understand the effect of packing parameters such as vibration frequency and particle characteristics such as shape and surface texture on packing density of mixtures. This section presents the literature available on the effect of vibration, shape and surface texture on packing density of particulate mixtures.

### **2.8.1 Effect of vibration on packing density**

Densification of mixtures by means of vibration, known as Vibro-compaction, is widely used in industry. These techniques involve the exertion of energy to the particles at a specific frequency and amplitude for a certain duration. However, for different particulate mixtures, determination of the most suitable parameters (such as vibration frequency and amplitude) to achieve "maximum density" is still an open problem. Many external factors such as friction, particle shape & size, material density, the geometry of container and the initial state before vibration affect the behavior (An, 2013). Hence, the achievement of densest packing has been a complicated problem

and different approaches (i.e.: experimental studies, numerical analysis, computer simulations) have been taken to model the behaviour of particulate systems in different conditions. Prediction of packing density is important in many applications such as concrete optimization, ceramic industry, powder technology, packing technology etc. hence, it is important to know the packing density of a particular mixture to effectively utilize the available resources (Jones et al., 2002).

A number of theoretical, empirical and semi-empirical packing models have been developed to predict the packing density of discrete and continuous particulate mixtures. Most of these models are based on several basic assumptions such as spherical particles, smooth texture, natural packing etc. (Aim & Le Goff, 1968; Andreasen & Andersen, 1930; Fuller and Thompson, 1907; Kwan et al., 2013; Stovall et al., 1986; Toufar et al., 1976). Though the particles used are in different shapes, different textures and the packing is done by either mechanical vibration or tapping (forced packing) in general applications.

Many studies on the effect of vibration on packing densification of particulate mixtures can be found. One of the first studies on this subject was done by McGeary in 1961. In his studies, spherical metal beads were packed in glass containers by mechanical vibration and packing structure and the dynamic procedure of packing were studied. He found out that single size spheres packed in an orthorhombic arrangement with a density 62.5% of theoretical density. He also noticed that to achieve high-density packings, size ratio between sphere sizes should be at least 0.15. Furthermore, he achieved 95.1% of theoretical density from spheres with diameter ratios 1:7:38:316 and volume compositions 6.1:10.2:23.0:60.7%, respectively.

Several major studies on vibration on the packing of mixtures with different shapes of particles were done by Xi-Zhong An. (An, 2013; An & Chai, 2016; An & Li, 2013; An et al. 2016; An et al., 2009; An et al., 2008; Li et al., 2011; Qian et al., 2016; Xie et al., 2017; Yu et al., 2006). An et al. in 2008 performed a numerical study of the packing of uniform spheres under three-dimensional (3D) vibration using the discrete element method (DEM), concentrating on the effects of vibration amplitude and frequency and inter-particle sliding and rolling frictions. It is revealed that the increase

of the vibration amplitude or frequency makes packing density to increase to a maximum value and then decrease. An et al. (2009) studied the packing of single sized spheres on one-dimensional (1D) vibration. The effects of packing conditions (i.e.: vibration amplitude  $A$  and vibration frequency  $\omega$ , feeding method on packing density) have been investigated. The results show that there are optimum values for  $A$  and  $\omega$  to accomplish the maximum packing density. The effects of  $A$  and  $\omega$  cannot be characterized by a single parameter (i.e. vibration intensity  $\Gamma=A\omega^2$ ) but must be considered discretely. An (2013) numerically reproduced two packing mixtures with the maximum packing densities of 0.64 and 0.74 for the amorphous state and crystalline state, in the packing densification of equal spheres subjected to 1D and 3D vibrations using the discrete element method (DEM), and the results were validated using experiments. In the latest study of An et al. (2015 a) packing densification of binary mixtures of spheres and cubes, (large cubes with small spheres and large spheres with small cubes), under 3D vibrations was studied experimentally. The study analyzed the effects of vibration conditions such as vibration time, frequency, amplitude, vibration intensity, the volume fraction of large particles, and container size on the packing densification and the optimal parameters were identified. An et al. (2015 b) also reveals similar results as in An et al. (2015 a) using only spheres.

A plethora of literature on the effect of size ratio on the packing density of a binary particulate mixture has been published. Majority of these studies reveal that lesser the size ratio higher the packing density. Wiącek et al. (2017) studied geometrical parameters of binary mixtures with several particle size ratio and influence of the particle size fractions. In this study, a micromechanics of binary mixtures with the ratio of the diameter of small and large spherical particles and effect of small particles were evaluated using discrete element simulations of confined uniaxial compression (Wiącek et al. , 2017). An et al. (2015) also studied the effect of size ratio on binary spherical mixtures and revealed that the packing density varies monotonically with size ratio where the increase of size ratio decreases the packing density linearly (An et al., 2015). Yu (1997) also studied the effect of size ratio and on the modeling of the packing of fine particles. He concluded that the use of packing size ratio and porosity can be used to derive equations for modeling of packing density (Yu et al. , 1997).

In addition to a large amount of literature dealing with the packing densification of monodisperse spheres and binary sphere mixtures, plenty of studies have been carried out on ternary, quaternary and continuous mixtures (Ayer & Soppet, 1965; Dinger & Funk, 1993; Funk & Dinger, 1994; He et al., 1999; Itoh et al., 1986; Jones et al., 2002; Kwan & Fung, 2009; Liu & Ha, 2002; Nowak et al., 1997; Pirzado et al. , 2016; Roquier, 2017; Scott & Kilgour, 1969; Shi & Zhang, 2006; Sohn & Moreland, 1968; Yu et al., 2006; Zheng et al., 1995). Despite studies on individual effects on packing density, investigations on the combined effect of vibration frequency ( $\omega$ ), size ratio (R) and large particle fraction (X) are lacking. This study investigates the combined effect of aforementioned factors on the packing density and develops a regression model and design graphs to predict the behavior of packing density under vibration frequency ( $\omega$ ), size ratio (R) and large particle fraction (X).

### **2.8.2 Effect of shape on packing density**

Ozol (1978) wrote: “The increasing use of crushed stone for both coarse and fine aggregate, along with perhaps recycled concrete and other recycled materials, forecasts that the effects and significance of shape, texture and surface area will be prominent considerations in the future.”

Characterization and measurement of a shape of irregular aggregate particle is one of the major need in scientific community and industry. Measurement of particle or aggregate shape is an important aspect in concrete technology, materials science and many other industries. For example, if the aggregate shape is known, enhanced concrete mixtures can be produced through accurate predictions of properties of concrete. Green strength, rheological properties, compressive strength, cement content etc. are directly or indirectly affected by the shape of aggregates. There have been many attempts to define particle shape and characterize the shape related properties of particles. Different definitions address different shape properties of particles hence it is important to understand the definitions of particle shape properties first.

There are two general concepts that can be followed to classify numerous definitions of shape characteristics available to define particle shape. First concept is that different scales can be used to measure, define or classify the shape of a particle. Visual

examination of particles will provide a basic set of observations like spherical, rounded, angular, elongated etc. Further examination can reveal whether the surface is rough or smooth, crushed or uncrushed, have sharp edges or not etc. This concept does not particularly quantify the shape characteristics and subjected to the examiners' decision making and expertise. Hence it is not widely accepted in scientific community.

The second concept is that the particle can be defined by various terms which gives a quantified value of a certain parameter of a particle. For example, area of an arbitrary projection of a particle, ratio of volume of a particle to surface area etc. Barrett (1980) proposed that the shape of a particle can be defined by form (overall shape), roundness (large scale smoothness) and surface texture (fine scale smoothness). These three definition methodologies are geometrically independent and might have some correlation when related to a process which involves some application. The following sections will describe the parameters that define shape under these three categories. As explained earlier definitions of shape are more qualitative and recent definitions have provided a quantitative approach to measure the shape of a particle. One of the early definitions of aggregate particle shape, a qualitative approach founded on visual observations, is shown in Figure 2.12 (a) and Figure 2.12 (b).

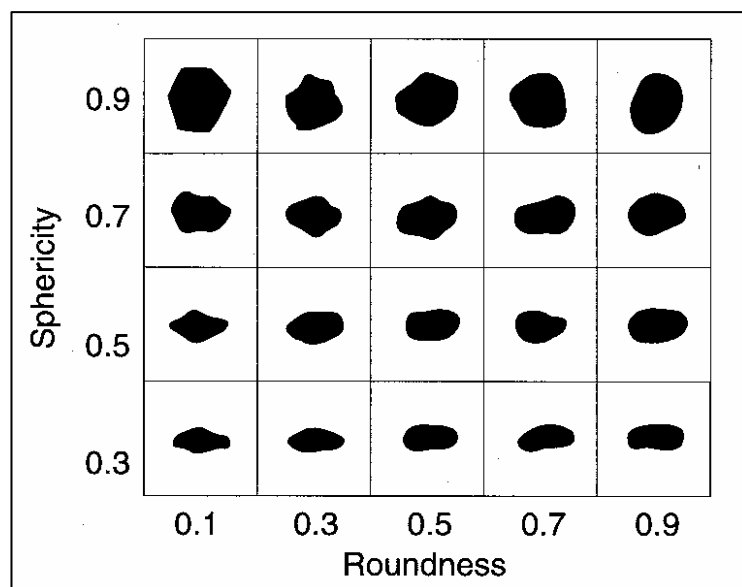


Figure 2.12 (a)

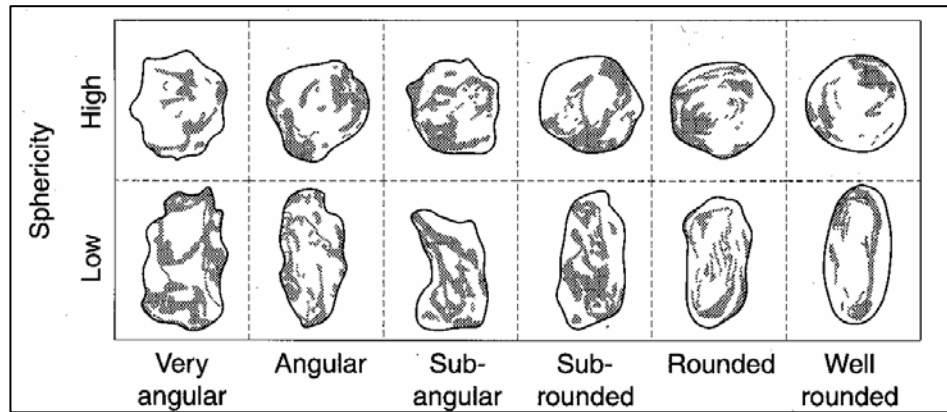


Figure 2.12 (b)

Figure 2.12: Visual assessment of particle shape (a) Derived from Measurements of sphericity and roundness, (b) Based upon visual observations

These are basic definitions that is defined in early stages. Hence, it does not characterize the fine surface features and three-dimensional shape features. The terms such as sphericity and roundness given in these definitions are not further defined and it will roughly provide an idea about the particle shape. Also, angularity is used to measure the macro surface characteristics, yet a fine definition is hard to find. The following are several shape parameters/indices often cited in the literature: sphericity, roundness, angularity, shape factor, fullness ratio, flatness (flakiness) ratio, elongation ratio, convexity ratio etc. Such terms are presented in the subsequent sections.

### 2.8.2.1 Shape of a particle

It is well known that the shape of particles can affect many properties of particulate mixtures such as packing density, porosity, rheology etc. Shape of particles used in a mixture has a significant effect on packing density. The characteristics of packing density with various shapes has been studied over the past decade by many researchers. Irregular shapes create more voids in between particles leading to low packing density mixtures. On the other hand, symmetrical particles such as cubes, spheres make dense mixtures with lesser voids. Hence, the shape is a critical factor that needs to be considered when developing a theoretical model to predict packing density.

The characterization of particle shape has been studied and various methods have been proposed to measure the shape of a particle in the past century. These methods can be

either simple approximations by visual observation or can be complex methods using advance mathematics or digital image processing techniques. Even though the advancement in this subject area is significant, there are uncertainties and drawbacks to all methods. The most common drawback is that many of these methods are using two-dimensional approach. Hence, the true three-dimensional shape will not be explained by these methods.

Another main drawback is that many of these methods may render one or many values due to complex shape characteristics and undefined measuring method. One may measure the length connecting the longest edges and one may measure the length at a mid-point. Likewise, the measurement of shape characteristics can be highly subjective. Following section explains some commonly used shape parameters and approaches with their equations.

### **Sphericity**

Sphericity is a measure of the shape or form of the particle and it is also called form factor (Rao & Tutumluer, 2000). Sphericity varies with ratio of surface area of the particle to its volume, the relative dimensions of its principal axes or those of the confining rectangular prism (Mather, 1966). This definition is very broad and vague. Another good definition is stated by Ozol in 1978. According Ozol (1978) sphericity is a measure of how closely equal the three axes or dimensions of a particle are, based on the ratio of the volume of particle to the volume of sphere whose diameter is the maximum dimension of the particle (Ozol, 1978). The sphericity of a sphere is 1.0 and the cube is 0.37. Sphericity value will provide a good understanding about the particle shape since it is a measure of how close a shape of a particle to a perfect sphere. Sphericity is a precise example of a compactness measure of a shape.

Wadell (1932) defined sphericity as the ratio of surface area of a hypothetical sphere (s) of the same volume as a particle to the actual surface area of the particle (S) as given in Equation 2.29 (Wadell, 1932).

$$\text{Sphericity} = \frac{s}{S} \quad \dots\dots\dots \text{Equation 2.29}$$

From Wadell's equation, the sphericity value of a sphere is 1 and cube is 0.806.



Measurement of surface area of an irregular particle is a tedious process. Hence, a more practical definition for sphericity is:

$$S(\emptyset) = \frac{D_n}{D_{cs}} \quad \dots\dots\dots \text{Equation 2.30}$$

Where;

$D_n$  : Diameter of the sphere of the same volume as the particle (nominal diameter)

$D_{cs}$  : Diameter of the circumscribing sphere (Wadell, 1932).

This relationship was derived mathematically and presented in equation 2.31.

$$S(\emptyset) = \left(\frac{V_p}{V_{cs}}\right)^{\frac{1}{3}} = \frac{\left(\frac{\pi}{6}D_n\right)^{\frac{1}{3}}}{\left(\frac{\pi}{6}D_{cs}\right)^{\frac{1}{3}}} = \frac{D_n}{D_{cs}} \quad \dots\dots\dots \text{Equation 2.31}$$

Where;

$V_p$  : Volume of the particle

$V_{cs}$  : Volume of the circumscribing sphere

Krumbein (1941) used the multiplication of the principal dimensions of a circumscribing triaxial ellipsoid of the particle to estimate and define sphericity as in Equation 2.32.

$$S(\emptyset) = \frac{\left(\frac{\pi LWT}{6}\right)^{\frac{1}{3}}}{\left(\frac{\pi L^3}{6}\right)^{\frac{1}{3}}} = \left(\frac{WT}{L^2}\right)^{\frac{1}{3}} \quad \dots\dots\dots \text{Equation 2.32}$$

$$\text{Sphericity} = \sqrt[3]{\frac{\text{Thickness} \times \text{Breadth}}{\text{Length}^2}} \quad \dots\dots\dots \text{Equation 2.33}$$

(Krumbein, 1941)

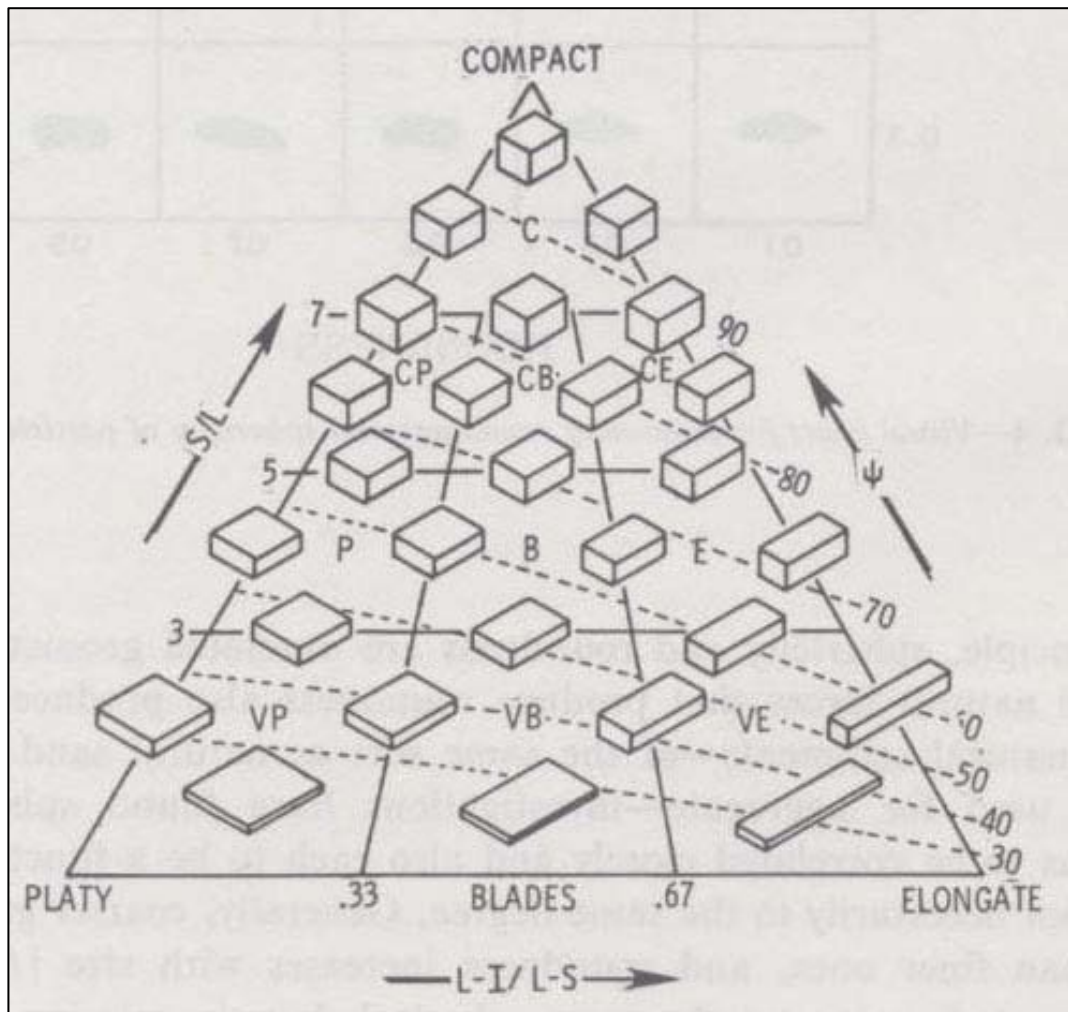


Figure 2.13: Form triangle of Sneed and Folk (1958)

L – Longest dimension (Length), I – Intermediate dimension (Thickness), S – Shortest dimension (Width)

Sneed and Folk (1958) developed a triangular diagram to plot Thickness / Length versus (Length-Width) / (Length-Thickness), making an outline for the joint specification of form and sphericity. Figure 2.13 shows this diagram (The symbolization I is used for width, and S is used for thickness, in Figure 2.13). Each block in the diagram is having equal volume. The independence of form and sphericity can be shown by following an iso-sphericity contour from the left to the right (Sneed & Folk, 1958).

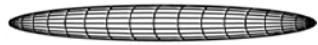

## Shape factor

According to Aschenbrenner (1956), the shape factor is defined by Equation 2.34:

$$F = \frac{(W/L)}{(T/W)} = \frac{LT}{W^2} \quad \dots\dots\dots \text{Equation 2.34}$$

$$\text{Shape factor} = \frac{\text{Thickness} \times \text{Length}}{\text{Breadth}^2} \quad \dots\dots\dots \text{Equation 2.35}$$

Table 2.2: Shape factor variation with particle shape

Shape factor (F)	Particle shape	
F > 1	Prolate (rod-like)	
F < 1	Oblate (disk-like)	

As explained in Table 2.2, for prolate particles thickness and breadth are similar and shape factor becomes greater than 1. For oblate particles the length and breadth are similar and shape factor becomes less than 1. This supplementary knowledge allows the particle geometry to be specified by Wadell sphericity and Aschenbrenner shape factor, as seen in Figure 2.14.

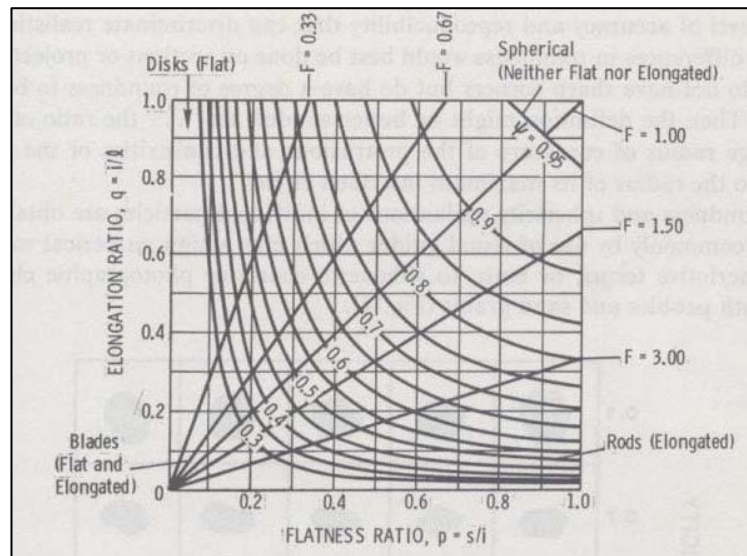


Figure 2.14: Particle Shape as defined by Wadell sphericity ( $\psi$ ) and Aschenbrenner shape factor (F) (Ozol, 1978)

Two other parameters proposed to define particle shape are elongation and flakiness. Elongation relates the longest dimension of the particle to the intermediate dimension while flakiness relates the intermediate dimension to the shortest dimension. These terms are clarified in Equation 2.36 and Equation 2.37, where L, W and T represent the longest, intermediate and shortest dimension of a particle.

**Flakiness ratio**

The flakiness ratio is expressed as the ratio between thickness and breadth. It is also known as flatness ratio. The value explains how flaky a particle is and can be used to get a reasonable idea of the particle. But since only two dimensions are taken in to account it does not help to get a three-dimensional idea of the particle.

Flakiness ratio =  $W/T$  ..... Equation 2.36

**Elongation ratio**

The elongation ratio is calculated by the ratio between breadth and length. Elongation ratio also provides a reasonable idea about how elongated the particle is and as flakiness ratio it also does not provide a three-dimensional view on the particle. However, both flakiness ratio and elongation ratio together can be used to get a good understanding about the shape of a particle.

Elongation ratio =  $L/W$  ..... Equation 2.37

Some scientists have used the opposite of Equations 2.36 and 2.37 as elongation and flakiness parameters. Different specifications use different values to specify elongated and flaky particles and a value of 3 or 5 is used commonly.

When an aggregate material is considered, the shape can be different for different size fractions. When the reduction ratio of crushing increases, the particle shape becomes flat and elongated. For gyratory, jaw or cone crusher machines this effect is larger and for impact type machines this effect is lesser. Impact type machines produce more cubicle or equidimensional particles. The speed of the crusher also influences particle shape (Ozol, 1978).

## Roundness

Roundness measures how rounded the particle is. Roundness is independent of sphericity and form and is the opposite of angularity. As cited by Powers (1953), Pettijohn (1949) defined roundness as the ratio of the mean radius of curvature of edges and corners of the particle to the radius of the maximum inscribed circle (Powers, 1953).

Roundness is divided in to two parts. First part is the corner roundness and the second part is the particle outline roundness. Corner roundness is the opposite of sharpness of corners which is an important factor in abrasion and particle outline roundness is the overall roundness of the particle which is measured using convexity. Overall roundness is important in packing density when determining the ability of interlocking of particles.

The roundness has also been defined as the level to which the contour of a particle fits the curvature of the largest sphere that can be contained within the particle (Ozol, 1978).

According to Wadell (1932), roundness is the mean radius of curvature of all the corners divided by the radius of the largest inscribed circle:

$$Roundness = \sum \frac{(r_i/R)}{N} \dots\dots\dots Equation 2.38$$

Where,

$r_i$  is the radius of curvature of corner  $i$

$R$  is the radius of the largest inscribed circle

$N$  is the number of corners

From the above equation it can be derived that both a sphere and a cylinder capped with two hemispheres have a roundness of 1.0. shapes with sharp corners of  $90^\circ$  such as cubes have a roundness of 0.843

Typically, both roundness and sphericity are determined using visual guides (Figure 2.13). Sphericity and roundness are inter connected but not to the same degree. A small increase in sphericity may incur a huge variation in roundness.

**Angularity**

Angularity measures the sharpness of corners and edges and this is exactly the opposite measurement of roundness. Angular particles may affect the packing density of mixtures. As described in roundness section, angularity can be identified by two aspects. First being the sharpness of edges and the second being the angularity of total particle which is measure by convexity of a particle (Mora & Kwan, 2000).

**Convexity ratio**

Convexity ratio measures the convexity of the particle. the convexity ratio is measured from the two-dimensional projection of the particle because of the difficulty of measuring shape parameters in three dimensions, it is defined as:

$$Convexity\ ratio = \frac{Area}{Convex\ area} \dots\dots\dots Equation\ 2.39$$

where the convex area is the area of the minimum convex boundary circumscribing the particle. Figure 2.15 explains the convexity.

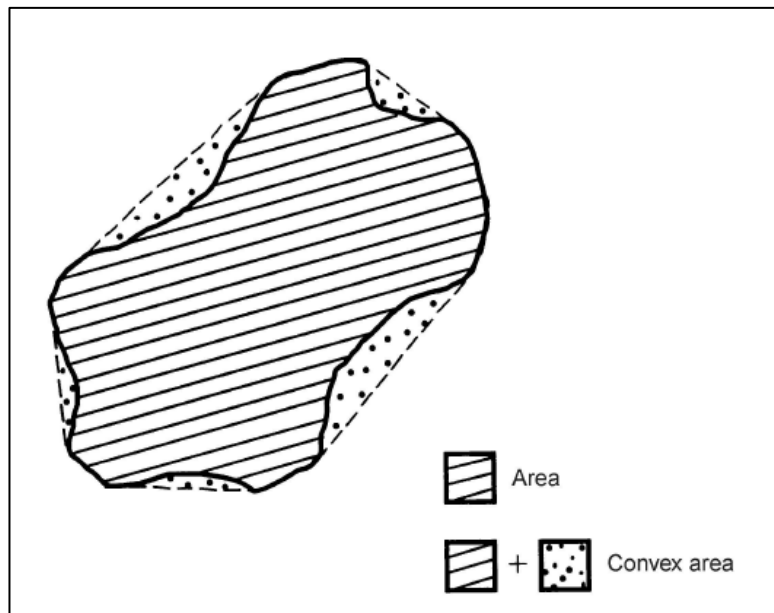


Figure 2.15: Convexity of a particle

### **Fullness ratio**

Fullness ratio is another measure of convexity. It is also estimated from the two-dimensional projection of the particle. It is defined by Equation 2.40;

$$Fullness\ ratio = \sqrt{\frac{Area}{Convex\ area}} \dots\dots\dots Equation\ 2.40$$

Both convexity ratio and fullness ratio are measures of concavity and are indirectly linked to roundness and angularity (Mora & Kwan, 2000).

### **2.8.3 Effect of surface texture on packing density**

Surface texture is another major factor that affects the packing density of a particulate mixture. Smooth particles tend to move quickly and rearrange in a more stable arrangement to improve the packing density of the mixture. Rough particles generate interparticle friction and hinder the ability to move freely. Hence, the rough particles take lot of energy and time to rearrange its structure to a high dense packing. Hence, the packing density of rough particles are usually lower than that of small particles. The effect of surface texture on packing density is investigated to account the surface texture effects into the model. Even though there are many research on effect of shape on packing density, there are only handful of research on effect of surface texture on packing density.

Alexander and Mindess (2005) have stated that the packing density of a mixture is affected by surface texture of an aggregate and packing models should account the surface texture. Mangulkar and Jamkar (2013) have reviewed the use of packing models in concrete mix proportioning. They have stated that the particles with improved surface texture provides better results in properties of concrete. Further, they have mentioned that the reason for such improvements is the effect of surface texture in packing density.

Lamond and Pielert (2006) has emphasized that aggregate surface texture has a direct influence on the porosity of a mixture. Figure 2.16 shows how surface texture is related to porosity.

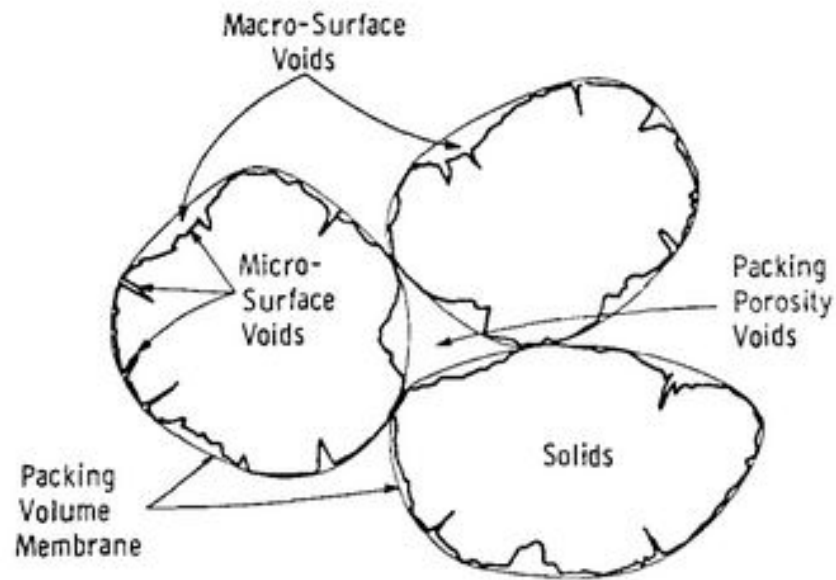


Figure 2.16: Particle packing volume and macro-surface voids and micro-surface voids enclosed by packing volume membrane (Lamond & Pielert, 2006)

Apart from above mentioned researches, there are many researches that indirectly indicate the effect of surface texture on particle packing and performances. Janoo (1998) has mentioned in a special report prepared for US army corps of engineers together with Vermont agency of transportation that the aggregate surface texture and shape has a direct effect on properties of base materials due to packing of particles (Janoo, 1998).

Little et al. (2003) have stated that the voids in a compacted mass of rough-textured aggregate usually are higher. Further, the rough textured particles hinder the workability and mobility of particles due to surface texture.

Erdoğan and Fowler (2005) have studied on effect of aggregate shape and texture on rheological properties of concrete. In their study they have coated smooth glass spheres to gain different surface textures. The study reveals the packing of mixtures are greatly affected by the surface texture and shape of particles.



### 2.8.3.1 Measurement of surface texture

Surface texture measures the unevenness or waviness of particle surface. It can also be identified as a microlevel measurement of surface roughness and texture is totally independent from roundness and form. Mora and Kwan (2000) stated that surface texture can be measured in terms of the magnitude and sharpness of the protrusions and indentations on the particle boundary.

A surface texture comprises of two independent geometric properties;

- 1) The level of surface relief, also called roughness or rugosity,
- 2) The surface area per unit of dimensional or projected area. This property, even though it is the ratio of areas, it has been defined as the roughness factor (Wenzel, 1949):

$$R = \frac{A}{a} \quad \dots\dots\dots \text{Equation 2.41}$$

Where;

A - True/real surface area and

a - Apparent/projected surface area

Apart from quantitative evaluation of roughness, the forms of roughness are of importance. The comparative importance of undulatory (smooth, wavelike) and abrupt rugosity was measured by Blanks (1949). According to Blanks (1949) the surface texture depends on hardness, grain size, pore structure and texture of the particle and the amount of external factors such as forces and weathering have been affected on the surface. Hard, dense, fine-grained material will generally have smooth surfaces.

The surface texture of a particle influences the properties of the material. Surface texture is defined as the degree of fineness and uniformity (Terzaghi & Peck, 1967). Terzaghi and Peck (1967) proposed qualitative terminologies such as smooth, sharp, gritty, etc., to define the texture. A roughness scale was used by Barskale and Itani (1989) to measure the surface texture of aggregates. The roughness of the surface was measured using visual examination and an index of 0 to 1000 was used to define

roughness. 0 of the index for glassy smooth particles and 1000 was used to measure very rough particles.

Bikerman (1966) suggested a method involving coating of asphalt on a flat sawed aggregate surface and then scraped to the surface of the aggregate. The asphalt left on the surface will be used as an indicator of the surface texture. This technique evaluates the micro-texture of the surface and is an index to the roughness of the surface.

Wright (1955) proposed a method to evaluate the surface texture of aggregate particles by means of 19mm particles. The aggregate will be submerged in a synthetic resin and after hardening the resin, the aggregate is cut into thin parts of approximately 2.5 x 10~2 mm thick. This thin section is magnified 125 times by a microscope and the unevenness of the surface is traced. The length of the trace is measured and compared with an uneven line drawn as a series of chords as shown in Figure 2.17. The difference between these two lines is defined as the roughness factor.

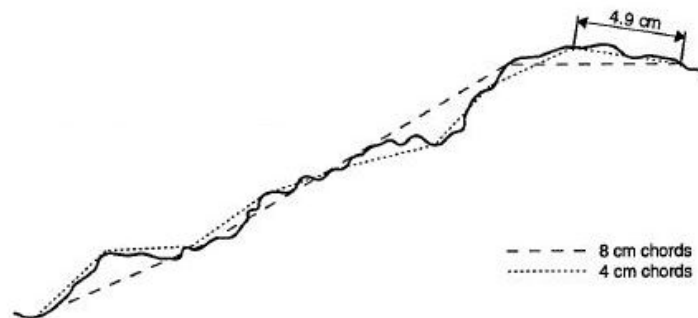


Figure 2.17: Measurement method for characterizing the surface texture of an aggregate (Wright, 1955).

### 2.8.3.2 Determination of surface characteristics using image analysis

Measurement of surface texture of particles is a challenging problem. Many researches have been carried out to develop reasonable methods to quantify the surface texture of particles. Most of these methods involve image processing techniques. Methods explained in previous sections are tedious and time consuming. Hence, digital image processing technologies based on computers have been developed for analyzing purposes of particle surface and shape characteristics such as shape, angularity and

roughness. Wilson et al., (1997) studied the feasibility of this technology for federal highway administration (FHWA) and the tests were carried out on fine sands both manufactured and natural. The results revealed that the technology was feasible for measurement of shape and angularity of particles. They also developed indices to measure roundness and angularity of particles. Their method captures images of the aggregates to be measured using a high-resolution camera and a computer application is used to analyze the images, distinguish and trace the boundaries of aggregates. These traces are further analyzed, and surface characteristics are measured using an algorithm in the application.

It is evident from the previous sections that the determination of particle surface texture is a time consuming and tedious task. Different approaches have been taken by engineers and scientists to deduce these features from the mass properties of the particles. British pendulum number is one such method that can be easily utilized to determine the surface texture characteristics of particles.

### **2.8.3.3 British pendulum number**

British pendulum number (BPN) can also be used to measure the surface texture. British pendulum test was originally developed to determine the skid resistance of surfaces. However, several studies have revealed that there is a significant correlation between BPN and surface texture.

Liu et al. (2004) however found that BPN depends on both surface micro texture and macrotecture. Corley-Lay (1998) also found that the variation of BPN from section to section resembles the variation of SN. Goodman (2009) also found a good correlation between texture depth and BPN using the data collected from several asphalt mix gyratory samples. Further Ahmed and Susan confirmed that fairly good correlations were found among the British Pendulum number (BPN), ribbed tire skid number (SN) and mean texture depth (MTD) rejecting the hypothesis that BPN is a measure of only surface micro-texture and ribbed tire skid number is insensitive to surface texture (Ahammed & Tighe, 2011).

## **2.9 Summary of findings**

Particle optimization is important in materials science and related industries. For example, optimization of concrete aggregates can produce high quality concrete, ecological concrete, high performance concrete, permeable concrete, light weight concrete etc. Hence, the optimization has immense advantages in not only in concrete industry, but also in many industries which involve packing of different particles. When the concrete industry is considered it was revealed that the packing has a great influence on properties of concrete such as water demand and cement particle spacing, flowability etc. Thus, determination of packing density is very important and plenty of models have been developed to predict the packing density of particle mixtures. However, most of these models are based on many assumptions hence applicability of such models in realistic complex applications such as concrete is still questionable. Most of these models do not incorporate vibration, shape and surface texture of particles to predict the packing density. However, literature revealed that each parameter influences the packing density greatly and needs to be accounted when calculating packing density of particulate mixtures. According to literature and experimental studies it was revealed that 3-parameter model can be effectively modified incorporating vibration, shape and surface texture. However, measurement of vibration, shape and surface texture are challenges faced by scientists and most suitable methods were adopted for the study based on accuracy and easiness of reproduction.

## CHAPTER 3

### 3 METHODOLOGY

#### 3.1 Introduction

Measurement of packing density in a particulate mixture is a tedious process. The packing density is the ratio between the solid volume and total volume of the mixture. Hence, the measurement of packing density involves the measurement of solid volume of particles and the measurement of total volume occupied by the particles. This chapter explains how the experimental work were carried out to determine the variation of packing density with respect to various vibration frequencies, various shape factors and various surface textures.

#### 3.2 Measurement of solid volume of particles ( $V_s$ )

The measurement of solid volume ( $V_s$ ) is straightforward for spherical particles. The volume of a sphere and number of spheres in the mixture is known. Hence, the total volume can be calculated by the Equation 3.1.

$$V_s = V_1N_1 + V_2N_2 \dots\dots\dots\text{Equation 3.1}$$

Where,

- $V_s$  - Total solid volume of the mix
- $V_1$  - Volume of sphere (Size class 1)
- $V_2$  - Volume of sphere (Size class 2)
- $N_1$  - Number of size class 1 spheres in the mix
- $N_2$  - Number of size class 2 spheres in the mix

However, the measurement of total solid volume of the mixture gets complicated when irregular particles are present. In this situation, the solid volume is measured using the Equation 3.2.

$$V_s = \frac{W_1}{\gamma_1} + \frac{W_2}{\gamma_2} \dots\dots\dots\text{Equation 3.2}$$

Where,

- $W_1$  - Weight of particles of size class 1
- $W_2$  - Weight of particles of size class 2
- $\gamma_1$  - Average specific gravity/density of size class 1 particles
- $\gamma_2$  - Average specific gravity/density of size class 2 particles

### 3.3 Measurement of total volume of the mixture ( $V_T$ )

Total volume (bulk volume) of the mixture was calculated by measuring the height of the mixture after achieving the maximum packing as shown in Figure 3.1. A Vernier caliper was used to measure the h value. Four different readings from four different locations were measured and average was taken as the h.

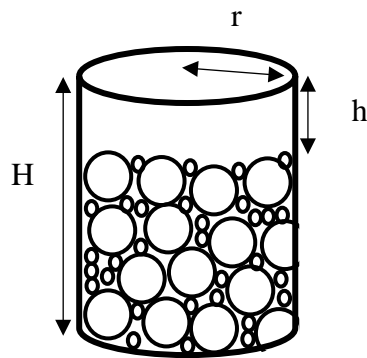


Figure 3.1: Measurement of total volume

$$V_T = \pi r^2(H - h) \dots \dots \dots \text{Equation 3.3}$$

Where,

- $V_T$  - Total volume
- $r$  - Inner radius of the container
- $H$  - Total height of the container
- $h$  - Height from the top of the mixture to top of the container

### 3.4 Application of vibration frequency

Two different sizes of particles were taken for the study at a time and mixture was prepared in volume proportions to measure the packing density. A plunger was placed on top of the mixture to apply vertical confinement. Dial gauge was placed to measure the displacement of plunger and vibration was applied until the dial gauge reading shows a maximum value (Maximum packing state). Figure 3.2 shows the schematic diagram of apparatus.

The experiment was repeated with various vibration frequencies (50 Rad/s – 150 Rad/s), various size ratios (diameter ratio between two particle sizes) ranging from 0.1 to 0.9 and various large particle volume proportions ranging from 0 to 1 to determine the effect of vibration frequency, size ratio and large particle volume fraction on the packing density. Shape factor and surface texture were held constant as shown in Table 3.1.

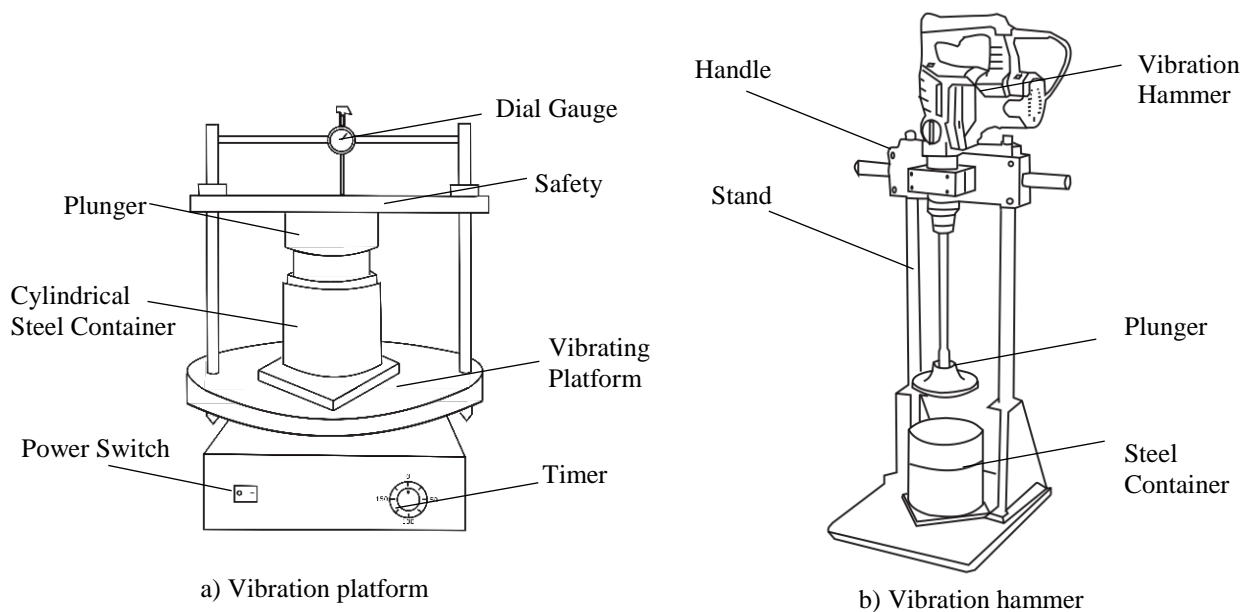


Figure 3.2: Schematic diagram of experimental setup

The vibration was applied to the particle mixture by means of a vibration table and a vibrating hammer. Vibration table was used to apply vibration to the bed of particles while vibration hammer was used to apply vibration to the top of mixture. The effect of both methods on packing density was measured and packing density results showed that there is no significant effect on applying vibration to bed or to the top. Table 3.1 presents the variables of the study and number of samples obtained from the experiment to analyze the effect. The shape (spherical – shape factor of 1) and surface texture (glass 12 BPN) were held constant to determine the effect of vibration. (Refer Appendix A)

Table 3.1: Vibration analysis data

<b>Vibration (Rad/s)</b>	<b>Number of samples to be used for the model development</b>	<b>Number of samples to be used for the model validation</b>
50	60	60
75	60	60
100	60	60
125	60	60
150	60	60

### **3.5 Measurement of shape factor**

Even though there are many parameters to measure the shape, according to Kwan and Mora (2001), Shape factor and convexity ratio parameters affect the packing density of particulate mixtures mostly. Convexity ratio is difficult to measure without a proper digital image processing apparatus. However, shape factor can be simply measured using a Vernier caliper. Hence, for this study shape factor is used as the shape parameter to develop the model (Refer Equation 2.35).



Aggregates passing the 25mm sieve and retaining the 19mm sieve were taken for the study. Vernier caliper was used for the measurement of dimensions. Since aggregates are in irregular shapes measurement was carried out in following order. First the longest dimension was selected as the length. Secondly, the shortest dimension perpendicular to length was measured as the thickness and finally, the remaining dimension perpendicular to both length and thickness was selected as breadth. The shape factor of particles was measured manually and categorized in to 5 groups. Figure 3.3 shows the dimensions of a particle and Figure 3.4 (a), (b), (c), (d) and (e) show the selected aggregates with shape factors of 0.15,0.3,0.45,0.75 and 0.9 respectively. The vibration frequency was kept at 110 Rad/s and surface texture of 25 BPN was used and kept constant for the experiment. Table 3.2 presents the constants and variables of the study and number of data obtained from the experiment to analyze the effect. (Refer Appendix B)

Table 3.2: Shape analysis data

<b>Shape factor</b>	<b>Number of samples to be used for the model development</b>	<b>Number of samples to be used for the model validation</b>
0.15	60	60
0.30	60	60
0.45	60	60
0.75	60	60
0.90	60	60

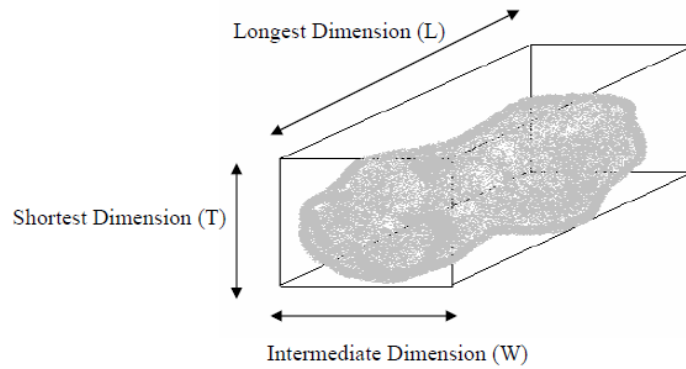


Figure 3.3: Dimensions of a particle



(a) 0.15

(b) 0.3

(c) 0.45

(d) 0.75

(e) 0.9

Figure 3.4: Selected aggregates for the experiment (a) Shape factor 0.15 (b) Shape factor 0.3 (c) Shape factor 0.45 (d) Shape factor 0.75 (e) Shape factor 0.9

### 3.6 Measurement of surface texture of particles using British pendulum test

Digital imaging techniques are complicated and difficult to execute in common laboratories. The objective of this study is to develop a theoretical packing model that can be used to determine the packing density of different mixtures with different shapes and textures, it is important to keep the tests involved with the model to be simple and easy to execute. Therefore, BPN method was selected to measure the aggregate surface texture. The relationship is developed with BPN value and packing density. Even though BPN is a measure of skid resistivity, it is also a measure of surface texture indirectly. The spherical glass beads were coated with different sizes of dust powders to achieve different surface textures.

The BPN value for different surfaces were measured using British pendulum test (Figure 3.5) (ASTM E303-93(2013)). Samples were prepared as shown in Figure 3.6 to measure the texture using British pendulum tester. 8 different surface textures were prepared for the study. Glass surface had a BPN of 12 while roughest surface had a BPN of 45. Rest of the textures were in between BPN 12 and 45 where real aggregates had a BPN value of 25. The coated spherical beads (constant shape factor 1) as shown in Figure 3.7 were then used for the determination of packing density under constant vibration frequency (110 Rad/s). Binary mixtures were prepared with different large particle proportions. Table 3.3 presents the constants and variables of the study and number of data obtained from the experiment to analyze the effect. (Refer Appendix C)

Table 3.3: Surface texture analysis data

<b>Surface texture (BPN)</b>	<b>Number of samples to be used for the model development</b>	<b>Number of samples to be used for the model validation</b>
12	40	40
14	40	40
18	40	40
25	40	40
33	40	40
35	40	40
39	40	40
45	40	40

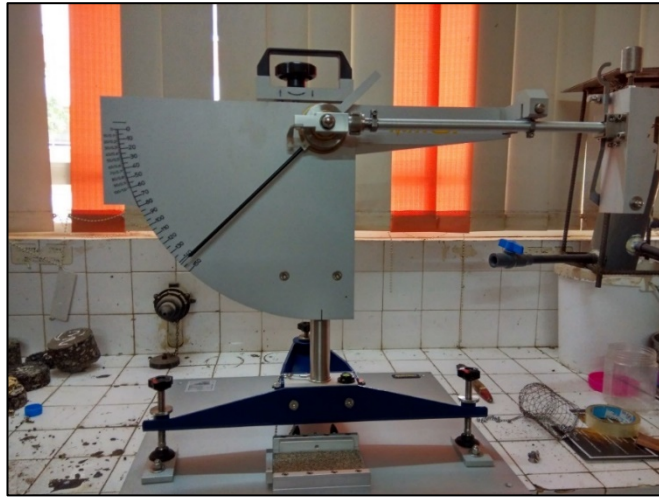


Figure 3.5: British pendulum test apparatus



Figure 3.6: Samples prepared for different surface textures



Figure 3.7: The coated spherical beads

## CHAPTER 4

### 4 VALIDITY OF PACKING MODELS

#### 4.1 Introduction

Optimization of packing of aggregate is the process of determining the most suitable aggregate particle sizes and distribution to minimize the voids content of an aggregate mix. An optimized aggregate mix will have lesser voids which needs to be filled with cement paste resulting low cement, high quality concrete (Richardson, 2005). Optimization of aggregates to achieve higher strengths with lower cement content has been studied for various applications over the past decade (Ley et al., 2012). Though those studies were successful for more generalized applications, there were limitations when applying the results for specialized applications such as zero slump concrete, precast concrete, roller compacted concrete, self-compacting concrete, high performance concrete etc. (Chun et al., 2007). The main reason for such limitations in generalized approach is the variation of the required properties of concrete in each application. (Mangulkar & Jamkar, 2013)

Interlocking concrete block pavers (ICBP) are one of the main pavement materials which needs vibration and compression in the packing of aggregates in concrete mixture. According to Ishai (2003) the absolute values of construction plus the maintenance cost of ICBP are always equal or less than that of flexible pavements and rigid pavement. Hence, ICBP is popular in many parts of the world. Concrete mixes used in ICBP industry seem to be far less economical and highly unsustainable. The manufacturers use high amount of cement to achieve higher strengths. There are high variations in strength within the same batch of blocks. Various issues such as non-availability of proper guidelines, volume batching methods, water/cement (W/C) ratio issues etc. can be the reasons for such variations.

The objective of this study is to determine the validity of aggregate packing models in mixture design of interlocking concrete block pavers and improve the concrete mixture design method by adopting aggregate packing concepts.

## 4.2 ICBP Manufacturing process and characteristics

Hydraulic molding machines use vibration and compression, commonly known as vibro-compression to cast the blocks. Semi dry concrete mix allows to remove the mold from the fresh block soon after casting which facilitates efficient production. Hence higher green strength is required to produce quality blocks. Typically, quarry dust, natural sand, 10 mm to 12 mm coarse aggregate, cement and pigments are used for the concrete mixture. Figure 4.1 shows the hydraulic block making process in a local factory.

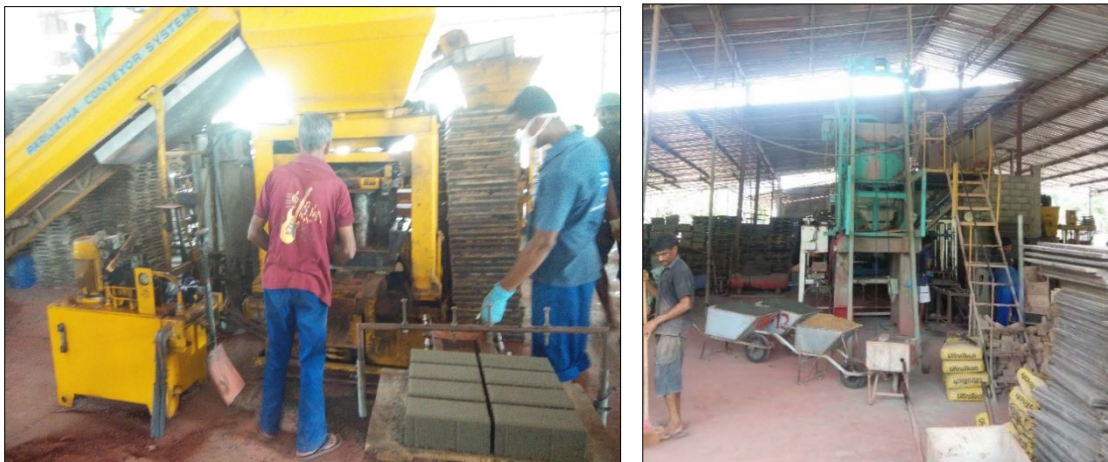


Figure 4.1: Hydraulic machine used in industry

Water/cement (W/C) ratio may vary from 0.3 to 0.4 depending on the required degree of surface texture. Water content should be optimum to produce a quality block since high amount of water may produce a slumpy block and low water content may produce a dry block which will crack soon after de-molding. A field survey was carried out to understand the industrial ICBP manufacturing procedure. Figure 4.2 shows the 0.45 power curve for aggregate gradation used for various grades of concrete used by the selected manufacturer with standard limits proposed by South African (SA) standards (SANS1058, 2012). 0.45 power maximum density line provides a guide to blend aggregates to get the maximum density. Similarly, the Indian standard (IS15658, 2006) proposes a coarse aggregate to fine aggregate mix of 60:40 for ICBP manufacturing. As shown in Figure 4.2, the South African standard specified limits are also closer to the maximum density line. It is evident that the industrial aggregate mix is not within

the minimum and maximum lines specified by SA standards (SANS1058, 2012) as well as distant to the maximum density line. The high percentage (35% to 45%) passing the 0.075mm sieve is also a major concern. These mixes may have high amount of voids (40%) which will eventually result in either low strength or high cement paste consumption.

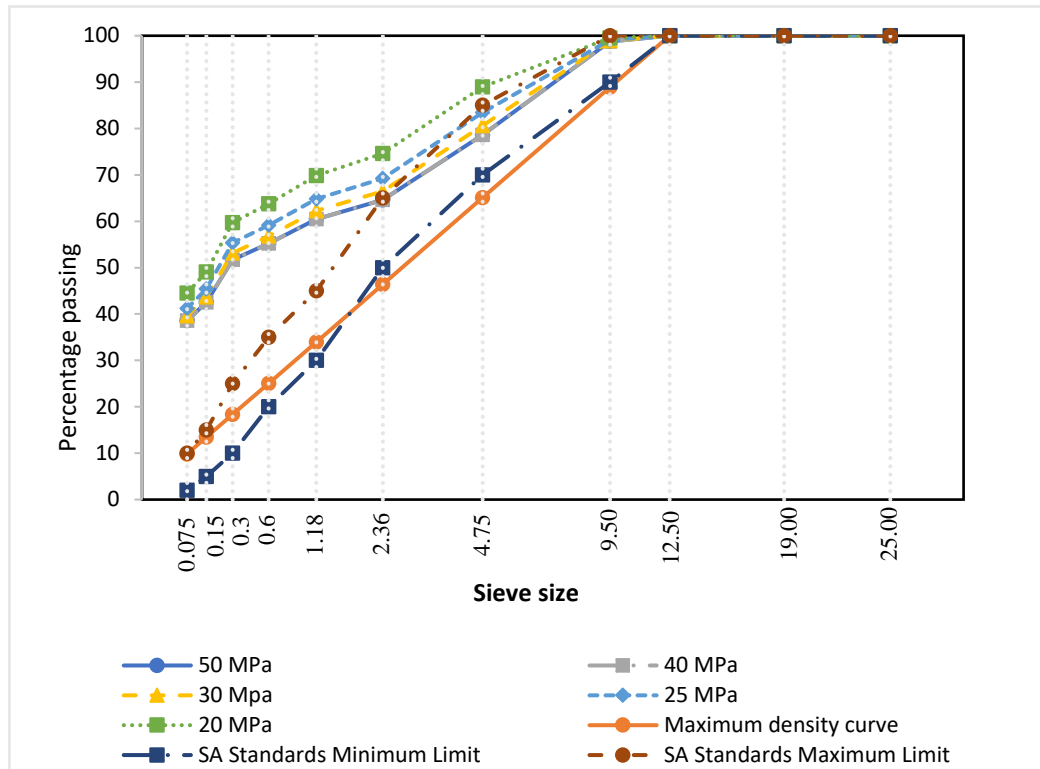


Figure 4.2: 0.45 Power curve and aggregate size distribution at an industrial block manufacturer

### 4.3 Determination of mix design characteristics

Considering the concrete mix requirements particle packing optimization was found to be the most suitable mix design methodology to follow. 12 mm coarse aggregates, manufactured sand and natural sand were used as aggregates for the mix. According to Indian standard for precast concrete blocks for paving IS 15658 (2006) the nominal maximum aggregate size is limited to 12 mm considering the block size. Since the vibration and compaction plays a major role in aggregate packing density, it is essential to select the optimum vibration time and compression stress. Figure 4.3 and Figure 4.4



show the variation of packing density with respect to vibration time and compression respectively.

The saturated solid density and oven-dried solid density of the aggregate were determined in accordance with BS EN 1097-3:1998 as  $2589 \text{ kg/m}^3$  and  $2560 \text{ kg/m}^3$  respectively. Moisture content was measured to determine the air dried solid density of the aggregate and it was  $2572 \text{ kg/m}^3$ . Then the solid volume of the aggregate in the container was calculated as the average weight of the aggregate in the container divided by the air-dried solid density of  $2572 \text{ kg/m}^3$ .

#### 4.3.1 Optimum Compression and Vibration

The optimum vibration period was selected as 6 seconds as shown in Figure 4.3 and the optimum compaction was selected as 1.8 MPa as shown in Figure 4.4. The results were used for the selection of aggregate proportions.

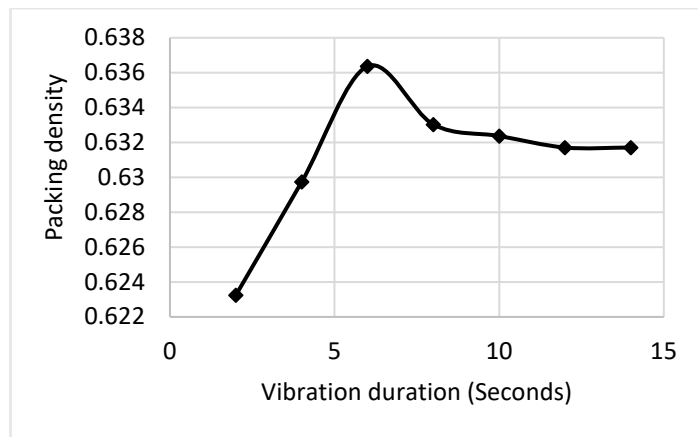


Figure 4.3: Packing density vs. Vibration

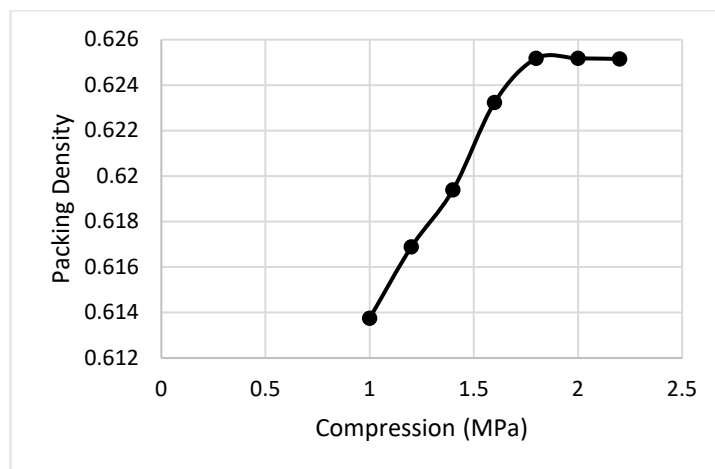


Figure 4.4: Packing density vs. Compression



### 4.3.2 Coarse aggregate to fine aggregate ratio

Aggregates were mixed in proportions by volume and selected vibration (6 seconds) and compression (1.8 MPa) was applied and the packing density of each mixture was determined. 10 mm coarse aggregates, 2.36 mm downsize fine aggregate were selected for the study. Figure 4.5 shows the variation of packing density with respect to aggregate proportions.

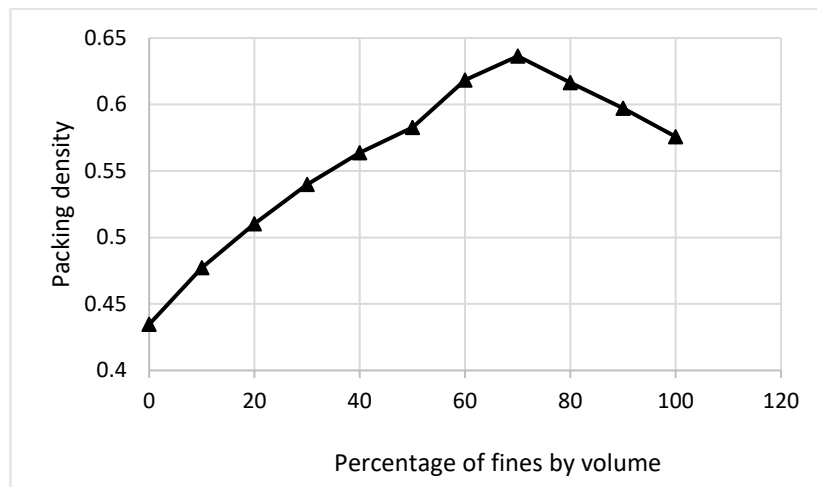


Figure 4.5: Packing density vs. Fine aggregate percentage (%) in the mix

Addition of fine aggregate increases the packing density of the mix. However, the packing density of aggregate mixture decreases after 70:30 fine to coarse ratio. Initially when coarse particles are dominant, voids in between coarse particles are high, resulting a low packing density. Introduction of fine particles will fill the voids in between coarse particles resulting a high packing density. The packing of coarse particles is disturbed and the amount of voids further increase with the introduction of fine particles. The mix proportion which produces the highest packing density is taken as the optimum mix.

### 4.3.3 Natural sand to manufactured sand proportion

Natural sand to manufactured sand proportion in the mix is selected considering the characteristics of ICBP. Previous studies have found that addition of 50% to 80%

manufactured sand to the total fine aggregate would increase the strength of the concrete (Arivalagan, 2013; Fate, 2014; Jadhav & Kulkarni, 2013; KrishnaRao et al., 2013; Uma & Banu, 2015; Zeghichi, et al. , 2012). Since the mold is removed as soon as the block is cast, it is necessary to maintain high green strength in fresh concrete. When the manufactured sand percentage is higher, the green strength is high due to the interlocking action in angular manufactured sand particles. But on the other hand, high amount of manufactured sand will increase the voids in the mix due to the shape factor (Uma & Banu, 2015). Natural sand is round and produces more workable concrete hence it can be easily used to fill the voids in coarse aggregates (Vitton, et al. 2008). The application of ICBP requires high green strength over workability to preserve the shape after removal of the mold. Hence, considering the above limitations, to maintain high green strength with a workable concrete, 70% manufactured sand and 30% natural sand was selected from total fine aggregates.

#### 4.3.4 Water/Cement Ratio

Water/cement ratio is critical in ICBP concrete mix. Since a dry concrete mix is used to cast blocks, the water/cement ratio needs to be kept to an optimum level. But too dry a mix will break the fresh block after casting as well as the required surface texture cannot be achieved. On the other hand, too wet a concrete mix will slump the block after casting and stripping of mold is difficult due to a sticky concrete mix. Therefore, to select the most suitable W/C ratio, box test was carried out (Cook, et al. , 2014). Box test revealed that 0.34 to 0.38 W/C ratio provides a better concrete mix which satisfies the required criteria. Figure 4.6 (a), 3.6 (b) and 3.6 (c) show the surface texture resulted in box tests with respect to the W/C ratio of 0.3, 0.35 and 0.4 respectively.



(a) 0.3 W/C

(b) 0.35 W/C

(c) 0.4 W/C

Figure 4.6: Results of box test for different Water/Cement ratios.

### 4.3.5 Effect of cement paste on strength

Excessive cement paste is the amount of cement paste that will remain after filling all the voids in the aggregate matrix. Excessive cement paste will coat the aggregate and act as a bonding agent for aggregates. Increase of excessive cement paste will increase thickness of the bond between two aggregates thus improving the strength of the bond. Since the aggregate is packed as densely as possible and the water/cement ratio is kept to an optimum level it is the excessive cement paste that will improve the strength of the concrete. According to Taylor, et al., (2012) excessive cement paste can be increased up to 130% to increase the strength of the concrete. As shown in Table 4.1 when the excessive cement paste is increased the strength of the concrete increases. Appendix E shows the calculation steps of the mix design.

Table 4.1: Effect of cement paste on strength

<b>Excessive cement paste (%)</b>	<b>Manufactured sand (kg/m<sup>3</sup>)</b>	<b>Natural Sand (kg/m<sup>3</sup>)</b>	<b>Coarse aggregate (kg/m<sup>3</sup>)</b>	<b>Cement (kg/m<sup>3</sup>)</b>	<b>Water (kg/m<sup>3</sup>)</b>	<b>7day Strength (N/mm<sup>2</sup>)</b>	<b>28day Strength (N/mm<sup>2</sup>)</b>
10	610	406	435	600	228	9.02	15.36
15	590	395	420	627	238	13.8	20.12
20	570	380	407	653	248	22.4	28.3
25	550	366	394	681	258	25.67	34.12
30	530	353	378	710	269	28.91	37.26
35	510	340	364	735	279	32.4	43.25
40	490	327	350	762	289	40.2	55.15

#### **4.4 Estimation of field packing density in laboratory (Laboratory packing).**

Field packing density was measured using similar aggregates used in industrial block manufacturing plants. Aggregates mixed in volume proportions and measured the packing density in laboratory to compare with theoretical models. The aggregates were mixed and both vibration and compression were applied by means of a vibration platform and a plunger to simulate actual conditions. Laboratory packing density curve in Figure 4.7 shows the variation of packing density with respect to aggregate proportions.

#### **4.5 Comparison of packing densities from models and experiments**

Toufar model, CPM and 3-parameter models were selected for the comparison. Chapter 2 section 2.5 explains each model and the reasons for the selection of each model. According to Figure 4.7, the packing density values predicted by these models are 4% to 16% lower than the packing density obtained from laboratory experiments. The compressible packing model underestimates the packing density for the selected aggregates by 16% while 3-parameter model estimates packing density correctly when the finer particle percentage is within 0 to 0.4 range. Toufar model also underestimates the packing density but compared to the CPM, Toufar model predictions are closer to experimental packing and laboratory packing. However, when maximum packing is concerned, all models apart from 3-parameter model predicts the same range of finer percentage. Toufar, CPM, experimental packing and laboratory packing suggests finer percentage of 0.6 to 0.8 will result the maximum packing density while 3-parameter model predicts finer percentage of 0.4 as the optimum mix ratio to obtain maximum packing density. Even though Toufar, CPM, experimental packing and laboratory packing suggest same range of finer percentage, their packing density predictions have considerable differences which may lead to different cement contents. Hence, it is crucial to identify the most related packing variation when selecting a theoretical packing model for mix design process. Table 4.2 shows the comparison of different packing models with experimental results.

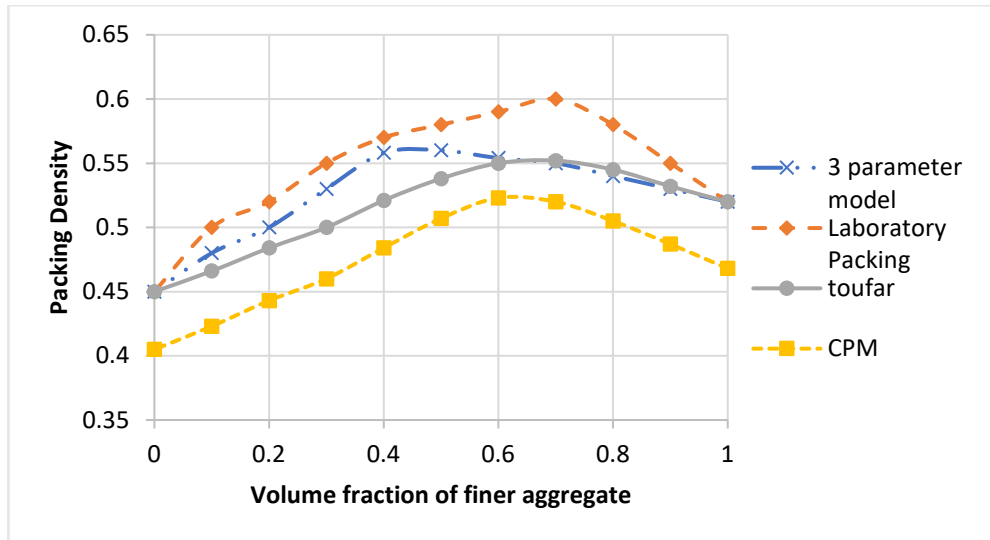


Figure 4.7: Comparison of packing models

The results shown in Figure 4.7 indicates that the predicted packing densities by selected models are not accurate for the given conditions. The selected models could only predict the packing density for pre-defined packing process. Both Toufar model and 3-parameter model do not consider method of packing into the calculation. Even though the compressible packing model considers method of packing, K value given for vibration in the model does not satisfy the vibration and compression process applied in the packing process.

#### 4.6 Determination of compressive strength of ICBP

From the results obtained through the study, concrete mix proportions were determined using packing density method. For each model, the mix proportion of large particles (Coarse) to smaller particles (fine) which gives the maximum packing density was selected for the concrete mix design. Excessive cement paste was selected as 35% for the study. Water cement ratio was selected as 0.35 for trial mixes and unconfined compressive strength was performed to check the strength. The results are given in Table 4.3. Figure 4.8 shows the fresh blocks soon after demolding. The blocks were made using the optimized mix design method and the blocks were having a very good green strength to hold its shape and the mixture was suitable to maintain fine details of the texture. Table 4.4 presents the strength of the blocks. As seen on Table 4.4, the optimized mixture was able to gain high various strength grades.

Table 4.2: Comparison of packing models with experimental results

Volumetric fraction of large particles	Laboratory packing density	Experimental packing density	3- parameter model (3PM)	Toufar model	Compressible Packing Model (CPM)
0	0.52	0.57	0.52	0.52	0.468
0.1	0.55	0.59	0.53	0.532	0.487
0.2	0.58	0.61	0.54	0.545	0.505
0.3	0.6	0.63	0.55	0.552	0.52
0.4	0.59	0.62	0.554	0.55	0.523
0.5	0.58	0.58	0.56	0.538	0.507
0.6	0.57	0.56	0.558	0.521	0.484
0.7	0.55	0.54	0.53	0.5	0.46
0.8	0.52	0.51	0.5	0.484	0.443
0.9	0.5	0.47	0.48	0.466	0.423
1.0	0.45	0.43	0.45	0.45	0.405

Table 4.3: Concrete mix proportions and strengths

<b>Packing model</b>	<b>Fine (kg/m<sup>3</sup>)</b>	<b>Coarse (kg/m<sup>3</sup>)</b>	<b>Cement<sup>1</sup> (kg/m<sup>3</sup>)</b>	<b>Water (kg/m<sup>3</sup>)</b>	<b>7-day Strength (kN/m<sup>2</sup>)</b>	<b>28-day Strength (kN/m<sup>2</sup>)</b>	<b>Cement Reduction<sup>2</sup> (%)</b>
Experimental results	850	364	735	262	32	43	27.9
3PM	432.5	649	870	304.5	33	45	14.7
Toufar	644	346.5	910	318.5	31	42	10.7
CPM	555.5	370	950	333	33	41	6.8
ACI Method (G40)	575	910	840	290	27.15	40.7	17.6
Industrial Mix	1310	340	1020	N/A	30	45	-

<sup>1</sup> 35% Excessive cement content

<sup>2</sup> Reduction of cement is calculated as a percentage compared to the industrial mix.



Figure 4.8: Sample ICBP using optimized concrete mixture

Table 4.4: Results obtained from field experiments

<b>Sample</b>	<b>Excessive cement content %</b>	<b>3-day strength (N/mm<sup>2</sup>)</b>	<b>7-day strength (N/mm<sup>2</sup>)</b>	<b>28-day strength (N/mm<sup>2</sup>)</b>
1	20	12.4	18.9	26.3
2	25	15.2	21.4	30.5
3	30	18.6	27.6	36.4
4	35	22.6	30.1	43
5	40	28.3	37.4	52.1



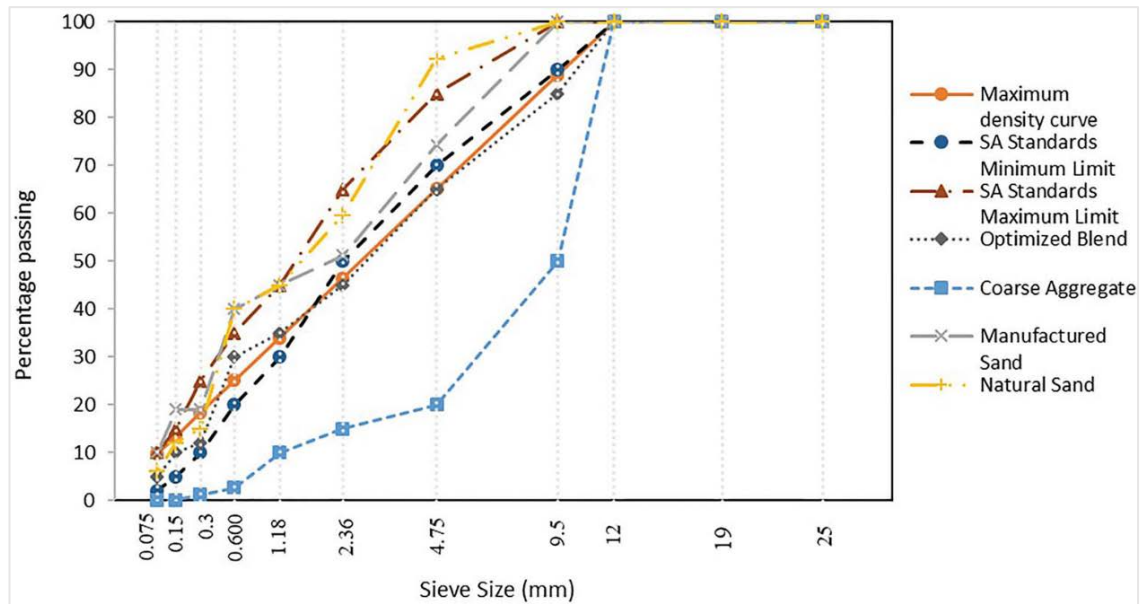


Figure 4.9: Gradation of aggregates used in the study and optimized blend

Figure 4.9 shows the aggregate gradation used in the study. The optimized blend proposed by the study is very close to the maximum density line and the lower limit of SA standards (SANS1058, 2012).

#### 4.7 Summary of findings

Particle packing optimization is a well-recognized and widely used method to enhance the performance of concrete. Several theoretical packing models are used to determine the packing density and different packing models apply different approaches to accurately predict the packing densities of irregular aggregate mixes. Due to non-homogeneity of the aggregate particle mixes, it is a very challenging task to accurately predict the packing densities or void ratios of a mix of aggregates. Due to this reason, it is crucial to select the most suitable packing model for the application. Selection of a suitable packing model should be done based on the applicability of packing model.

This study determined the applicability of three widely used packing models, 3-parameter model, Toufar model and Compressible packing model for the use of ICBP manufacturing. The theoretical models were compared with controlled laboratory experiments as well as field experiments to determine the applicability of them in ICBP manufacturing. Concrete mixes were produced using the optimum mix ratios

predicted by each theoretical model as well as the experimental programs. From the results of unconfined compressive strength, it was observed that the theoretical models can be used to optimize the current industrial mix design and the 3-parameter, Toufar and CPM models have reduced the cement consumption by 14.7%, 10.7 % and 6.8% respectively for the application of ICBP when compared to the current industrial mix design. Even though the theoretical packing models could produce the required strength, it was evident that experimental mix design could also achieve the same strength using lesser amount of cement. Hence, the study recommends a more accurate and reliable theoretical packing model incorporating shape and texture factors as well as compaction method which focuses and specializing in application is needed for the ICBP and precast concrete industry.

#### **4.8 Recommendations**

From the study, it is evident that even though the existing packing models can be used to optimize the concrete mixtures to a certain extent, further optimization can be done if packing models are developed incorporating realistic conditions such as vibration, particle shape and surface texture. Hence, the study recommends a packing model development incorporating vibration, particle shape and surface texture. To accommodate these factors into a model it is important to analyse the effect of these factors on packing density. The following chapters present the experimental work carried out to determine the effect of vibration, shape and surface texture and the analysis of the results.

## CHAPTER 5

### 5 COMBINED EFFECT OF VIBRATION FREQUENCY, SIZE RATIO AND LARGE PARTICLE VOLUME FRACTION

#### 5.1 Introduction

Densification of mixtures by means of vibration, known as Vibro-compaction, is widely used in industry. These techniques involve the exertion of energy to the particles at a specific frequency and amplitude for a certain duration. However, for different particulate mixtures, determination of the most suitable parameters (such as vibration frequency and amplitude) to achieve "maximum density" is still an open problem. Many external factors such as friction, particle shape & size, material density, the geometry of container and the initial state before vibration affect the behavior (X.-z. An, 2013). Hence, the achievement of the densest packing has been a complicated problem and different approaches (i.e.: experimental studies, numerical analysis, computer simulations) have been taken to model the behavior of particulate systems in different conditions. Prediction of packing density is important in many applications such as concrete optimization, ceramic industry, powder technology, packing technology etc. Hence, it is important to know the packing density of a particular mixture to effectively utilize the available resources (Jones et al., 2002).

A number of theoretical, empirical and semi-empirical packing models have been developed to predict the packing density of discrete and continuous particulate mixtures. Most of these models are based on several basic assumptions such as spherical particles, smooth texture, natural packing etc. (Aim & Le Goff, 1968; Andreasen & J. Andersen, 1930; Fuller and Thompson, 1907; Kwan et al., 2013; Stovall et al., 1986; Toufar et al., 1976). Though the particles used are in different shapes, different textures and the packing is done by either mechanical vibration or tapping (forced packing) in general applications. The objective of this chapter is to determine the combined effect of vibration frequency, size ratio and large particle volume fraction on packing density of binary mixtures. The study further develops a regression model and design graphs to predict packing density.

The experiment was conducted as described in section 3.4. The study focused on the packing density of binary spheres hence, the packing arrangements and packing structure were not particularly studied. Since the vibration was applied until the point of maximum packing, it was noticed that by both methods, similar maximum packing density can be achieved. However, the time taken to achieve the maximum packing are different. It was observed that the mixtures on vibration table achieve maximum packing sooner than the vibration applied using vibration hammer.

## 5.2 Vibration time

The time taken to achieve maximum packing density of each composition was measured. Figure 5.1 shows the variation of vibration time with respect to different mixture compositions for various vibration frequencies. When the vibration frequency is 110 rad/s, the mixtures tend to reach the maximum packing density sooner. Interestingly, it was found that for a fixed vibration frequency, the minimum time is observed around mixtures with 0.7 large particle volume fractions which is the optimum combination for maximum packing density. Table 5.1 shows the values of vibration time with respect to various vibration frequencies. The particle composition may provide a better freedom to rearrange in a more stable setting. This can be the possible reason for such behavior and further studies are recommended to analyze the particle packing behavior under vibration.

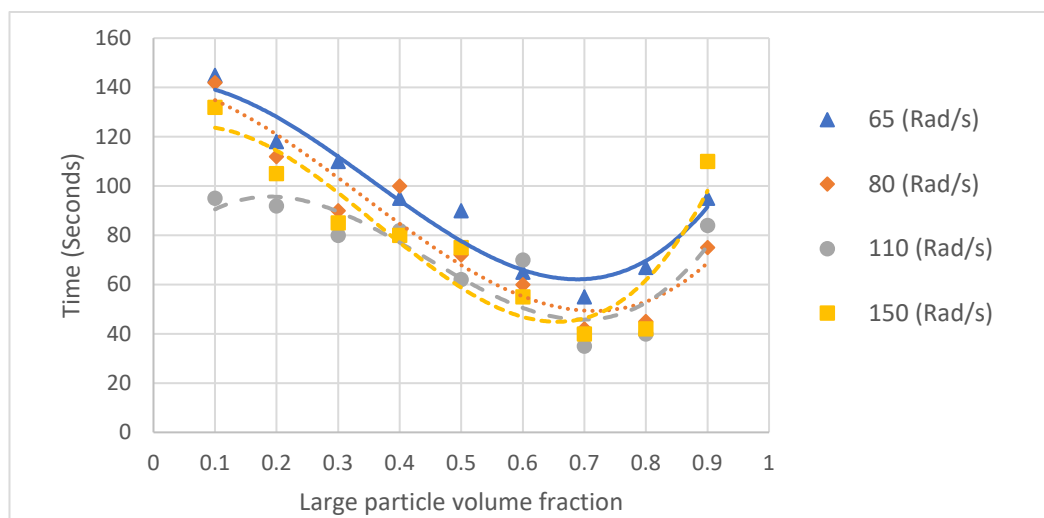


Figure 5.1: Vibration time required for maximum packing

Table 5.1: Time for maximum packing with vibration for various large particle volume fractions.

Large particle volume fraction	Time (Seconds)			
	65 (Rad/s)	80 (Rad/s)	110 (Rad/s)	150 (Rad/s)
0.1	145	142	95	132
0.2	118	112	92	105
0.3	110	90	80	85
0.4	95	100	82	80
0.5	90	72	62	75
0.6	65	60	70	55
0.7	55	42	35	40
0.8	67	45	40	42
0.9	95	75	84	110

### 5.3 Container wall effect

Spherical glass beads with the diameters of 20mm, 10mm, 5mm, and 3mm were used for the study and a steel container with a diameter of 200mm was used to reduce the wall effect due to the container. According to McGeary (1961) and Ayer and Soppet (1965), when large particle diameter to container diameter ratio ( $d/D$ ) is less than 0.1, the effect of container wall can be neglected. Based on this information, a container of diameter 200 mm was used where maximum  $d/D$  for the experiments is 20/200 (0.1). Also, according to the Ayer and Soppet (1965), the maximum value for container wall effect for the selected spherical beads and container was found to be  $4.3 \times 10^{-3}$  which is a very small value. Hence, the container wall effect is assumed to be negligible in this study.

However, further experimental studies were performed to confirm variation of packing density with respect to the container diameter. For the study, seven different diameter containers were selected. The vibration and large particle fraction were maintained constant and packing density variation was measured with different container

diameters. Figure 5.2 shows the packing density variation with respect to the large particle diameter to container diameter ratio ( $d/D$ ). The results shown in Figure 5.2 further confirm that the container wall effect can be neglected when the  $d/D$  is less than 0.1. When all the other factors are held constant, the container wall effect significantly affects the packing density when  $d/D$  is greater than 0.1. The results further validate and confirm the findings of McGeary (1961) and Ayer and Soppet (1965). Table 5.2 shows the packing density values with respect to the large particle diameter to container diameter ratio ( $d/D$ ) for a vibration frequency of 110 Rad/s and a large particle volume fraction of 0.7.

Table 5.2: Packing density values with respect to the large particle diameter to container diameter ratio ( $d/D$ )

Particle diameter/Container diameter ( $d/D$ )	Packing density		
	20mm	10mm	5mm
0.4	-	0.6	-
0.2	0.71	0.71	-
0.16	-	0.756	-
0.1	0.8	-	0.64
0.08	0.81	0.761	-
0.067	-	0.759	-
0.05	-	0.762	0.65
0.04	0.81	0.761	0.65
0.033	0.81	-	-
0.025	0.81	-	-
0.02	0.81	-	0.65
0.017	-	-	0.65
0.0125	-	-	0.65
0.01	-	-	0.65

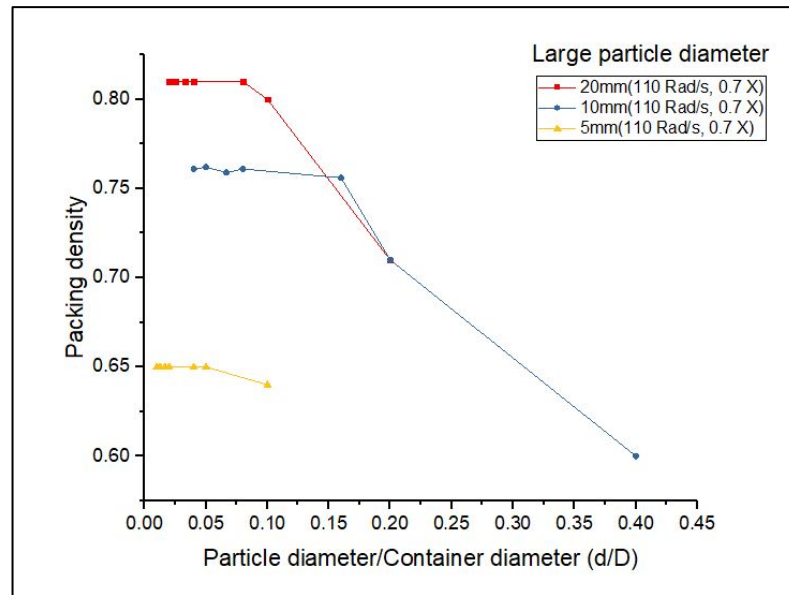


Figure 5.1: Packing density variation with respect to the large particle diameter to container diameter ratio ( $d/D$ )

#### 5.4 Analysis and development of model

Literature review and previous studies confirm that the packing density of a binary mixture depends on the proportion of large and small particles, vibration, the size ratio of the two particle classes, shape and surface texture of particles. Shape and surface texture were kept constant throughout the study by selecting spherical and smooth glass beads to isolate their effect on packing density. The variation of packing density was studied for various size ratios (0.6,0.5,0.3,0.25,0.15), various vibrations (65 rad/s to 150 rad/s) and for various mix proportions (0.1 to 0.9). Figure 5.3 shows the packing density variation with respect to vibration for binary mixtures with various coarse aggregate proportions. The size ratio of the binary mixture was kept at 0.15 (20mm and 3mm spherical beads).

The increase of the vibration frequency improves the mobility of individual particles by means of kinetic energy, allowing the particles to achieve more stable position. Further increase of vibration frequency inputs extra energy to the mixture, disturbing the stable packing structure and forcing particles to move from the stable packing position to unstable dispersed packing position, reducing the packing density of the mixture. This phenomenon was observed in the experimental study. The maximum

packing density was achieved around 100-120 rad/s and the further increase of vibration frequency reduces the packing density as shown in Figure 5.3. The results further validate the findings of An, et al., (2016). They also found that when vibration frequency increases, the packing density increases to a maximum and then reduces with further increase of vibration similar to Figure 5.3.

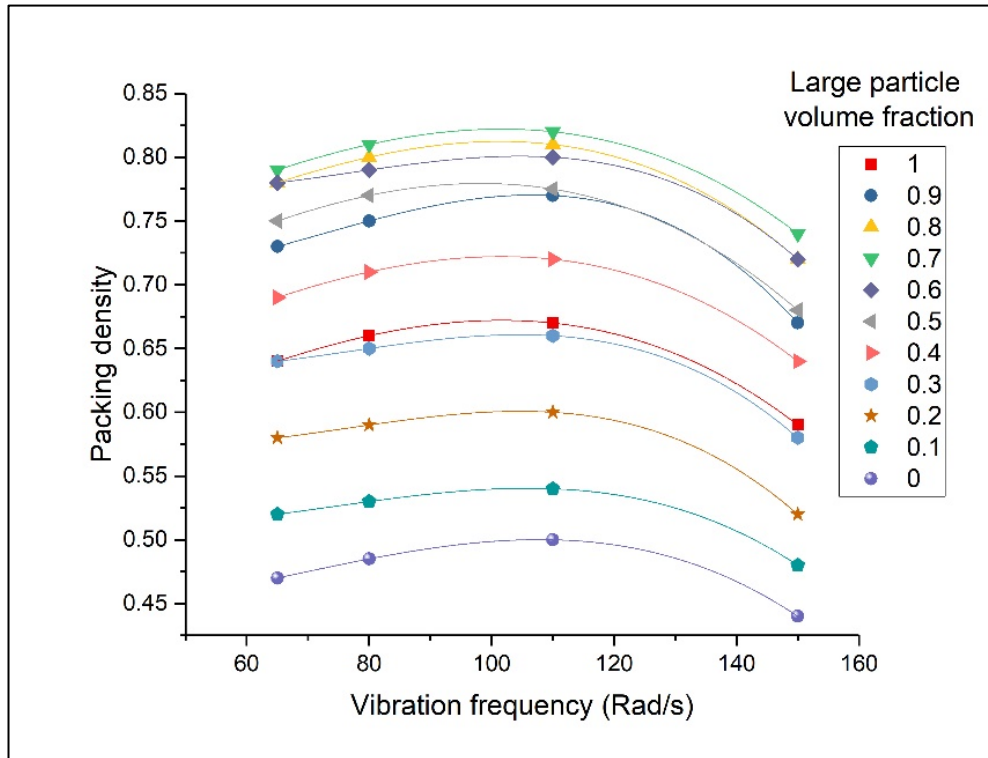


Figure 5.2: Effect of vibration frequency on packing density for various large particle fractions at size ratio of 0.15.

The images of the sample before and after vibration show that the particles arrangement is more ordered after vibration is applied than the initial random arrangement. As shown in Table 5.3, the photographic evidence suggests that the particles may rearrange in a more orderly manner to increase the packing density of the mixture. The top view and the side view of the sample after vibration indicate that the particle rearrangement is more ordered than the initial random arrangement. However, further investigations are encouraged to confirm the particle rearrangement structure and packing arrangement under vibration.



Table 5.3: Particle arrangement before and after vibration



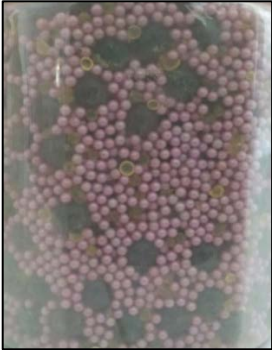



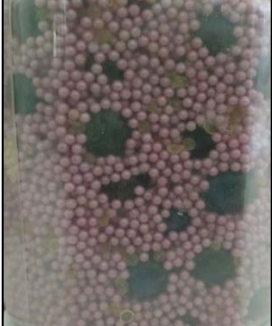
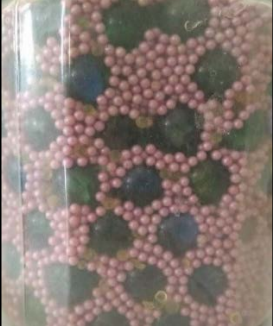
Particle mixture	Top view		Side view	
	Before Vibration	After Vibration	Before Vibration	After Vibration
10 mm and 3 mm particle mixture				
20 mm and 3 mm particle mixture				

Figure 5.4(a) shows the variation of packing density with respect to the larger particle volume fraction. Maximum packing density can be achieved when the large particle volume fraction is closer to 0.7. Introduction of small particles to a mixture of large particles will increase the packing density of the mixture by occupying free voids in between large particles. The packing will reach a maximum value and further input of smaller particles will start to disturb the packing of larger particles (loosening effect). Thus, the packing density of the mixture will start to reduce. Hence, there is an optimum mixture composition that will yield the maximum packing density.

Figure 5.4(b) shows the variation of packing density with the size ratio of two particle sizes under 110 Rad/s vibration frequency at large particle volume fraction of 0.7. Four different particle sizes were selected for the study (20mm,10mm,5mm,3mm) and 5 different size ratios were selected by combining to achieve 0.15,0.25,0.3,0.5,0.6 size ratios.

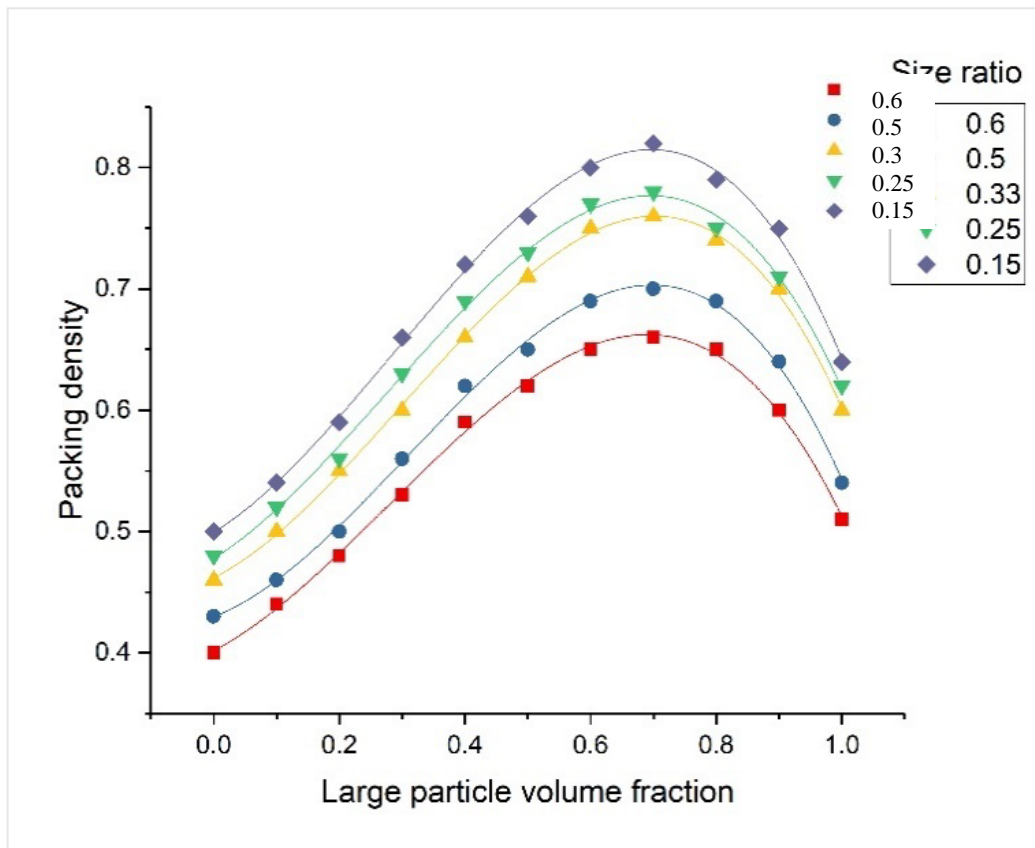
When size ratio is small, small particles will easily fill the voids in between large particles. Higher the size ratio, more difficult for smaller particles to fill the voids in larger particles. Thus, loosening effect may occur reducing the packing density of the mixture as shown in Figure 5.4(b). According to McGeary (1961), the packing density variation with respect to particle size ratio is a curve with two linear sections. When size ratio is in between 1 to 0.1 the packing density variation is linear with a steep gradient and when size ratio is less than 0.1 the variation becomes linear with a mild gradient. Hence, the curve has two linear sections with a sharp curve around size ratio 0.1. Figure 5.4(b) shows only the first linear section. Therefore, the model will be accurate only within the range of 1-0.1 size ratio.

The relationship between the packing density and large particle fraction is a polynomial curve of third order ( Eq 4.1 ) with the adjusted  $R^2$  value of 0.98. Fitted curve is shown in Figure 5.4(a).

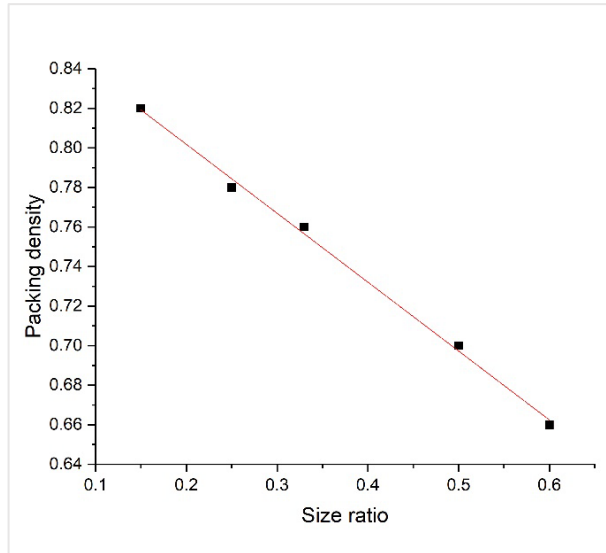
Where A , B, C and D parameters are functions of size ratio and vibration frequency while  $X$  is the volumetric fraction of large particles. Table 5.4 shows the values for A, B, C, and D for 110 Rad/s vibration frequency.

Table 5.4: A, B, C and D Parameters (110 Rad/s)

Size ratio	A	B	C	D
0.6	-1.0159	0.8549	0.2715	0.4017
0.5	-1.1966	1.1084	0.2011	0.4297
0.3	-1.188	1.0676	0.2611	0.4618
0.25	-1.1053	0.9202	0.3246	0.4778
0.15	-1.216	1.0431	0.3162	0.4994



(a) Variation of packing density with large particle fraction



(b) Variation of packing density with size ratio

Figure 5.3: Effect of large particle fraction and size ratio on packing density

The variation of A, B, C and D parameters with respect to size ratio was observed. A, B and C curves show a second order polynomial relationship with  $R^2$  of 0.95 and D shows a linear relationship with  $R^2$  of 0.94. Figure 5.5 shows the variation of A, B, C and D parameters with respect to size ratio for fixed vibration frequency of 110 Rad/s. Curve fitted equations for A, B, C and D were found to be in the form of Equation 5.2 to Equation 5.5 respectively.

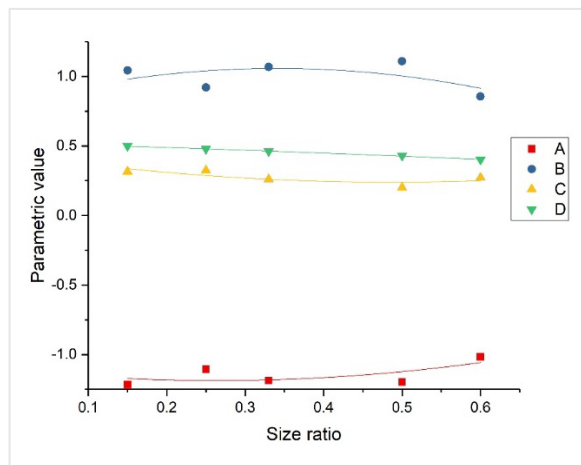


Figure 5.4: Variation of A, B, C and D parameters with size ratio

$$A = A_1R^3 + A_2R^2 + A_3R + A_4 \quad \dots\dots\dots\text{Equation 5.1}$$

$$B = B_1R^3 + B_2R^2 + B_3R + B_4 \quad \dots\dots\dots\text{Equation 5.2}$$

$$C = C_1R^3 + C_2R^2 + C_3R + C_4 \quad \dots\dots\dots\text{Equation 5.3}$$

$$D = D_1R^2 + D_2R + D_3 \quad \dots\dots\dots\text{Equation 5.4}$$

Where, R is the size ratio of two particle classes.

$$R = \frac{d_1}{d_2} \quad \dots\dots\dots\text{Equation 5.5}$$

Where d1 and d2 are diameters of small particle and large particle respectively.

Similarly, variations were plotted for different vibration frequencies and behavior of A, B, C and D were observed. Similar behavior was observed for different vibration frequencies. To determine the relationship between vibration frequency and packing density, the variation of A<sub>1</sub>, A<sub>2</sub>.....D<sub>3</sub> was plotted against vibration frequency ( Figure 5.6). Table 5.5 shows the values of sub parameters with various vibration frequencies.

Table 5.5: Variation of A, B, C and D sub-parameters (A<sub>1</sub>, A<sub>2</sub>, A<sub>3</sub>, B<sub>1</sub>, B<sub>2</sub>, .....D<sub>1</sub>, D<sub>3</sub>)

Sub parameter	Vibration frequency (Rad/s)			
	65	80	110	150
A1	7.1265	7.1265	7.1265	7.1265
A2	-11.9156	-11.8978	-11.8717	-11.8565
A3	6.27345	6.2874	6.3072	6.3168
A4	-1.61375	-1.6775	-1.7645	-1.7965
B1	-8.723	-8.723	-8.723	-8.723
B2	13.7538	13.7292	13.6908	13.662
B3	-6.68708	-6.7077	-6.7422	-6.7742
B4	1.61105	1.7078	1.8608	1.9808
C1	1.4292	1.4292	1.4292	1.4292
C2	-1.5565	-1.5442	-1.525	-1.5106
C3	0.2585	0.2645	0.2765	0.2925
C4	0.0256	-0.0074	-0.0734	-0.1614
D1	-0.1323	-0.1323	-0.1323	-0.1323
D2	0.044125	0.0352	0.0295	0.0471
D3	0.66225	0.681	0.678	0.59

Table 5.6: Equation parameters for A1, A2, A3, B1, B2, .....D2, D3.

Sub Parameter	Coefficients ( $\tau = \alpha + \beta\omega + \gamma\omega^2$ )			Equation 5.7
	$\alpha$	$\beta$	$\gamma$	
A1	0.0000	0.0000	7.1265	Eq (5.7 a)
A2	-0.000007	0.0022	-12.029	Eq (5.7 b)
A3	-0.000006	0.0018	6.1818	Eq (5.7 c)
A4	0.00003	-0.0086	-1.1815	Eq (5.7 d)
B1	0.0000	0	-8.723	Eq (5.7 e)
B2	0.000008	-0.0028	13.902	Eq (5.7 f)
B3	0.000005	-0.0021	-6.5717	Eq (5.7 g)
B4	-0.00003	0.0108	1.0358	Eq (5.7 h)
C1	0.0000	0.000	1.429	Eq (5.7 i)
C2	-0.000004	0.0014	-1.6306	Eq (5.7 j)
C3	0.0000	0.00040	0.2325	Eq (5.7 k)
C4	0.0000	-0.0022	0.1686	Eq (5.7 l)
D1	0.0000	0.000	-0.1323	Eq (5.7 m)
D2	0.000009	-0.0019	0.1296	Eq (5.7 n)
D3	-0.00003	0.0056	0.425	Eq (5.7 o)

Figure 5.6 shows the variation of A<sub>1</sub>, A<sub>2</sub>, .....D<sub>3</sub>s with respect to vibration frequency( $\omega$ ). The curve fitting correlation was found to be in between 0.89 being the lowest for D<sub>1</sub> and 0.999 being the highest for A<sub>2</sub>. Table 5.6 shows the equations (Eq(5.7a) to Eq(5.7 o)) for each parameter (A<sub>1</sub> to D<sub>3</sub>).

The final model incorporating three independent variables, (1) vibration frequency ( $\omega$ ), (2) size ratio (R) and (3) large particle fraction ( X) was developed.

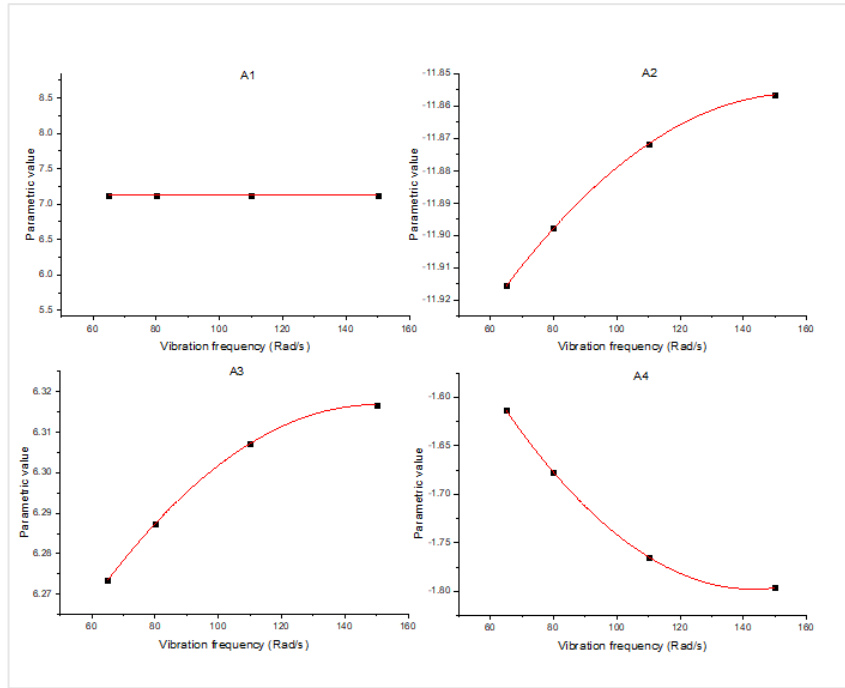


Figure 5.6 (a): Sub parameters of A

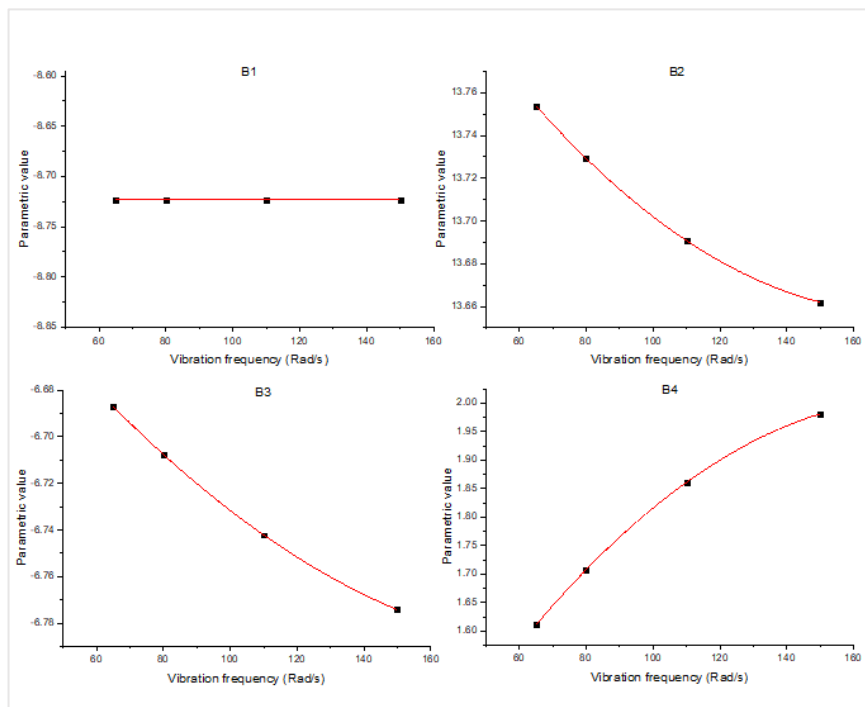


Figure 5.6 (b): Sub parameters of B

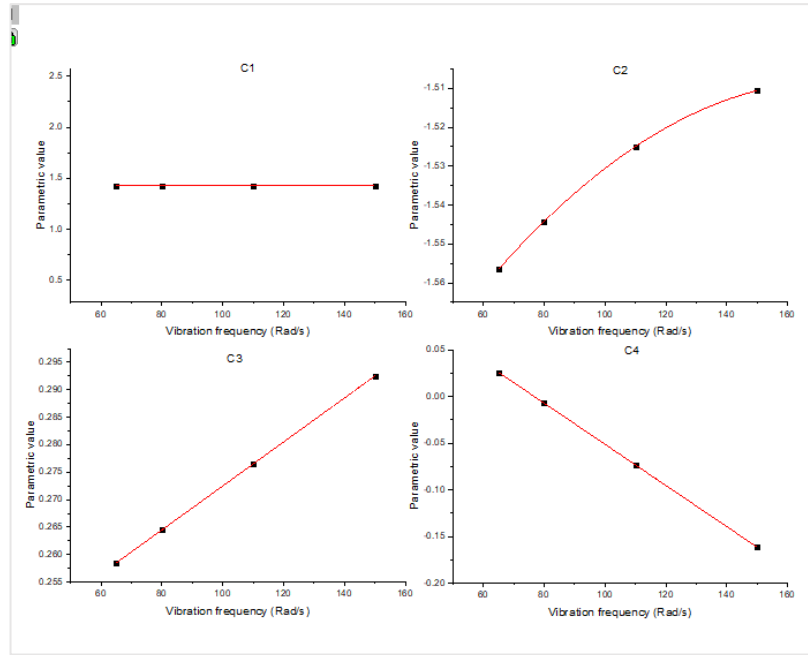


Figure 5.6 (c): Sub parameters of C

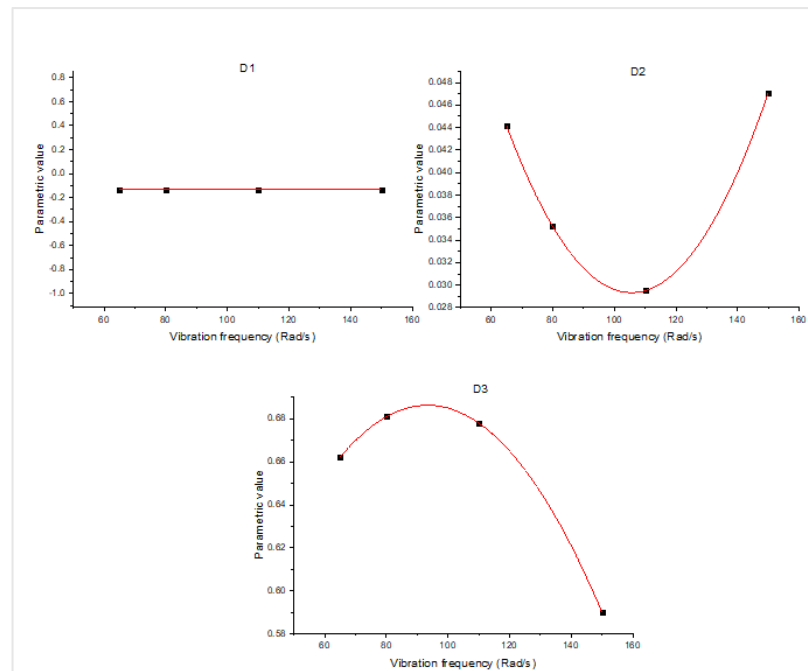


Figure 5.6 (d): Sub parameters of D

Figure 5.5: Variation of  $A_1, A_2, A_3, B_1, B_2, \dots, D_1, D_3$  with vibration frequency



### Summary of the model:

$$A_1 = 7.1625 \quad \text{Eq (4.7a)}$$

$$A_2 = -7 \times 10^{-6} \omega^2 + 0.0022 \omega - 12.029 \quad \text{Eq (4.7b)}$$

$$A_3 = -6 \times 10^{-6} \omega^2 + 0.0018 \omega + 6.1818 \quad \text{Eq (4.7c)}$$

$$A_4 = 3 \times 10^{-5} \omega^2 - 0.0086 \omega - 1.1815 \quad \text{Eq (4.7d)}$$

$$B_1 = -8.713 \quad \text{Eq (4.7e)}$$

$$B_2 = 8 \times 10^{-6} \omega^2 - 0.0028 \omega + 13.902 \quad \text{Eq (4.7f)}$$

$$B_3 = 5 \times 10^{-6} \omega^2 - 0.0021 \omega - 6.5717 \quad \text{Eq (4.7g)}$$

$$B_4 = -3 \times 10^{-5} \omega^2 + 0.0108 \omega + 1.0358 \quad \text{Eq (4.7h)}$$

$$C_1 = 1.429 \quad \text{Eq (4.7i)}$$

$$C_2 = -4 \times 10^{-6} \omega^2 + 0.0014 \omega - 1.6306 \quad \text{Eq (4.7j)}$$

$$C_3 = 0.0004 \omega + 0.2325 \quad \text{Eq (4.7k)}$$

$$C_4 = -0.0022 \omega - 0.1686 \quad \text{Eq (4.7l)}$$

$$D_1 = -0.1323 \quad \text{Eq (4.7m)}$$

$$D_2 = 9 \times 10^{-6} \omega^2 - 0.0019 \omega + 0.1296 \quad \text{Eq (4.7n)}$$

$$D_3 = -3 \times 10^{-5} \omega^2 + 0.0056 \omega + 0.425 \quad \text{Eq (4.7o)}$$

### 5.4.1 Validation of the model

The model was validated for 300 independent samples and the correlation coefficient of experimental data and model predicted data is 0.967 which shows a very good correlation of the model. Hence the model is selected for the development of design graphs. Model predictions are plotted against experimental values in Figure 5.7.

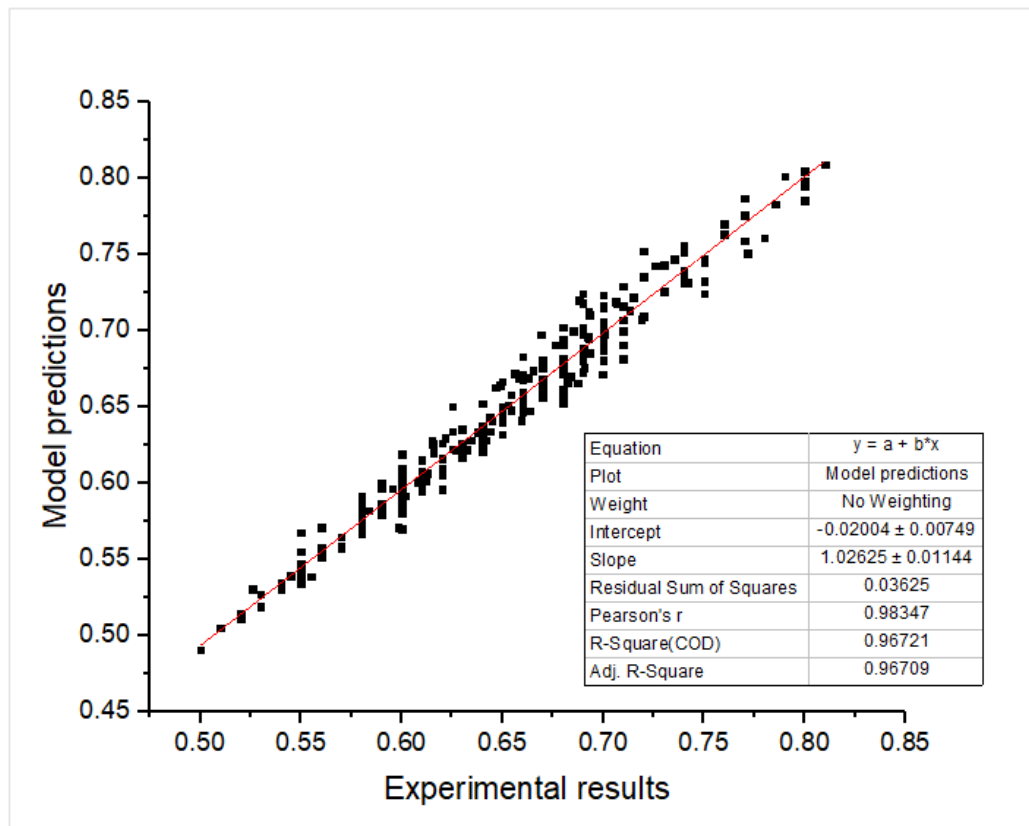


Figure 5.6: Correlation between model and experimental results

### 5.4.2 Cross check of the model

Since the size ratio and packing density is having a linear relationship for a constant vibration frequency and large particle fraction, the model can be cross-checked by verifying if the model predictions are following the same relationship. Figure 5.8 shows the model predicted packing density variation with size ratios for three different randomly selected vibration frequency and large particle fraction. As expected, the model predictions are also showing a linear relationship with a correlation coefficient of 0.99, validating the model for the use of practical and analysis purposes.

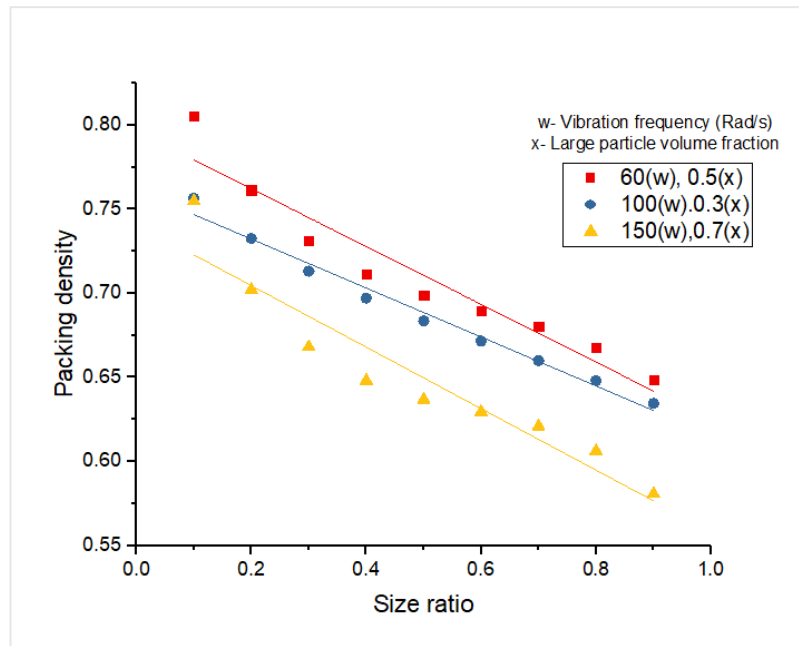


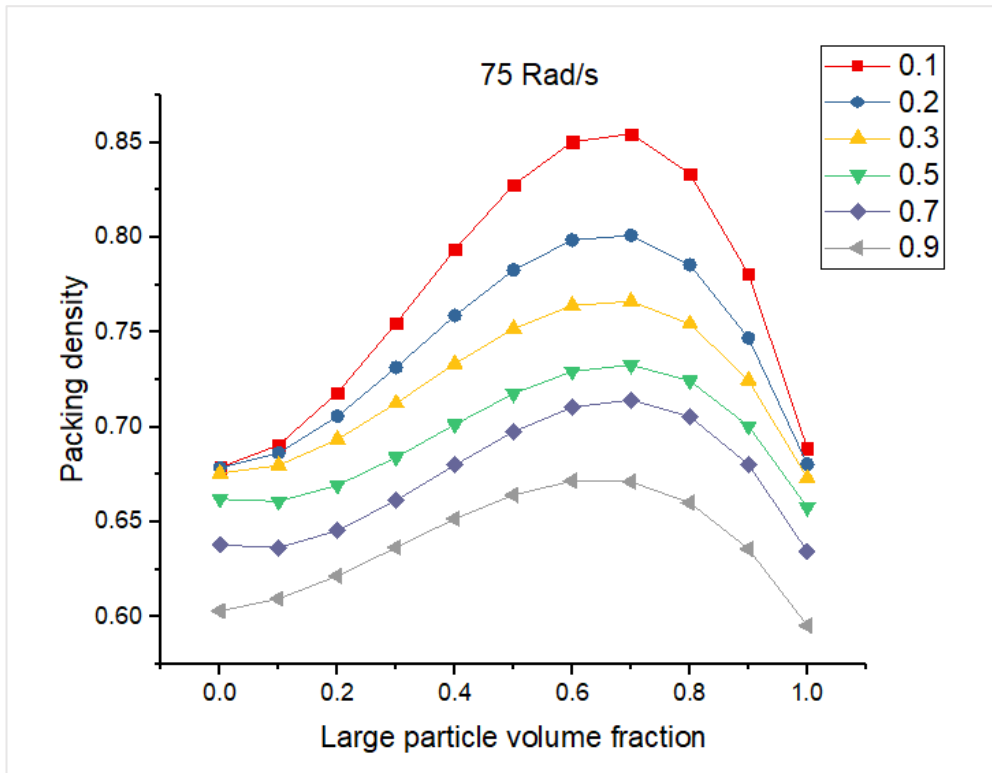
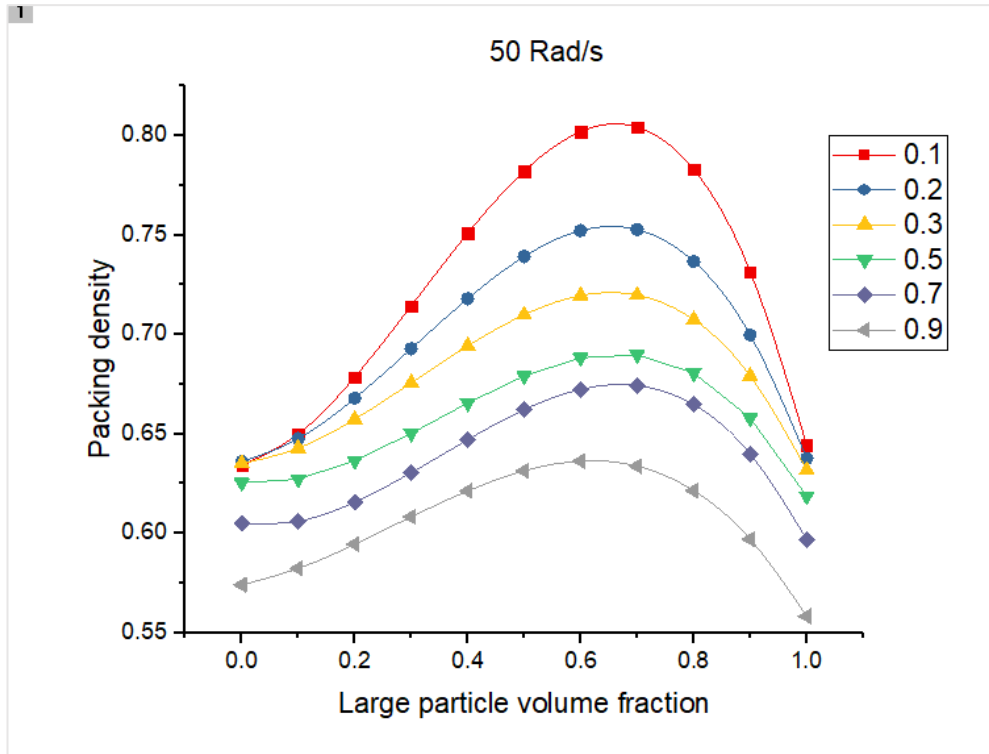
Figure 5.7: Model predicted packing density with size ratio

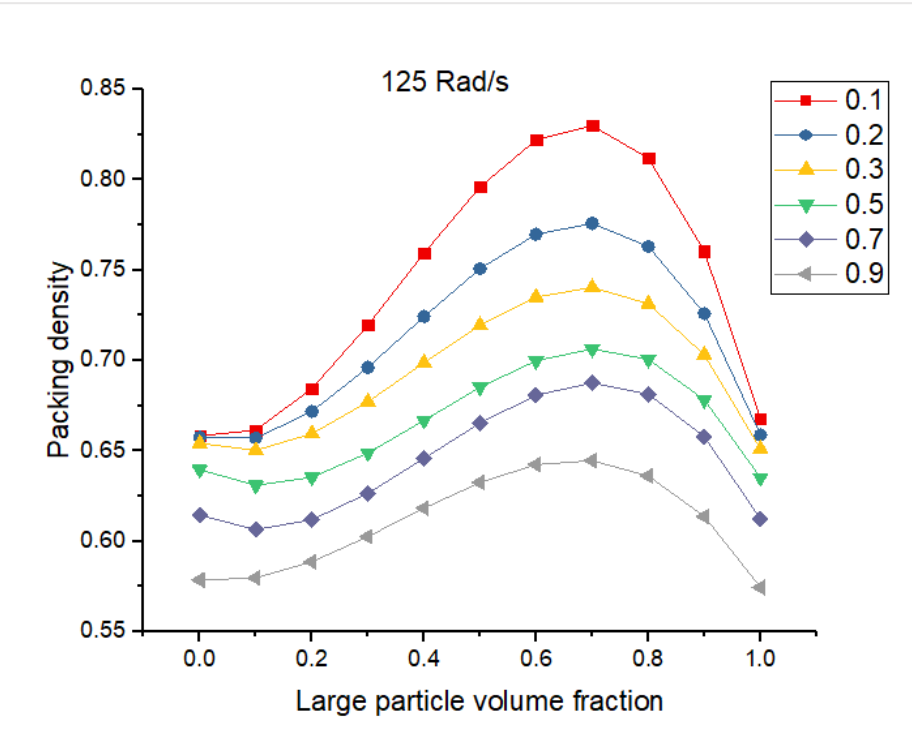
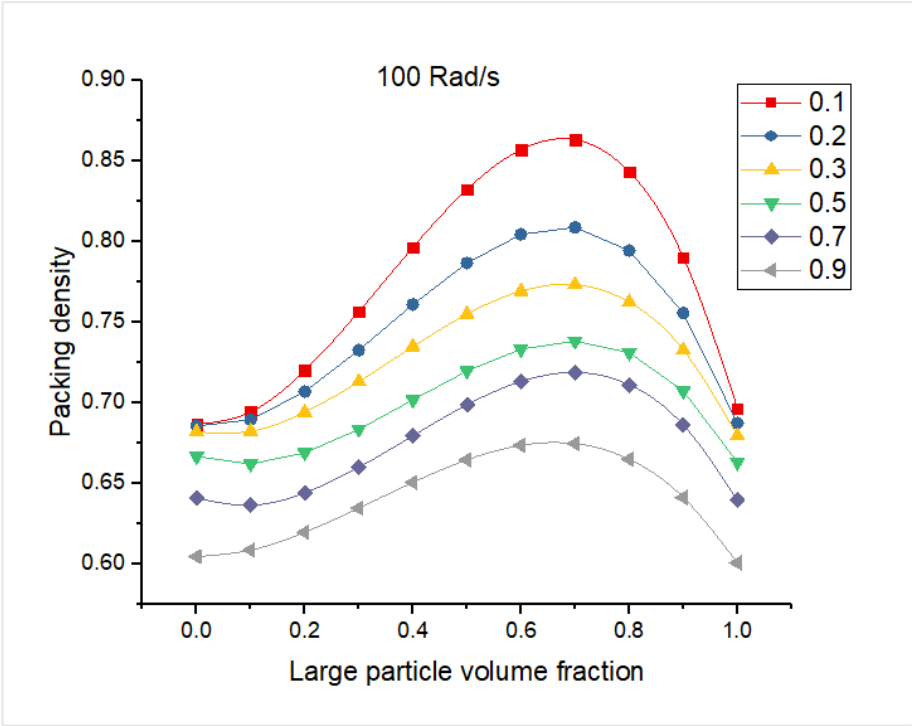
### 5.4.3 Limitations of the model

The model was validated for the vibration frequency range of 50 Rad/s to 150 Rad/s. Hence, the accuracy of the model for vibration frequencies beyond the specified vibration frequency is limited. However, most of the equipment in the industry having a vibration frequency within the given range. Hence, the applicability of design graphs is valid for various applications in the industry. Another limitation of the model is, it does not consider the effect of vibration amplitude. The model was developed keeping vibration amplitude a constant. Therefore, it can be effectively used for a given equipment with a constant amplitude (Most equipment in the industry has a constant amplitude). Furthermore, for the simplicity, the model is developed for spherical, smooth particles.

### 5.5 Design graphs

Use of model equation is complicated hence design graphs were developed for the easiness of use. Following set of graphs can be effectively used to determine the packing density for selected vibration frequency. Figure 5.9 shows the design graphs with different vibration frequencies.





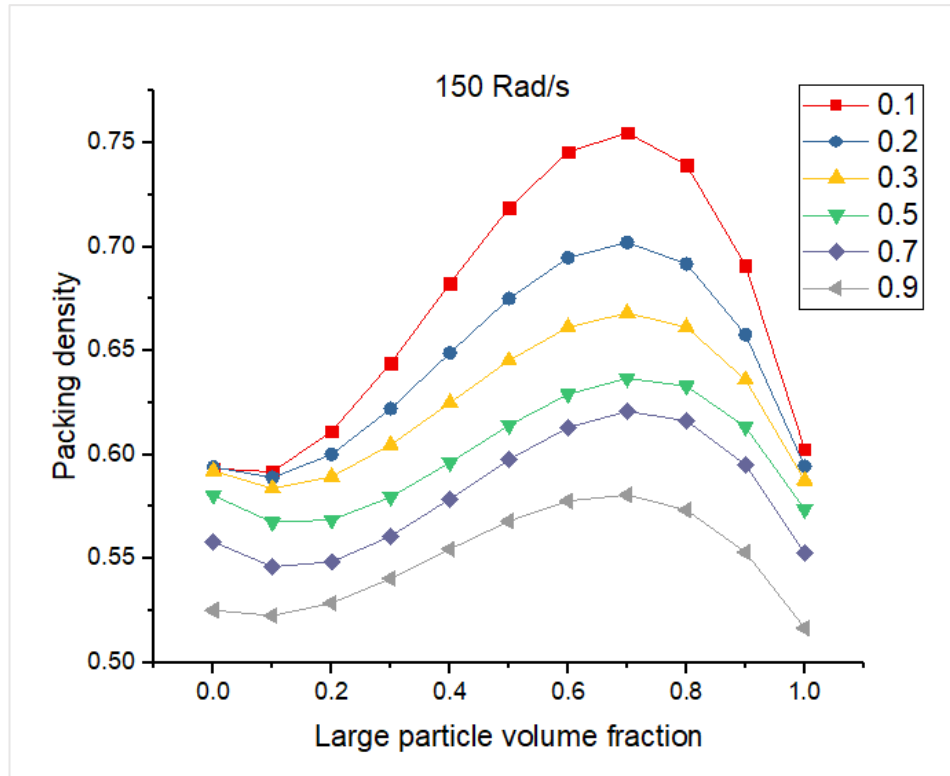


Figure 5.8: Design graphs for various vibration frequencies

## 5.6 Summary of findings and recommendations

The packing density of binary mixtures with various vibration frequencies and various size ratios was studied experimentally to analyze the behavior of mixtures under vibration. From experimental results, an analytical model was developed to predict the packing density of binary spherical mixtures under vibration. Further, design graphs were also developed to simplify the usability of the developed model. The following conclusions can be drawn from the results,

- a) Vibration frequency is playing a major role in packing densification of binary spherical mixtures. The packing density increases to a maximum as the vibration frequency increases and reduces as further increase of vibration frequency of the mixture.

- b) The packing density reaches a maximum value when the volume fraction of large spheres is around 0.7.
- c) The variation of packing density with size ratio is observed to be linear. When the size ratio is close to 1 (Size of two particles is approximately similar), the packing density is low and when the size ratio is closer to 0 (Size of two particles is considerably different), the packing density is high.
- d) Based on the observations, an analytical packing model was developed and design graphs were produced from the model to easily determine the packing density of a binary spherical mixture.
- e) It is recommended that the graphs should be used for the given range of vibration frequencies and further studies are required to develop the model beyond the specified range of vibration frequency.
- f) Vibration amplitude was held constant throughout the study. Hence the design graphs can be effectively used for constant vibration amplitude and further studies are required to incorporate vibration amplitude in the model.
- g) Further studies are recommended to investigate the behavior of particles under vibration and identify the packing arrangement of binary spherical mixtures subjected to vibration.

## CHAPTER 6

### 6 COMBINED EFFECT OF SHAPE, SURFACE TEXTURE AND VIBRATION ON PACKING DENSITY

#### 6.1 Introduction

As explained in previous chapters, packing density is one of the key factors that affect the properties of materials such as concrete, asphalt, ceramic etc. Some applications require maximum packing density while some require maximum porosity. Either way measuring the packing density of particulate mixtures is a prime concern in the materials industry. Material optimization, advancement of properties, development of high density materials and lightweight materials are some of the applications of packing density. Though there are many advantages of packing density, measurement of packing density in a particulate mixture is a tedious process. The problem gets complicated due to involvement of various factors such as particle shape, surface texture, mixture proportion, size ratio, method of packing etc. Hence, a number of approaches have been taken to identify the behavior of particle packing and develop reasonably accurate analytical and numerical models to predict the packing density of particulate mixtures. These models have been utilized for applications such as concrete, asphalt etc. making several assumptions such as spherical aggregates, smooth surfaces, random loose packing state etc. which is far from the reality. The real-world particles are in various shapes, various textures and various packing methods are used to make dense packing. Thus, the accuracy and applicability of basic packing models are limited. There are many packing models that have been developed to address these factors. Majority of these models have been developed by taking only one factor at a time keeping all other factors a constant. There is no packing model that gets the combined effect of the shape, texture and vibration together to predict the packing density. The objective of this study is to develop a packing model by taking effect of particle shape, particle surface texture and vibration frequency.



## **6.2 Development of particle packing models**

Packing density is the ratio of solid volume to bulk volume of a particle mixture. Higher the solid volume, higher the packing density. High packing density means less voids in the mixture. Hence, many applications are required to maintain an optimum, minimum or maximum amount of voids in the particulate mixtures. To achieve the required level of packing it is important to know the packing density of a mixture of two or more components. Since measuring the packing density manually is tedious and impractical, particle packing models are used to predict the packing density of mixtures. Chapter 4 explains the packing models that have been developed so far. As explained in Chapter 4, most of these models were developed based on number of basic assumptions such as spherical particles, smooth surfaces, random loose packing conditions etc. Nevertheless, the real conditions are far from the assumptions and packing density may vary greatly with non-spherical, rough particles subjected to vibration as explained in Chapter 2. Chapter 5 considered the effect of vibration alone on packing density to develop an analytical model and design graphs for prediction of packing density of binary spherical mixtures. This chapter describes the effect of particle shape and surface texture separately. Further a combined effect of shape, surface texture and vibration is analyzed to modify the existing 3-parameter model to predict the packing density of irregular shaped particles with various surface textures under various vibration frequencies.

## **6.3 Effect of particle shape on packing density**

The packing density of aggregate mixtures with different shape factors were measured for different mixture proportions by varying the large particle volume fraction. The variation of packing density with respect to particle shape was found to be linear where increase of shape factor increases the packing density of the mixture. As expected the highest packing was observed when shape factor is closer to 1(Spherical) and for mixtures with 0.7 large particle volume fraction. Figure 6.1 shows the variation of packing density with respect to particle shape factor when all the other factors are held constant.

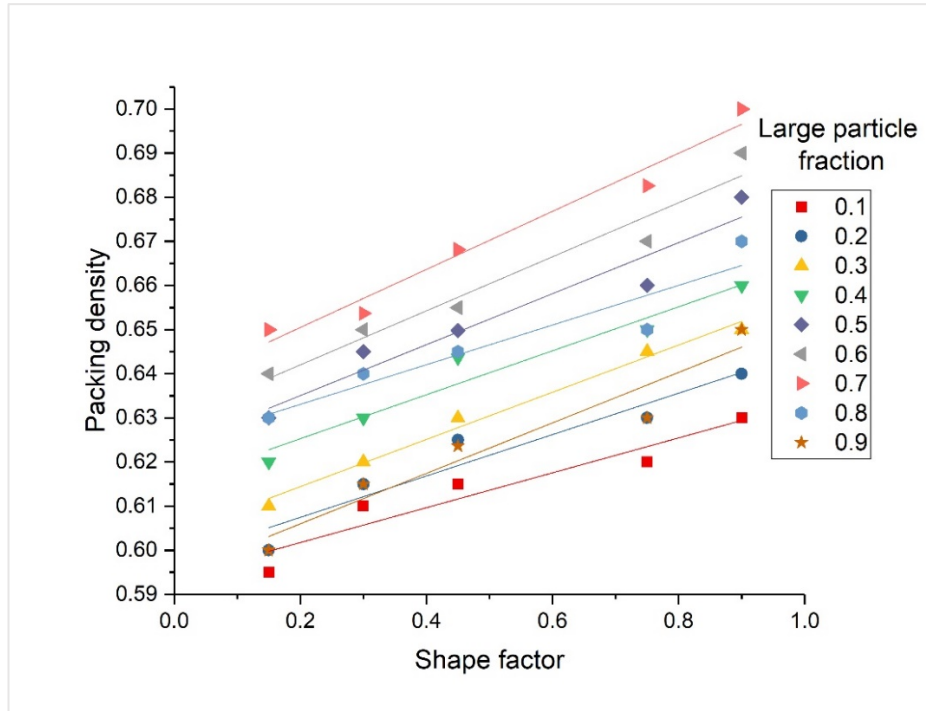


Figure 6.1: Effect of shape on packing density

The relationship found to be linear and the equation takes the shape of,

$$Y = m\sigma + c \quad \dots\dots\dots \text{Equation 6.1}$$

Where  $m$  and  $c$  are functions of large particle volume fraction ( $F$ ) and  $\sigma$  is the shape factor. The variation of  $m$  and  $c$  with respect to large particle fraction was considered. Table 6.1 shows the variation of  $m$  and  $c$  for large particle fraction. Figure 6.2 and Figure 6.3 show the variations graphically.

Table 6.1: Variation of  $m$  and  $c$  value with large particle fraction

Large particle fraction	$m$	$c$
0.1	0.0395	0.5938
0.2	0.0469	0.5981
0.3	0.0535	0.6037
0.4	0.0498	0.6153
0.5	0.0578	0.6235
0.6	0.0612	0.6298
0.7	0.0658	0.6373
0.8	outlier	0.6241
0.9	0.0572	0.5946

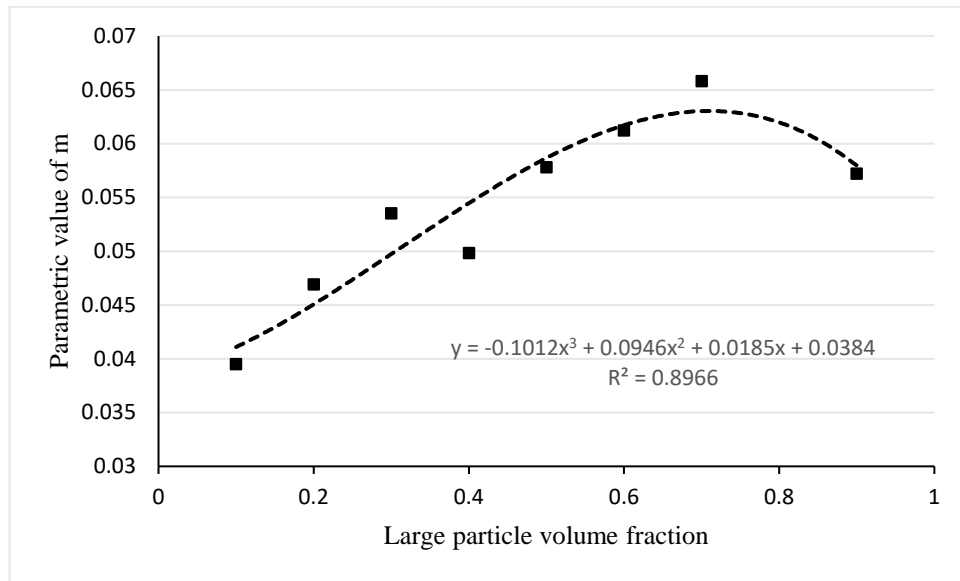


Figure 6.2: Variation of “m” with respect to large particle fraction

Variation of “m” found to be polynomial with 3<sup>rd</sup> order and the Pearson’s R<sup>2</sup> correlation coefficient of 0.8966.

$$m = -0.1012F^3 + 0.0946F^2 + 0.0185F + 0.0384 \dots\dots\dots \text{Equation 6.2}$$

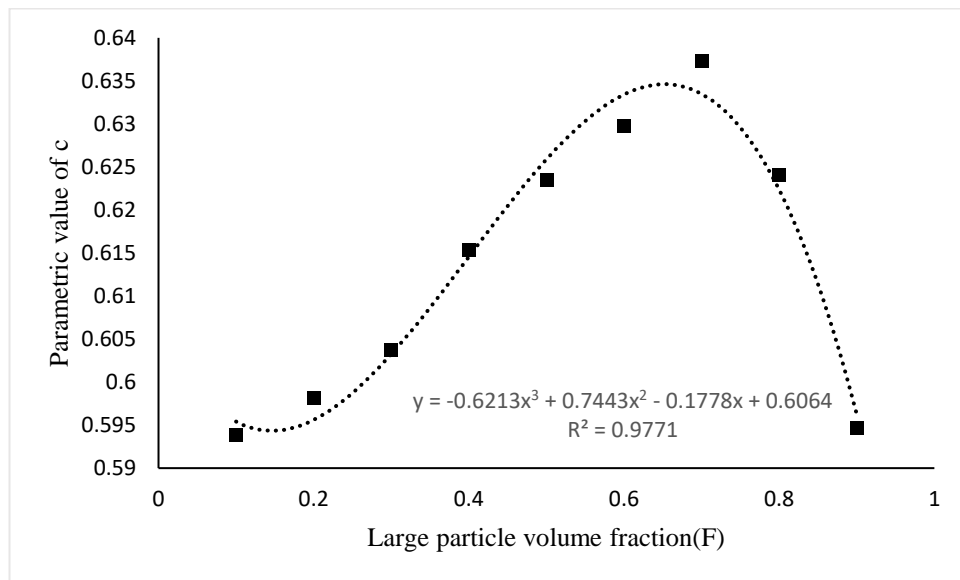


Figure 6.3: Variation of “c” with respect to large particle fraction

Variation of “C” found to be polynomial with 3<sup>rd</sup> order and the Pearson’s R<sup>2</sup> correlation coefficient of 0.977.

$$C = -0.6213 \times F^3 + 0.7443 \times F^2 - 0.1778 \times F + 0.6064 \dots\dots\dots \text{Equation 6.3}$$

Hence, the variation of packing density with respect to both shape factor and large particle fraction can be expressed using Equation 6.4;

$$P.D = (-0.1012F^3 + 0.0946F^2 + 0.0185F + 0.0384)\sigma + -0.6213 \times F^3 + 0.7443 \times F^2 - 0.1778 \times F + 0.6064 \dots\dots\dots \text{Equation 6.4}$$

Where F is the large particle volume fraction and  $\sigma$  is the shape factor.

The model correlation was found to be 0.97 for Pearson’s R<sup>2</sup> and 0.93 for adjusted R<sup>2</sup> as shown in Figure 6.4.

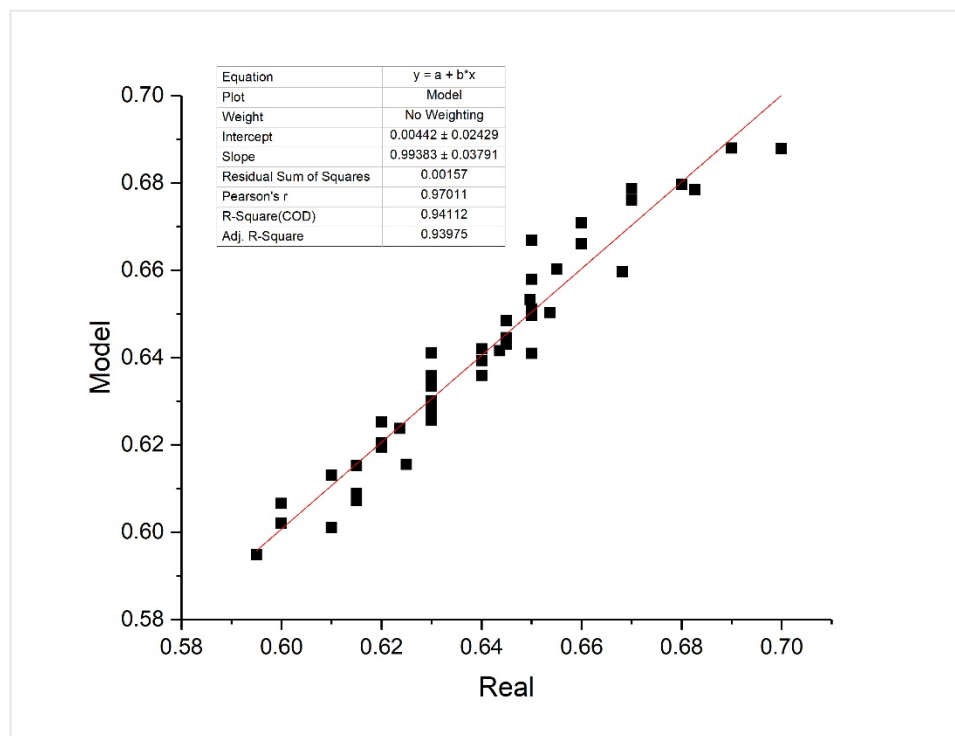


Figure 6.4: Correlation of model and experimental results

#### 6.4 Effect of surface texture on packing density

The effect of surface texture on packing density was studied as explained in section 3.6. Various surface textures were prepared by coating aggregate dust on spherical glass beads. The surface texture was measured using British pendulum test. The variation of packing density with respect to surface texture of the particles are presented in Figure 6.5. As shown in Figure 6.5, when the texture is rough the packing density reduces, and the variation is linear with respect to BPN value of the surface. The resistance of particles to move to more stable location due to the inter particle friction may be the possible reason for the reduction of packing density. Due to this inter particle friction, the particle arrangement becomes more irregular creating more voids in the mixture. Thus, the packing density reduces.

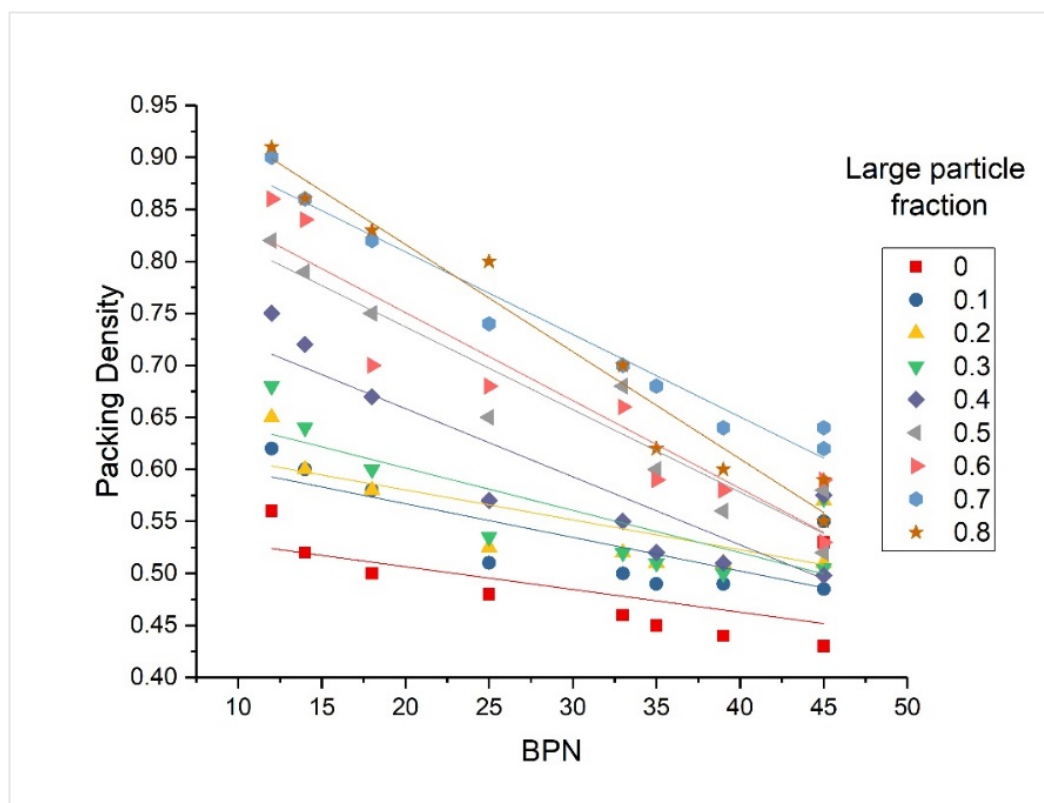


Figure 6.5: Effect of Surface texture on packing density

The equation takes the shape of,

$$Y = mx + c \quad \dots\dots\dots \text{Equation 6.5}$$

Where m and c are functions of large particle volume fraction(F) and x is the surface texture value in BPN.

$$C = 0.5933F + 0.5702 \quad \dots\dots\dots \text{Equation 6.6}$$

$$m = -0.0093F - 0.0032 \quad \dots\dots\dots \text{Equation 6.7}$$

The Pearson’s correlation coefficient for the model is 0.938 with adjusted R<sup>2</sup> value of 0.85 as shown in Figure 6.6.

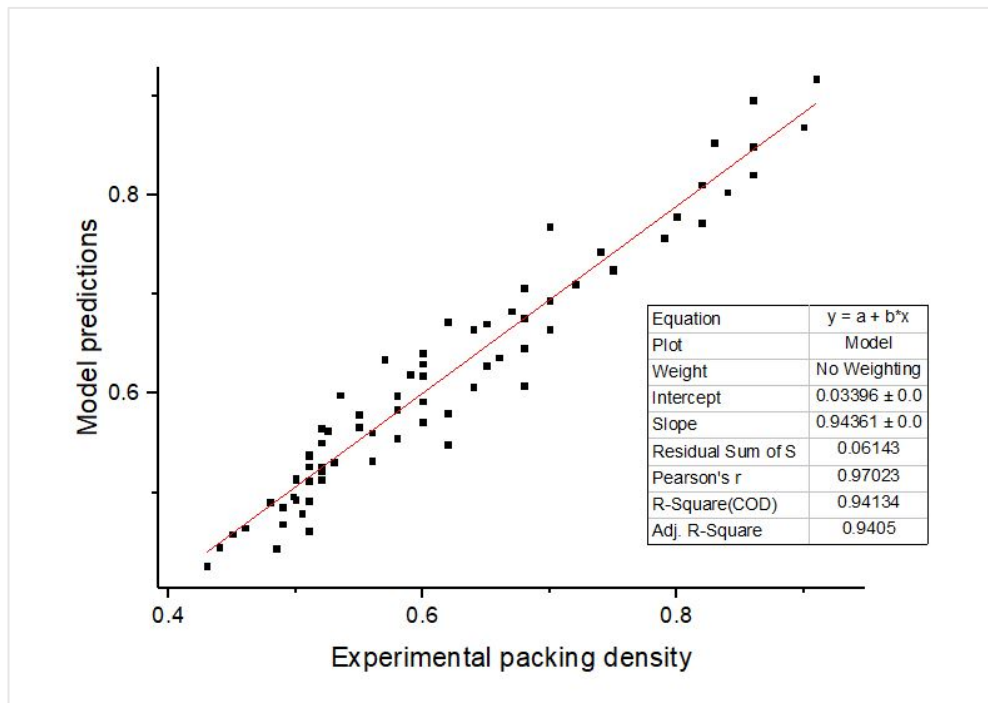


Figure 6.6: Correlation of model and experimental results

### 6.5 Combined effect of vibration, shape and surface texture on packing density

The combined effect of individual factors was studied to develop the model incorporating vibration, shape and surface texture. As explained in Chapter 2, 3-parameter model was selected as the base model for modification. The main reason for selecting this model is the introduction of wedging effect in addition to loosening and packing effects in 3-parameter model. Also, the validity of the packing models was

analyzed in Chapter 4 also confirmed that the 3-parameter model can be used to accurately predict the packing density compared to other theoretical packing models.

### 6.6 Modification of 3-parameter model

The 3-parameter model is modified to incorporate the vibration, surface texture and shape factor by modifying the following equations.

$$a = 1 - (1 - s)^{a_1} - a_2 \times s \times (1 - s)^{a_3} \quad \dots\dots\dots \text{Equation 6.8}$$

$$b = 1 - (1 - s)^{b_1} - b_2 \times s \times (1 - s)^{b_3} \quad \dots\dots\dots \text{Equation 6.9}$$

$$c = c_1 \cdot \tanh(C_2 s) \quad \dots\dots\dots \text{Equation 6.10}$$

The behavior of a, b and c parameters with respect to vibration, shape and surface texture were analyzed to determine the  $a_1, a_2, a_3, b_1, b_2, b_3, c_1$  and  $c_2$  equations.

Table 6.2: Values of sub-parameters

Table 6.2 (a): Values of  $b_2$  and  $b_3$  for different vibration frequencies

Vibration (Rad/s)	50	60	70	80	90	100	110	120	130	140	150
$b_2$	14	15	16	17	18	19	20	19	18	17	16
$b_3$	7	6.5	6	5.5	5	4.5	4	4.5	5	5.5	6

Table 6.2 (b): Values of  $b_1$  for different surface textures

Surface Texture	10	20	30	40	50
$b_1$	5	6	7	8	9

Table 6.2 (c): Values of  $a_3$  for different shape factors

Shape	1	0.8	0.6	0.4	0.2
$a_3$	2.2	3.2	4	4.5	5

The  $a_3$  found to be varying with shape factor linearly as shown in Figure 6.7. The curve fitting equation for  $a_3$  is given by,

$$a_3 = - 3.45 \times \text{Shape factor} + 5.85 \quad \dots\dots\dots \text{Equation 6.11}$$

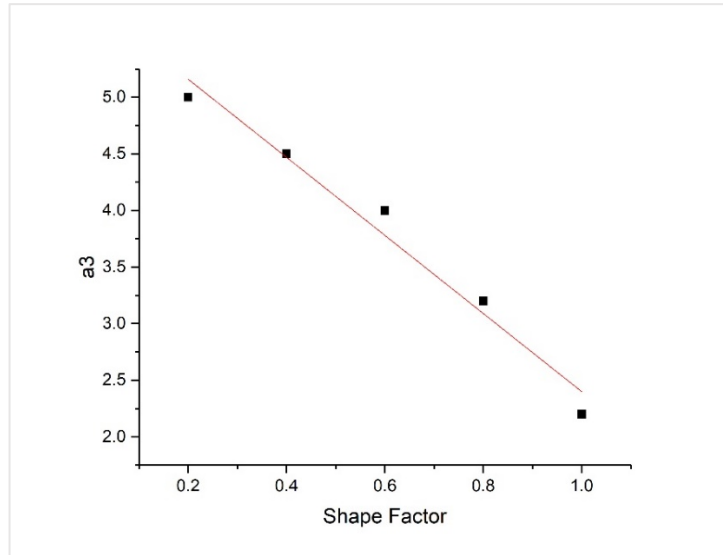


Figure 6.7: Variation of parameter  $a_3$  with respect to Shape factor

Both  $b_2$  and  $b_3$  varies with the vibration frequency and Figure 6.8 shows the variation of  $b_2$  and  $b_3$  with respect to vibration.

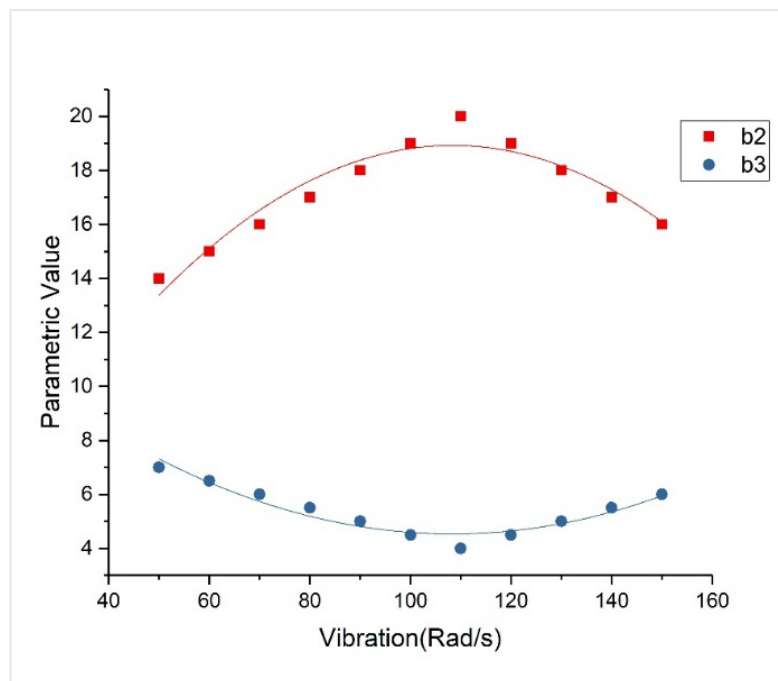


Figure 6.8: Variation of parameter  $b_2$  and  $b_3$  with respect to Shape factor



The variation of  $b_2$  and  $b_3$  are given by,

$$b_2 = -0.0016 \times \text{Vibration}^2 + 0.3536 \times \text{Vibration} - 0.2308 \dots \text{Equation 6.12}$$

$$b_3 = 0.0008 \times \text{Vibration}^2 - 0.1768 \times \text{Vibration} + 14.115 \dots \text{Equation 6.13}$$

And the parameter  $b_1$  found to be varying with the surface texture as shown in Figure 6.9. The variation of  $b_1$  with respect to surface texture is given by,

$$b_1 = 0.1 \times \text{Surface texture} + 4 \dots \text{Equation 6.14}$$

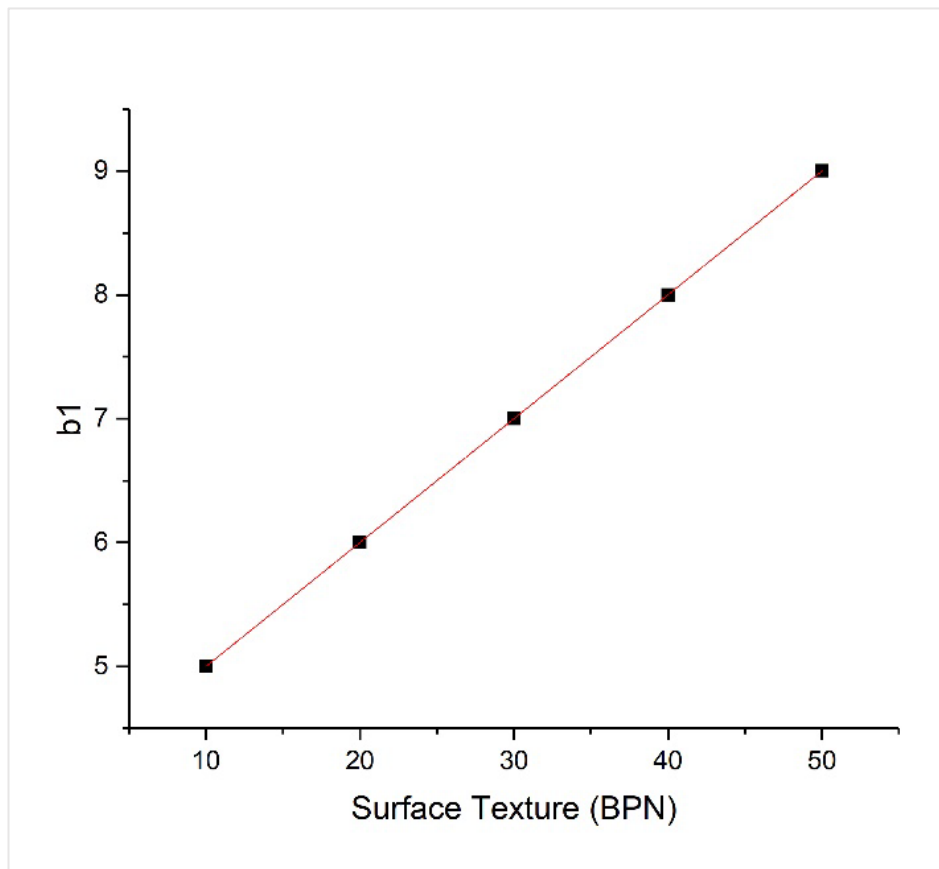


Figure 6.9: The variation of  $b_1$  with respect to surface texture

All the other parameters were found to be constant and the Table 6.3 gives the values of each parameter.

Table 6.3: Values and equations for each sub parameter

Parameter	Value / Equation
$a_1$	1.5
$a_2$	3
$a_3$	$= -3.45 \times \gamma + 5.85$
$b_1$	$= 0.1 \times \beta + 4$
$b_2$	$= -0.0016 \times \omega^2 + 0.3536 \times \omega - 0.2308$
$b_3$	$= 0.0008 \times \omega^2 - 0.1768 \times \omega + 14.115$
$c_1$	0.36
$c_2$	12

- $\gamma$  = Shape factor
- $\beta$  = Surface texture (BPN)
- $\omega$  = Vibration frequency (Rad/s)

Hence, the modified 3-parameter model incorporating vibration, surface texture and shape can be written as,

$$\frac{1}{\phi_i^*} = \left( \frac{r_i}{\phi_i} + \frac{r_j}{\phi_j} \right) - (1 - b)(1 - \phi_j) \frac{r_j}{\phi_j} [1 - c(2.6^{r_j} - 1)] \quad \dots\dots\dots \text{Equation 6.15}$$

$$\frac{1}{\phi_j^*} = \left( \frac{r_i}{\phi_i} + \frac{r_j}{\phi_j} \right) - (1 - a) \frac{r_i}{\phi_i} [1 - c(3.8^{r_i} - 1)] \quad \dots\dots\dots \text{Equation 6.16}$$

$$\phi_{mix} = \min(\phi_i^*, \phi_j^*) \quad \dots\dots\dots \text{Equation 6.17}$$

Where a, b and c are loosening effect, wall effect and wedging effect parameters

$$a = 1 - (1 - s)^{1.5} - 3 \times s \times (1 - s)^W \quad \dots\dots\dots \text{Equation 6.18}$$

$$b = 1 - (1 - s)^X - Y \times s \times (1 - s)^Z \quad \dots\dots\dots \text{Equation 6.19}$$

$$c = 0.36 \cdot \tanh(12 \cdot s) \quad \dots\dots\dots \text{Equation 6.20}$$

Where,

$$W = -3.45 \cdot \gamma + 5.85 \quad \dots\dots\dots \text{Equation 6.21}$$

$$X = 0.1 \times \beta + 4 \quad \dots\dots\dots \text{Equation 6.22}$$

$$Y = -0.0016 \cdot \omega^2 + 0.3536 \cdot \omega - 0.2308 \quad \dots\dots\dots \text{Equation 6.23}$$

$$Z = 0.0008 \times \omega^2 - 0.177 \times \omega + 14.1 \quad \dots\dots\dots \text{Equation 6.24}$$

The 3-parameter model was developed maintaining the W, X, Y and Z factors as constants. However, The variation of W, X, Y and Z parameters were compared with the constant values of 3-parameter model. Figure 6.10 to 6.13 show the variation of W,X,Y and Z respectively.

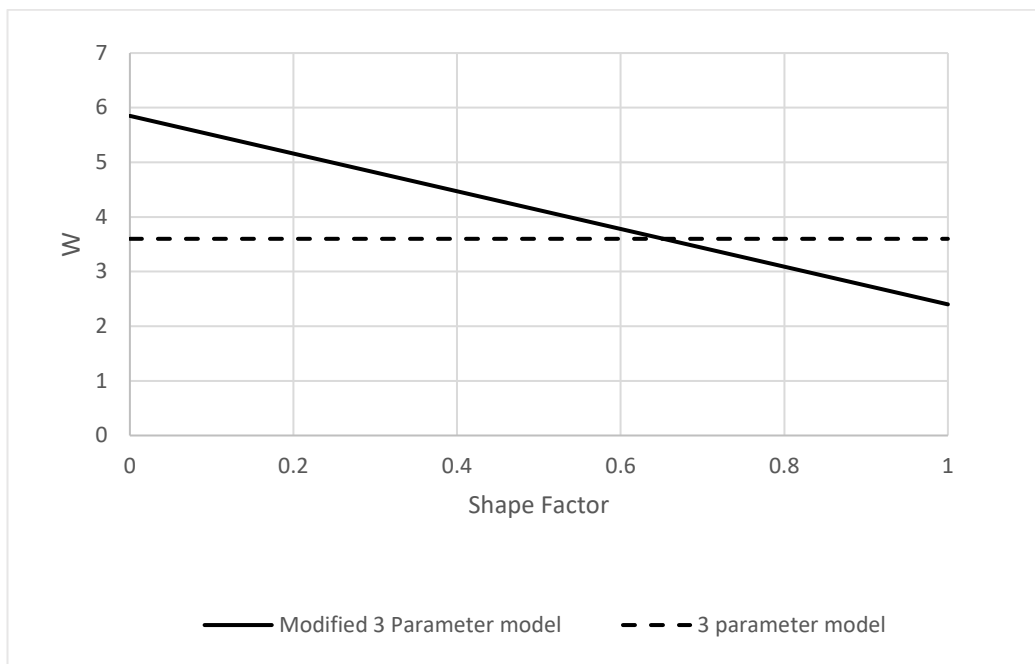


Figure 6.10: Variation of W with shape factor

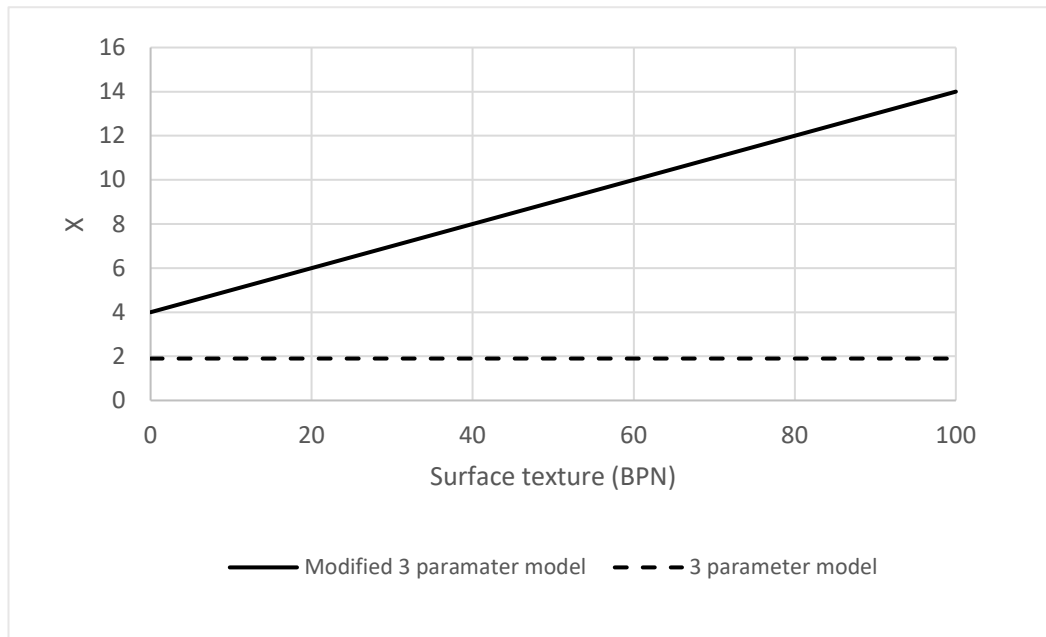


Figure 6.11: Variation of X with surface texture

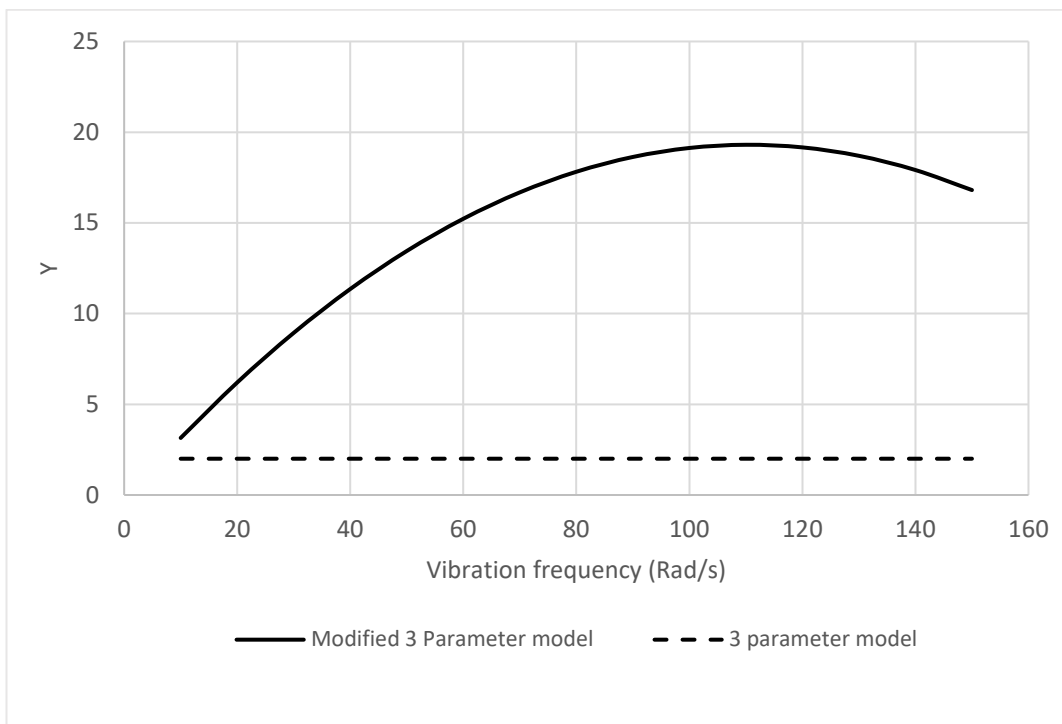


Figure 6.12: Variation of Y with vibration frequency

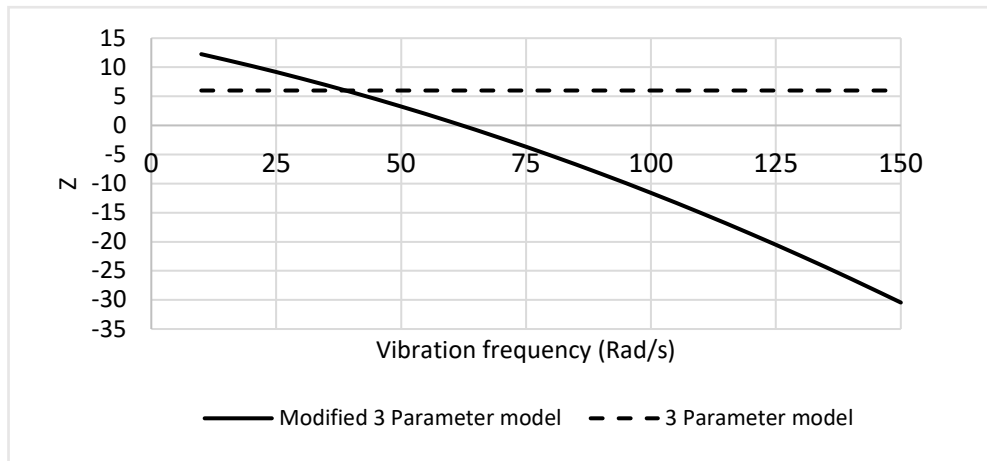


Figure 6.13: Variation of Z with vibration frequency

The final model was validated using more than 300 independent data. The adjusted  $R^2$  value of experimental packing density results and model predictions is 0.95. Figure 6.14 shows the correlation between experimental packing density results and model predictions.

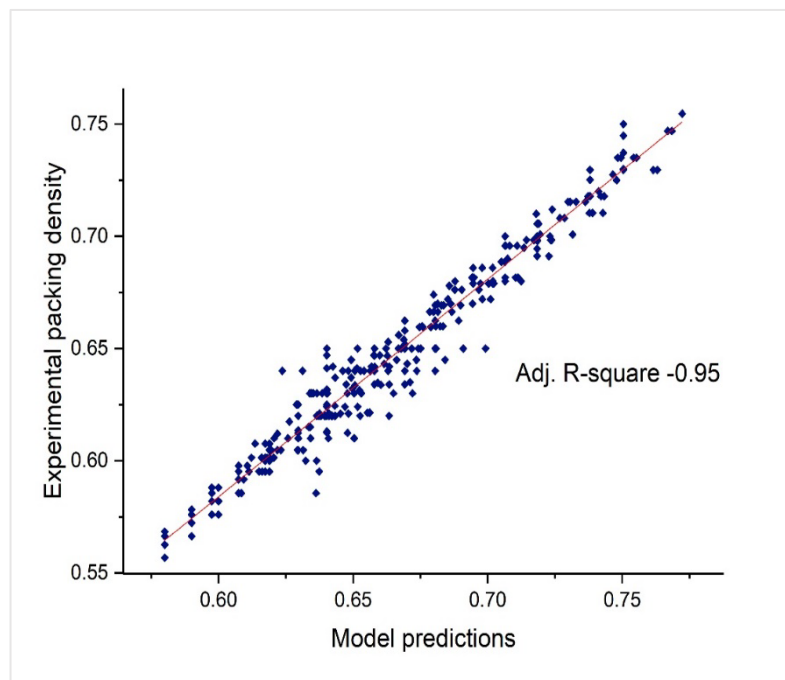


Figure 6.14: The correlation between experimental packing density results and model predictions

The validated model was compared with the results obtained from section 4.5 to verify the accuracy of the developed model. Figure 6.15 shows the comparison of modified 3-parameter model with laboratory packing density values obtained in Chapter 4 for ICBP application. It also presents the improvement of modified 3-parameter model from the basic three parameter model. The model incorporating only vibration in Chapter 5 was also compared and the improvement is presented in Figure 6.15.

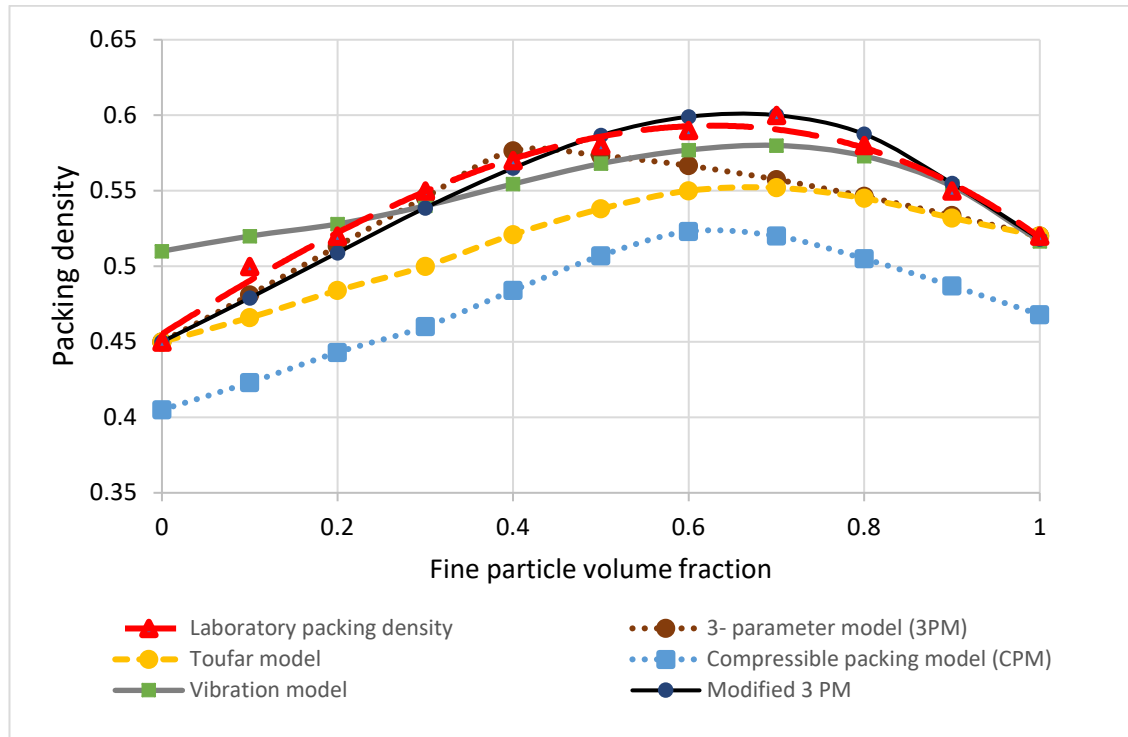


Figure 6.15: Verification of modified 3-parameter model

Table 6.4 presents the percentage error of each model compared with laboratory packing density values at optimum packing state. From the existing models, the compressible packing model yielded the highest error of 15.4% while modified 3-parameter model yielded an error of 7.6%. The model incorporating vibration showed an error of 3.4% which is an improvement from 3-parameter model. The modified 3-parameter model reduced the error from 7.6% to 1.1% making it more accurate than the existing 3-parameter model. Table 6.5 presents the percentage error at each fine particle volume fraction for different models.

Table 6.4: Percentage error of each model at optimum packing

<b>Packing model</b>	<b>Percentage error (%)</b>
Compressible packing model	15.4
Toufar model	8.7
3-parameter model	7.6
Vibration model	3.4
Modified 3-parameter model	1.1

Table 6.5: Percentage error of each model at various fine particle volume fractions

Fine particles volume fraction	Percentage error				
	Compressible packing model	Toufar model	3- parameter model	Vibration model	Modified 3- parameter model
1	11	0	0	1	0
0.9	13	3	3	1	1
0.8	15	6	6	1	1
0.7	15	9	8	3	1
0.6	13	7	4	2	2
0.5	14	8	1	2	1
0.4	18	9	1	3	1
0.3	20	10	1	2	2
0.2	17	7	1	2	2
0.1	18	7	4	4	4
0	11	0	0	12	0

### 6.6.1 Behavior of wall effect

The behavior of wall effect with size ratio for different surface textures and vibration were analyzed from the developed model. Figure 6.16 shows the wall effect variation with respect to size ratio for different surface textures and Figure 6.17 shows the wall

effect variation with respect to size ratio for different vibrations. As described earlier, wall effect parameter is influenced by surface texture and vibration. Hence, the wall effect varies with both surface texture and vibration. As shown in Figure 6.16 the wall effect is high when the surface texture is rough. When the wall surface is rougher, the inter particle friction is high. Thus, the mobility of particles is reduced, and disordered packing may occur. Hence, voids may form near to the wall of larger particles. This phenomenon can be described using Figure 6.16.

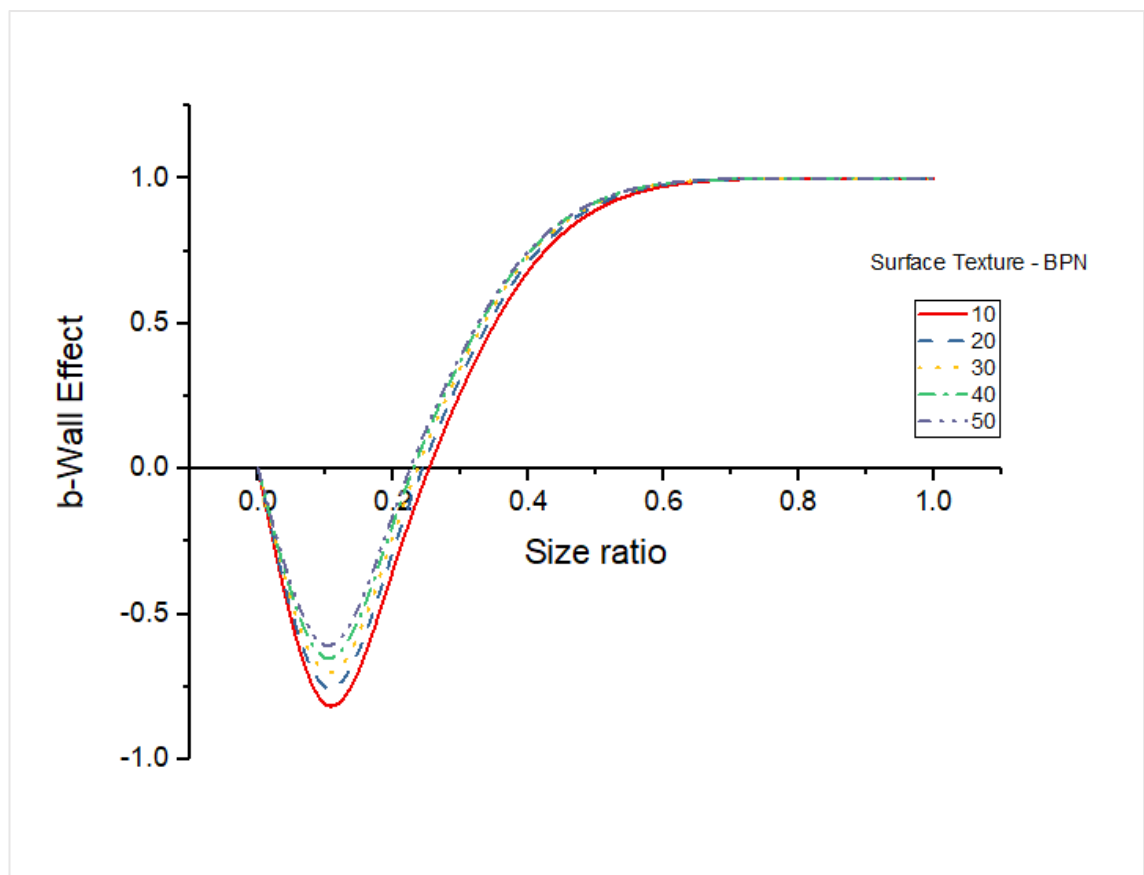


Figure 6.16: The wall effect variation with respect to size ratio for various surface textures

Figure 6.17 shows the variation of wall effect for different size ratios for various vibration frequencies. When the vibration frequency is higher, the wall effect is smaller and vice versa. Higher vibration frequencies allow particles to move freely and occupy stable and comfortable positions in the mixture. This mobility of particles fills up the voids and reduces the voids closer to the wall. However, further increase of vibration



frequencies provide extra energy to already formed packing and disturb the packing structure. Hence, when the vibration frequency is greater than the optimum value, the voids may form around the wall of the larger particles. Therefore, wall effect again increases. This phenomenon can be observed from Figure 6.17.

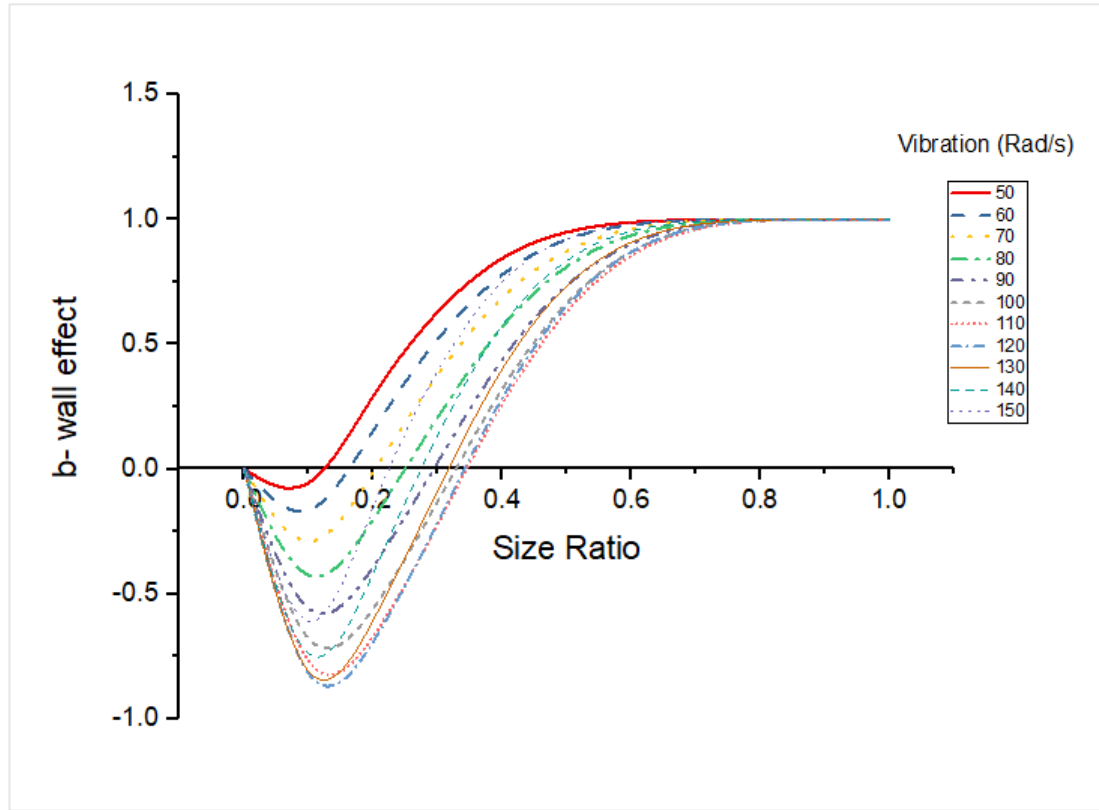


Figure 6.17: The wall effect variation with respect to size ratio for various vibration frequencies

### 6.6.2 Behavior of loosening effect

As shown in Figure 6.18 the loosening effect is higher when the shape factor is closer to 0. Which means irregular shaped particles tend to disturb the packing by loosening effect. Irregular shaped particles may loosen up the already formed packing by intruding into the voids in between larger particles. Figure 6.18 explains the behavior of loosening effect for different shape factors. Similarly, when the size ratio is higher the loosening effect is also higher. When size ratio is higher, the secondary particle is larger than the voids formed by dominant particle. Hence, the secondary particles will loosen the packing structure of dominant larger particles.

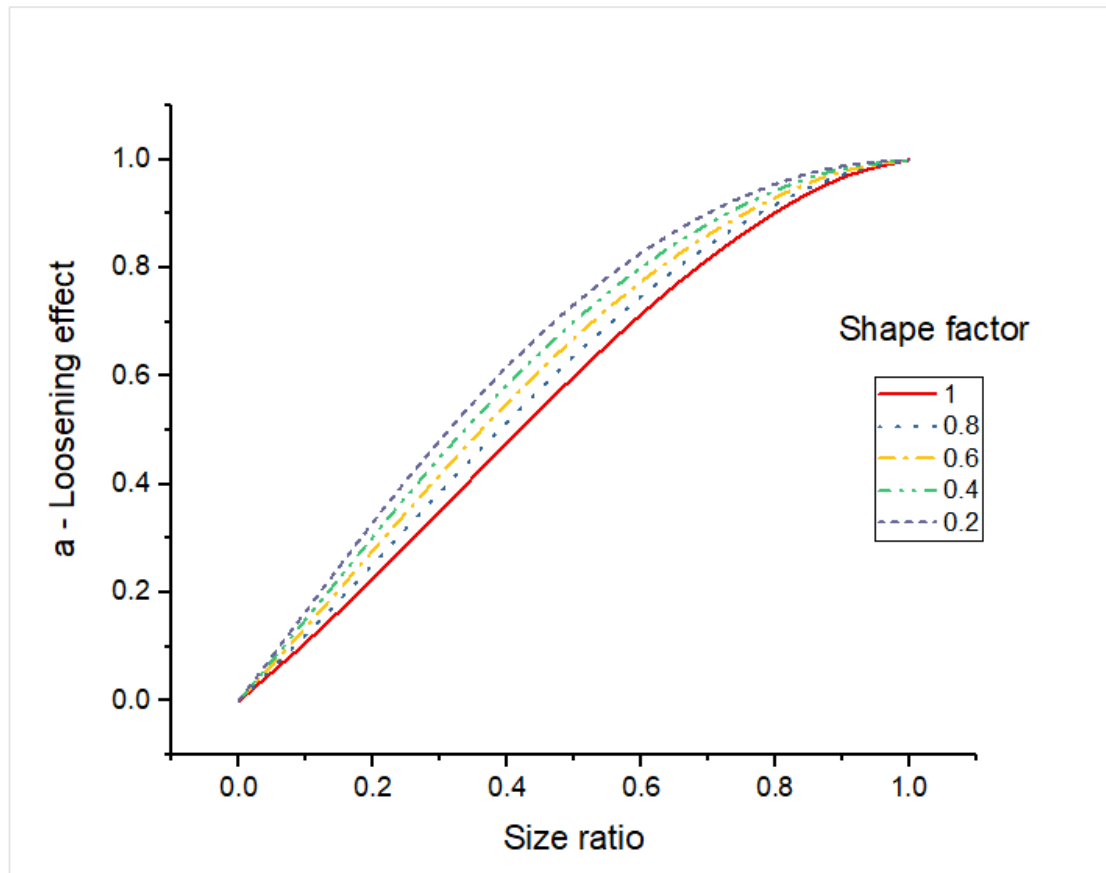


Figure 6.18: The loosening effect variation with respect to size ratio for various shape factors

### 6.6.3 Behavior of wedging effect

The wedging effect found to be not affected by any of the factors (vibration, shape or surface texture). This can be expected since any particle can act as a wedge at any point under any circumstance. The variation of wedging effect with size ratio is shown in Figure 6.19. The value of wedging effect is zero when size ratio is zero and increases rapidly until size ratio is around 0.2. When size ratio is greater than 0.2, the wedging effect does not change much, and the value is around 0.35 throughout. When the size ratio is closer to 0 the smaller particles are very small to act as a wedge and disturb the packing density. Hence, the wedging effect is small. However, when the size ratio is increased the smaller particles disturb the packing hence, the wedging effect increases rapidly. The wedging effect reaches a maximum value and further increase of size ratio does not change the wedging effect. The wedging formed by larger particles are not

stable and larger voids may fill up by particles in the mixture maintaining a constant wedging effect value. This behavior can be observed in Figure 6.19.

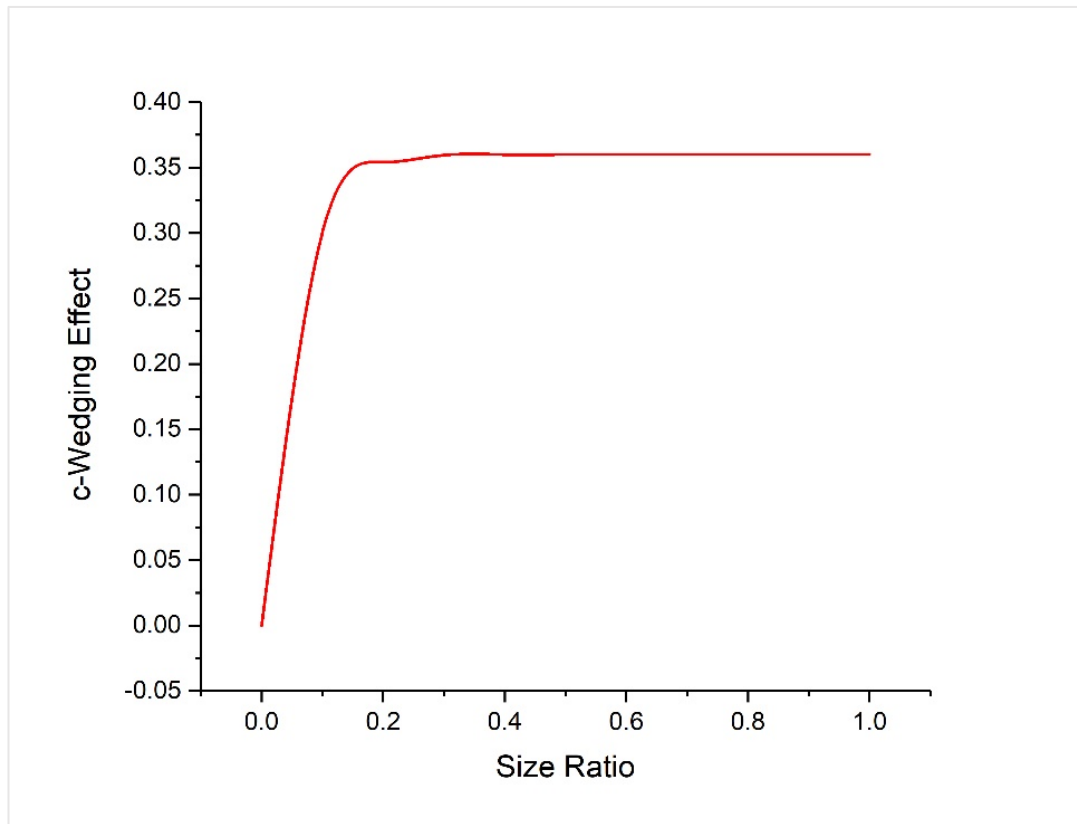


Figure 6.19: The wedging effect variation with respect to size ratio

## CHAPTER 7

### 7 CONCLUSIONS AND RECOMMENDATIONS

#### 7.1 Conclusions

Particle packing density is an important aspect in materials science. Determination of packing density for different mixtures is time consuming and laborious. Hence, use of packing models to predict packing density is in demand. The existing packing models can be effectively used to predict the packing density of a particulate mixture. However, those models do not accurately predict the packing density. These model make various assumptions such as spherical particles, smooth surface texture, random loose packing etc. Realistic conditions are far from the assumptions. Therefore, a packing model based on realistic assumptions is needed to accurately predict the packing density.

The initial research concluded that mixture design based on packing density can be effectively optimize the existing mixtures used for ICBP. The research showed that a mixture subjected to optimum vibration period and compression yields maximum packing density. The maximum packing density can reduce the amount of cement and increase the strength with excessive cement paste.

Following are the major conclusions derived from the study.

1. 3-parameter model can be effectively used to predict the packing density of binary mixtures. However, it can be further developed incorporating particle shape, texture and vibration frequency to accurately determine the packing density.
2. Vibration frequency affects the packing density. There is an optimum vibration frequency that produces maximum packing density. When vibration frequency is increased continuously packing density reaches to a maximum value and then decreases.

3. Particle shape affects the packing density linearly. Higher the shape factor higher the packing density. When particles are more irregular in shape, the packing density reduces due to occurrence of voids in mixtures
4. Particle surface texture affects the packing density linearly. When the surface is smooth, the particles pack easily increasing the packing density of the mixture. When the surface is rough, interparticle friction resist the particle movement. Hence, the packing density of the mixture is low.
5. Modified 3-parameter model can be used to predict the packing density accurately.
6. The wall effect is affected by both surface texture and vibration frequency.
7. The loosening effect is affected only by particle shape.
8. The wedging effect does not affect by vibration, surface texture or particle shape.

## **7.2 Limitations of the model and recommendations**

This study has opened a new door to understand the behavior of complex particulate mixtures and further validation and modification is recommended to develop the model for more complex applications. The developed model can be used to predict the packing density of binary mixtures. The effect of vibration amplitude, specific gravity of particles, effect of container wall on packing density have not been accounted in the model. Further, the model can be used for binary mixtures only. Hence, the study can be extended by evaluating the effect of vibration amplitude, specific gravity of particles, effect of container wall on packing density. It is further recommended to expand the model to incorporate ternary and multi component mixtures.

## REFERENCES

- Abrams, D. A. (1919). *Design of concrete mixtures* (Vol. 1): Structural Materials Research Laboratory, Lewis Institute.
- Ahamed, M. A., & Tighe, S. L. (2011). Asphalt pavements surface texture and skid resistance—exploring the reality. *Canadian Journal of Civil Engineering*, 39(1), 1-9.
- Aim, R. B., & Le Goff, P. (1968). Effet de paroi dans les empilements désordonnés de sphères et application à la porosité de mélanges binaires. *Powder technology*, 1(5), 281-290.
- Alexander, M. G. M. (2005). *Aggregates in concrete* (Vol. 1). Oxon: Taylor and Francis.
- An, X.-z. (2013). Densification of the packing structure under vibrations. *International Journal of Minerals, Metallurgy, and Materials*, 20(5), 499-503.
- An, X., & Chai, H. (2016). Packing densification of binary cylindrical particle mixtures under 3D mechanical vibrations. *Advanced Powder Technology*, 27(6), 2489-2495. doi:<https://doi.org/10.1016/j.appt.2016.09.024>
- An, X., He, S., Feng, H., & Qian, Q. (2015). Packing densification of binary mixtures of spheres and cubes subjected to 3D mechanical vibrations. *Applied Physics A*, 118(1), 151-162.
- An, X., & Li, C. (2013). Experiments on densifying packing of equal spheres by two-dimensional vibration. *Particuology*, 11(6), 689-694. doi:<https://doi.org/10.1016/j.partic.2012.06.019>
- An, X., Li, C., & Qian, Q. (2016). Experimental study on the 3D vibrated packing densification of binary sphere mixtures. *Particuology*, 27, 110-114.
- An, X., Li, C., Yang, R., Zou, R., & Yu, A. (2009). Experimental study of the packing of mono-sized spheres subjected to one-dimensional vibration. *Powder technology*, 196(1), 50-55.
- An, X., Yang, R., Zou, R., & Yu, A. (2008). Effect of vibration condition and inter-particle frictions on the packing of uniform spheres. *Powder technology*, 188(2), 102-109.
- Andreasen, A., & Andersen, J. (1930). About the Relationship between Density and Particle Spacing in Products Made of Loose Particles: Kolloid.
- Andreasen, A. M., & Andersen, J. (1930). Relation between grain size and interstitial space in products of unconsolidated granules. *Kolloid-Zeitschrift*, 50(3), 217-228.
- Arivalagan, S. (2013). Evaluate the properties of concrete using manufactured sand as fine aggregate. *World Journal of Engineering Sciences*, 1(5), 176-187.
- Ayer, J. E., & Soppet, F. E. (1965). Vibratory Compaction: I, Compaction of Spherical Shapes. *Journal of the American Ceramic Society*, 48(4), 180-183. doi:[10.1111/j.1151-2916.1965.tb14708.x](https://doi.org/10.1111/j.1151-2916.1965.tb14708.x)

- Barskale, R. D., & Itani, S. Y. (1989). Influence of aggregate shape on base behavior. *Transportation Research Record*(1227).
- Bikerman, J. (1966). Adhesion of asphalt to stone. *Journal Materials*.
- Blanks, R. F. (1949). *Modern concepts applied to concrete aggregate*. Paper presented at the Proceedings of the American Society of Civil Engineers.
- Bolomey, J. (1935). Granulation et prévision de la résistance probable des bétons. *Travaux*, 19(30), 228-232.
- Brouwers, H. (2006). Particle-size distribution and packing fraction of geometric random packings. *Physical review E*, 74(3), 031309.
- Brouwers, H., & Radix, H. (2005). Self-compacting concrete: theoretical and experimental study. *Cement and concrete research*, 35(11), 2116-2136.
- Chun, Y., Claisse, P., Naik, T. R., & Ganjian, E. (2007). *Sustainable Construction Materials and Technologies: Proceedings of the Conference on Sustainable Construction Materials and Technologies*. Coventry, United Kingdom: CRC Press.
- Cook, M. D., Ley, M. T., & Ghaeezadah, A. (2014). A workability test for slip formed concrete pavements. *Construction and Building Materials*, 68, 376-383.
- Corley-Lay, J. (1998). Friction and surface texture characterization of 14 pavement test sections in Greenville, North Carolina. *Transportation Research Record: Journal of the Transportation Research Board*(1639), 155-161.
- De Larrard, F. (1999). *Concrete mixture proportioning: a scientific approach*: CRC Press.
- De Larrard, F. (2000). Granular Structures and Concrete Formulation. *Études et recherches des laboratoires des ponts et chaussées*.
- De Larrard, F., & Sedran, T. (1994). Optimization of ultra-high-performance concrete by the use of a packing model. *Cement and concrete research*, 24(6), 997-1009.
- De Larrard, F., & Sedran, T. (2002). Mixture-proportioning of high-performance concrete. *Cement and concrete research*, 32(11), 1699-1704.
- Dewar, J. (2002). *Computer modelling of concrete mixtures*: CRC Press.
- Dhir, R., McCarthy, M., & Paine, K. A. (2005). Engineering property and structural design relationships for new and developing concretes. *Materials and structures*, 38(1), 1-9.
- Dinger, D. R., & Funk, J. E. (1993). Particle packing. IV: Computer modelling of particle packing phenomena. *Interceram*, 42(3), 150-152.
- Fate, S. (2014). Concrete with smart material (manufactured crushed sand)—a review. *IOSR Journal of Mechanical and Civil Engineering (IOSR-JMCE)*, 1, 27-29.
- Fennis, S. (2011). Design of ecological concrete by particle packing optimization.
- Fennis, S. A., & Walraven, J. C. (2012). Using particle packing technology for sustainable concrete mixture design. *Heron*, 57 (2012) 2.

- Feret, R. (1892). Sur la compacité des mortiers hydrauliques.
- Fu, G., & Dekelbab, W. (2003). 3-D random packing of polydisperse particles and concrete aggregate grading. *Powder technology*, 133(1-3), 147-155.
- Fuller, W. B. & Thompson, S. E. (1907). The law of proportioning concrete. *Transactions, American Society of Civil Engineers*, 59, 67-143.
- Funk, J., Dinger, D., & Funk Jr, J. (1980). Coal Grinding and Particle Size Distribution Studies for Coal-Water Slurries at High Solids Loading. *Alfred University Research Foundation, Alfred, New York*.
- Funk, J. E., & Dinger, D. R. (1994). *Predictive process control of crowded particulate suspensions: applied to ceramic manufacturing*: Springer Science & Business Media.
- Furnas, C. (1931). Grading aggregates-I.-Mathematical relations for beds of broken solids of maximum density. *Industrial & Engineering Chemistry*, 23(9), 1052-1058.
- Furnas, C. C. (1928). *Flow of gases through beds of broken solids*. Retrieved from
- Garas, V., & Kurtis, K. (2008). Assessment of methods for optimising ternary blended concrete containing metakaolin. *Magazine of Concrete Research*, 60(7), 499-510.
- Geisenhanslüke, C. (2009). *Einfluss der Granulometrie von Feinstoffen auf die Rheologie von Feinstoffleimen*: kassel university press GmbH.
- Glavind, M., Olsen, G. S., & Munch, C. (1993). Packing calculations and concrete mix design. *Nordic Concrete Research*, 13(2).
- Glavind, M., & Pedersen, E. (1999). Packing calculations applied for concrete mix design *Utilizing Ready Mix Concrete and Mortar* (pp. 121-130): Thomas Telford Publishing.
- Goltermann, P., Johansen, V., & Palbol, L. (1997). Packing of aggregates: An alternative tool to determine the optimal aggregate mix. *ACI Materials Journal*, 94(5), 435-443.
- Goodman, S. N. (2009). *Quantification of pavement textural and frictional characteristics using digital image analysis* (Vol. 71).
- Gram, A., & Silfwerbrand, J. (2007). Computer simulation of SCC flow. *Betonwerk und Fertigteil-Technik/Concrete Plant and Precast Technology*, 73(8), 40-48.
- He, D., Ekere, N., & Cai, L. (1999). Computer simulation of random packing of unequal particles. *Physical review E*, 60(6), 7098.
- Hunger, M. (2010). *An integral design concept for ecological self-compacting concrete*: University of Technology.
- Institution, S. L. S. (2011). Specification for Concrete Paving Blocks.
- International, A. (2013). ASTM E303 - 93(2013), Standard Test Method for Measuring Surface Frictional Properties Using the British Pendulum Tester. West Conshohocken.



- IS15658. (2006). *Precast concrete blocks for paving- Specification*. Retrieved from New Delhi:
- Itoh, T., Wanibe, Y., & Sakao, H. (1986). Relation between packing density and particle size distribution in random packing models of powders. *J. Jpn. Inst. Met.*, 50(8), 740-746.
- Ishai , I., (2003). Comparative Economic-Engineering Evaluation of Concrete Block Pavements. *Road Materials and Pavement Design*, 4(3), pp. 251-268.
- Jadhav, P. A., & Kulkarni, D. K. (2013). Effect of replacement of natural sand by manufactured sand on the properties of cement mortar. *International journal of civil and structural Engineering*, 3(3), 621.
- Janoo, V. C. (1998). *Quantification of Shape, Angularity, and Surface Texture of Base Course Materials* (Special Report 98-1). Retrieved from Vermont:
- Johansen, V. (1991). Particle packing and concrete properties. *Materials Science of Concrete II*, 111-147.
- Jones, M., Zheng, L., & Newlands, M. (2002). Comparison of particle packing models for proportioning concrete constituents for minimum voids ratio. *Materials and structures*, 35(5), 301-309.
- Kolonko, M., Raschdorf, S., & Wäsch, D. (2008). A hierarchical approach to estimate the space filling of particle mixtures with broad size distributions. *submitted to Powder Technology*.
- KrishnaRao, S., ChandraSekharRao, T., & Sravana, P. (2013). Effect of manufacture sand on strength characteristics of roller compacted concrete. *International Journal of Engineering Research and Technology*, 2(2), 1-9.
- Kronlöf, A. (1997). Filler effect of inert mineral powder in concrete. *VTT PUBLICATIONS*.
- Krumbein, W. C. (1941). Measurement and geological significance of shape and roundness of sedimentary particles. *Journal of Sedimentary Research*, 11(2).
- Kumar, S., & Santhanam, M. (2003). Particle packing theories and their application in concrete mixture proportioning: A review. *Indian concrete journal*, 77(9), 1324-1331.
- Kwan, A., Chan, K., & Wong, V. (2013). A 3-parameter particle packing model incorporating the wedging effect. *Powder technology*, 237, 172-179.
- Kwan, A., & Fung, W. (2009). Packing density measurement and modelling of fine aggregate and mortar. *Cement and Concrete Composites*, 31(6), 349-357.
- Kwan, A., & Mora, C. (2002). Effects of various, shape parameters on packing of aggregate particles. *Magazine of Concrete Research*.
- Kwan, A. K. H., Chan, K. W., & Wong, V. (2013). A 3-parameter particle packing model incorporating the wedging effect. *Powder technology*, 237(Supplement C), 172-179. doi:<https://doi.org/10.1016/j.powtec.2013.01.043>

- Kwan, A. K. H., Wong, V., & Fung, W. W. S. (2015). A 3-parameter packing density model for angular rock aggregate particles. *Powder technology*, 274(Supplement C), 154-162.
- Lagerblad, B., & Vogt, C. (2004). *Ultrafine particles to save cement and improve concrete properties*: Cement och Betong Institutet.
- Lamond, J. F., & Pielert, J. H. (2006). *Significance of tests and properties of concrete and concrete-making materials* (Vol. 169): ASTM International.
- Ley, T., Cook, D., & Fick, G. (2012). *Concrete pavement mixture design and analysis(MDA): Effect of aggregate systems in concrete properties* Retrieved from Ames:
- Li, C., An, X., Yang, R., Zou, R., & Yu, A. (2011). Experimental study on the packing of uniform spheres under three-dimensional vibration. *Powder technology*, 208(3), 617-622.
- Little, J. B., Priyantha Jayawickrama, Mansour, & Solaimanian, B. H. (2003). *Quantify shape, angularity and surface texture of aggregates using image analysis and study their effect on performance* (FHWA/TX-06/0-1707-4).
- Liu, S., & Ha, Z. (2002). Prediction of random packing limit for multimodal particle mixtures. *Powder technology*, 126(3), 283-296.
- Liu, Y., Fwa, T., & Choo, Y. (2004). Effect of surface macrotexture on skid resistance measurements by the British Pendulum Test. *Journal of Testing and Evaluation*, 32(4), 304-309.
- Mangulkar, M. N., & Jamkar, S. S. (2013). Review of Particle Packing Theories Used For Concrete Mix Proportioning. *International Journal Of Scientific & Engineering Research*, 4, 143-148.
- Mather, B. (1966). Shape, surface texture, and coatings *Significance of Tests and Properties of Concrete and Concrete-Making Materials*: ASTM International.
- McGeary, R. K. (1961). Mechanical Packing of Spherical Particles. *Journal of the American Ceramic Society*, 44(10), 513-522. doi:10.1111/j.1151-2916.1961.tb13716.x
- Mechling, J., Lecomte, A., & Diliberto, C. (2007). The influence of the clinker composition on concrete compressive strength. *Concrete under severe conditions: environment & loading CONSEC*.
- Mikulic, D., Gabrijel, I., & Milovanovic, B. (2008). *Prediction of concrete compressive strength*. Paper presented at the International RILEM Symposium on Concrete Modelling-CONMOD'08.
- Mora, C., & Kwan, A. (2000). Sphericity, shape factor, and convexity measurement of coarse aggregate for concrete using digital image processing. *Cement and concrete research*, 30(3), 351-358.
- Neville, A. M. (1995). *Properties of concrete* (Vol. 4): Longman London.

- Nowak, E., Knight, J., Povinelli, M., Jaeger, H., & Nagel, S. (1997). Reversibility and irreversibility in the packing of vibrated granular material. *Powder technology*, 94(1), 79-83.
- Ozol, M. (1978). —Shape, Surface Texture, Surface Area, and Coatings *Significance of Tests and Properties of Concrete and Concrete-Making Materials*: ASTM International.
- Palm, S., & Wolter, A. (2009). Determining and optimizing the void filling of dry particle systems. *Cem. Int*, 7, 2-8.
- Peronius, N., & Sweeting, T. (1985). On the correlation of minimum porosity with particle size distribution. *Powder technology*, 42(2), 113-121.
- Petersen, I. (1981). Report on packing models. *FL Schmidt & Co.*
- Pettijohn, F. J. (1957). Sedimentary rocks.
- Pirzado, A. A., Dintzer, T., & Janowska, I. (2016). Macronization/densification of graphenes via vibratory compaction. *Powder technology*, 295, 303-306. doi:<https://doi.org/10.1016/j.powtec.2016.03.050>
- Popovics, S. (1998). History of a mathematical model for strength development of Portland cement concrete. *Materials Journal*, 95(5), 593-600.
- Powers, M. C. (1953). A new roundness scale for sedimentary particles. *Journal of Sedimentary Research*, 23(2).
- Powers, T. C. (1969). The properties of fresh concrete.
- Qian, Q., An, X., Wang, Y., Wu, Y., & Wang, L. (2016). Physical study on the vibrated packing densification of mono-sized cylindrical particles. *Particuology*, 29(Supplement C), 120-125. doi:<https://doi.org/10.1016/j.partic.2016.01.009>
- Rao, C., & Tutumluer, E. (2000). Determination of volume of aggregates: New image-analysis approach. *Transportation Research Record: Journal of the Transportation Research Board*(1721), 73-80.
- Rao, V. K., & Krishnamoorthy, S. (1993). Aggregate mixtures for least-void content for use in polymer concrete. *Cement, Concrete and Aggregates*, 15(2), 97-107.
- Reschke, T. (2001). *Der Einfluss der Granulometrie der Feinstoffe auf die Gefügeentwicklung und die Festigkeit von Beton.*
- Richardson, D. (2005). *Aggregate gradation optimization-literature search*. Retrieved from Rolla:
- Roquier, G. (2017). The 4-parameter Compressible Packing Model (CPM) for crushed aggregate particles. *Powder technology*, 320(Supplement C), 133-142. doi:<https://doi.org/10.1016/j.powtec.2017.07.028>
- Roussel, N., Geiker, M. R., Dufour, F., Thrane, L. N., & Szabo, P. (2007). Computational modeling of concrete flow: general overview. *Cement and concrete research*, 37(9), 1298-1307.

- SANS1058. (2012). Standard specification for concrete paving blocks (2.01 ed.): South african bureau of standards.
- Schwanda, F. (1966). Das rechnerische Verfahren zur Bestimmung des Hohlraumes und Zementleimanspruches von Zuschlägen und seine Bedeutung für den Spannbetonbau. *Zement und Beton*, 37(8-17), 13.
- Scott, G., & Kilgour, D. (1969). The density of random close packing of spheres. *Journal of Physics D: Applied Physics*, 2(6), 863.
- Sedran, T., & De Larrard, F. (1999). *Optimization of self-compacting concrete thanks to packing model*. Paper presented at the Proceedings 1st SCC Symp, CBI Sweden, RILEM PRO7.
- Shi, Y., & Zhang, Y. (2006). *Simulation of random packing of spherical particles with different size distributions*. Paper presented at the ASME 2006 international mechanical engineering congress and exposition.
- Sinan Turhan Erdoğan, D. W. F. (2005). *Determination of aggregate shape properties using x-ray tomographic methods and the effect of shape on concrete rheology* (ICAR 106-1). Retrieved from Alexandria:
- Sneed, E. D., & Folk, R. L. (1958). Pebbles in the lower Colorado River, Texas a study in particle morphogenesis. *The Journal of Geology*, 66(2), 114-150.
- Snoeijer, J. H., van Hecke, M., Somfai, E., & van Saarloos, W. (2004). Packing geometry and statistics of force networks in granular media. *Physical review E*, 70(1), 011301.
- Sohn, H. Y., & Moreland, C. (1968). The effect of particle size distribution on packing density. *The Canadian Journal of Chemical Engineering*, 46(3), 162-167.
- Souwerbren, C. (1998). *Betontechnologie: studieboek voor de cursus betontechnoloog van de Betonvereniging: BetonPrisma*.
- Stovall, T., De Larrard, F., & Buil, M. (1986). Linear packing density model of grain mixtures. *Powder technology*, 48(1), 1-12.
- Stroeven, P., & Stroeven, M. (1999). Assessment of packing characteristics by computer simulation. *Cement and concrete research*, 29(8), 1201-1206.
- Talbot, A. N., & Richart, F. E. (1923). *The strength of concrete, its relation to the cement aggregates and water*. Retrieved from
- Taylor, P., Bektas, F., Yurdakul, E., & Ceylan, H. (2012). Optimizing cementious content in concrete mixtures for required performance.
- Terzaghi, K. P., & Peck, P. (1967). RB (1967). *Soil mechanics in engineering practice*.
- Toufar, W., Born, M., & Klose, E. (1976b). Contribution of optimisation of components of different density in polydispersed particles systems. *Freiberger Booklet A*, 558, 29-44.
- Uma, M., & Banu, S. (2015). Strength and durability studies on concrete with flyash and artificial sand. *International Journal of Engineering Research and General Science*, 3(1), 138-146.

- Vesilind, P. A. (1980). The Rosin-Rammler particle size distribution. *Resource Recovery and Conservation*, 5(3), 275-277.
- Vitton, S., Bausano, J. P., Williams, R. C., & Schafer, V. (2008). Fine aggregate angularity from geotechnical perspective. *Road Materials and Pavement Design*, 9(sup1), 243-268.
- Wadell, H. (1932). Volume, shape, and roundness of rock particles. *The Journal of Geology*, 40(5), 443-451.
- Walker Jr, W. J. (2003). Persistence of granular structure during compaction processes. *KONA Powder and Particle Journal*, 21, 133-142.
- Wenzel, R. N. (1949). Surface roughness and contact angle. *The Journal of Physical Chemistry*, 53(9), 1466-1467.
- Westman, A. R., & Hugill, H. (1930). The packing of particles. *Journal of the American Ceramic Society*, 13(10), 767-779.
- Wiącek, J., Parafiniuk, P., & Stasiak, M. (2017). Effect of particle size ratio and contribution of particle size fractions on micromechanics of uniaxially compressed binary sphere mixtures. *Granular Matter*, 19(2), 34.
- Wilson, J., Klotz, L. D., & Nagaraj, C. (1997). Automated measurement of aggregate indices of shape. *Particulate Science and Technology*, 15(1), 13-35.
- Wong, H., & Kwan, A. (2008). Packing density of cementitious materials: measurement and modelling. *Magazine of Concrete Research*.
- Wong, V., & Kwan, A. K. H. (2014). A 3-parameter model for packing density prediction of ternary mixes of spherical particles. *Powder technology*, 268(Supplement C), 357-367. doi:<https://doi.org/10.1016/j.powtec.2014.08.036>
- Wright, P. (1955). A method of measuring the surface texture of aggregate. *Magazine of Concrete Research*, 7(21), 151-160.
- Xie, Z., An, X., Wu, Y., Wang, L., Qian, Q., & Yang, X. (2017). Experimental study on the packing of cubic particles under three-dimensional vibration. *Powder technology*, 317, 13-22. doi:<https://doi.org/10.1016/j.powtec.2017.04.037>
- Yu, A., An, X., Zou, R., Yang, R., & Kendall, K. (2006). Self-assembly of particles for densest packing by mechanical vibration. *Physical review letters*, 97(26), 265501.
- Yu, A., Bridgwater, J., & Burbidge, A. (1997). On the modelling of the packing of fine particles. *Powder technology*, 92(3), 185-194.
- Yu, A., & Standish, N. (1987). Porosity calculations of multi-component mixtures of spherical particles. *Powder technology*, 52(3), 233-241.
- Yu, A., Zou, R., & Standish, N. (1996). Modifying the linear packing model for predicting the porosity of nonspherical particle mixtures. *Industrial & engineering chemistry research*, 35(10), 3730-3741.

- Zeghichi, L., Benghazi, Z., & Baali, L. (2012). Comparative study of self-compacting concrete with manufactured and dune sand. *Journal of Civil Engineering and Architecture*, 6(10), 1429.
- Zheng, J., Carlson, W. B., & Reed, J. S. (1995). The packing density of binary powder mixtures. *Journal of the European Ceramic Society*, 15(5), 479-483.
- Zheng, J., Johnson, P. F., & Reed, J. S. (1990). Improved equation of the continuous particle size distribution for dense packing. *Journal of the American Ceramic Society*, 73(5), 1392-1398.
- Zheng, J., & Stroeven, P. (1999). Computer-simulation of particle section patterns from sieve curves for spherical aggregate *Modern Concrete Materials: Binders, Additions and Admixtures* (pp. 559-566): Thomas Telford Publishing.

## APPENDICES

### Appendix A

#### Packing density results with respect to vibration

Vibration (Rad/s)	Large particle volume fraction	Size ratio				
		1.000	0.8	0.6	0.4	0.2
50	1	0.550	0.600	0.620	0.650	0.650
	0.9	0.560	0.640	0.650	0.660	0.700
	0.8	0.600	0.660	0.680	0.700	0.730
	0.7	0.610	0.680	0.700	0.730	0.760
	0.6	0.615	0.670	0.690	0.718	0.755
	0.5	0.610	0.665	0.680	0.705	0.735
	0.4	0.605	0.657	0.650	0.685	0.720
	0.3	0.602	0.630	0.642	0.677	0.700
	0.2	0.600	0.620	0.630	0.660	0.680
	0.1	0.580	0.610	0.625	0.650	0.660
	0	0.560	0.600	0.620	0.640	0.640
75	1	0.583	0.633	0.653	0.684	0.686
	0.9	0.595	0.676	0.687	0.699	0.742
	0.8	0.636	0.697	0.720	0.742	0.786
	0.7	0.646	0.718	0.740	0.773	0.810
	0.6	0.650	0.707	0.730	0.753	0.807
	0.5	0.644	0.701	0.719	0.742	0.786
	0.4	0.638	0.692	0.688	0.726	0.764
	0.3	0.634	0.665	0.679	0.717	0.744
	0.2	0.633	0.655	0.668	0.701	0.724
	0.1	0.614	0.647	0.665	0.693	0.706
	0	0.596	0.640	0.664	0.687	0.691
100	1	0.594	0.641	0.660	0.670	0.693
	0.9	0.606	0.685	0.696	0.708	0.752
	0.8	0.646	0.707	0.729	0.752	0.796
	0.7	0.656	0.727	0.750	0.784	0.825
	0.6	0.659	0.716	0.739	0.763	0.818

	0.5	0.653	0.710	0.728	0.752	0.796
	0.4	0.646	0.701	0.697	0.735	0.775
	0.3	0.643	0.673	0.689	0.727	0.754
	0.2	0.642	0.665	0.678	0.712	0.736
	0.1	0.625	0.658	0.677	0.706	0.721
	0	0.610	0.655	0.680	0.690	0.710
125	1.0	0.582	0.626	0.642	0.670	0.670
	0.9	0.592	0.669	0.677	0.687	0.729
	0.8	0.631	0.690	0.709	0.730	0.773
	0.7	0.640	0.709	0.729	0.761	0.800
	0.6	0.643	0.697	0.718	0.740	0.793
	0.5	0.636	0.691	0.707	0.729	0.772
	0.4	0.630	0.682	0.676	0.713	0.751
	0.3	0.628	0.656	0.669	0.706	0.732
	0.2	0.628	0.649	0.661	0.693	0.716
	0.1	0.613	0.645	0.662	0.690	0.704
150	0.0	0.600	0.644	0.669	0.693	0.697
	1.0	0.548	0.587	0.598	0.622	0.618
	0.9	0.554	0.626	0.630	0.635	0.673
	0.8	0.591	0.644	0.660	0.676	0.715
	0.7	0.597	0.662	0.678	0.706	0.740
	0.6	0.600	0.650	0.667	0.685	0.733
	0.5	0.594	0.644	0.656	0.674	0.712
	0.4	0.589	0.637	0.627	0.659	0.693
	0.3	0.588	0.612	0.621	0.654	0.676
	0.2	0.591	0.608	0.615	0.644	0.663
	0.1	0.578	0.606	0.620	0.645	0.654
	0.0	0.568	0.609	0.630	0.651	0.652



### Vibration model correlation analysis

Large particle volume fraction	Size ratio	Vibration Frequency (Rad/s)	Experimental Results	Model predictions
0.9	0.6	65	0.4	0.379
0.8	0.6	65	0.4	0.435
0.7	0.6	65	0.42	0.428
0.6	0.6	65	0.425	0.443
0.5	0.6	65	0.43	0.400
0.4	0.6	65	0.43	0.433
0.3	0.6	65	0.43	0.420
0.2	0.6	65	0.435	0.433
0.1	0.6	65	0.45	0.468
0.9	0.5	65	0.46	0.477
0.8	0.5	65	0.47	0.452
0.7	0.5	65	0.475	0.471
0.6	0.5	65	0.475	0.482
0.5	0.5	65	0.48	0.457
0.4	0.5	65	0.48	0.462
0.3	0.5	65	0.48	0.487
0.2	0.5	65	0.48	0.452
0.1	0.5	65	0.48	0.480
0.9	0.3	65	0.49	0.489
0.8	0.3	65	0.49	0.491
0.7	0.3	65	0.49	0.472
0.6	0.3	65	0.495	0.496
0.5	0.3	65	0.5	0.503
0.4	0.3	65	0.5	0.516
0.3	0.3	65	0.5	0.494
0.2	0.3	65	0.5	0.500
0.1	0.3	65	0.5	0.509
0.9	0.25	65	0.51	0.515

0.8	0.25	65	0.52	0.510
0.7	0.25	65	0.52	0.528
0.6	0.25	65	0.52	0.506
0.5	0.25	65	0.525	0.537
0.4	0.25	65	0.53	0.515
0.3	0.25	65	0.53	0.522
0.2	0.25	65	0.53	0.531
0.1	0.25	65	0.53	0.548
0.9	0.15	65	0.54	0.531
0.8	0.15	65	0.54	0.543
0.7	0.15	65	0.54	0.559
0.6	0.15	65	0.545	0.544
0.5	0.15	65	0.545	0.578
0.4	0.15	65	0.546	0.546
0.3	0.15	65	0.55	0.547
0.2	0.15	65	0.55	0.531
0.1	0.15	65	0.55	0.555
0.9	0.6	80	0.55	0.565
0.8	0.6	80	0.56	0.559
0.7	0.6	80	0.56	0.538
0.6	0.6	80	0.56	0.566
0.5	0.6	80	0.564	0.536
0.4	0.6	80	0.57	0.570
0.3	0.6	80	0.57	0.568
0.2	0.6	80	0.58	0.582
0.1	0.6	80	0.58	0.558
0.9	0.5	80	0.586	0.600
0.8	0.5	80	0.586	0.570
0.7	0.5	80	0.59	0.583
0.6	0.5	80	0.59	0.588

0.5	0.5	80	0.593	0.589
0.4	0.5	80	0.594	0.616
0.3	0.5	80	0.598	0.582
0.2	0.5	80	0.598	0.587
0.1	0.5	80	0.6	0.605
0.9	0.3	80	0.62	0.619
0.8	0.3	80	0.625	0.589
0.7	0.3	80	0.63	0.609
0.6	0.3	80	0.64	0.612
0.5	0.3	80	0.65	0.626
0.4	0.3	80	0.604	0.599
0.3	0.3	80	0.605	0.609
0.2	0.3	80	0.61	0.612
0.1	0.3	80	0.65	0.606
0.9	0.25	80	0.6	0.631
0.8	0.25	80	0.59	0.625
0.7	0.25	80	0.68	0.635
0.6	0.25	80	0.67	0.625
0.5	0.25	80	0.654	0.596
0.4	0.25	80	0.6647	0.645
0.3	0.25	80	0.645	0.619
0.2	0.25	80	0.633	0.588
0.1	0.25	80	0.62	0.608
0.9	0.15	80	0.62	0.598
0.8	0.15	80	0.62	0.638
0.7	0.15	80	0.62	0.641
0.6	0.15	80	0.624	0.592
0.5	0.15	80	0.63	0.583
0.4	0.15	80	0.625	0.647
0.3	0.15	80	0.63	0.622

0.2	0.15	80	0.615	0.657
0.1	0.15	80	0.621	0.651
0.9	0.6	110	0.68	0.627
0.8	0.6	110	0.67	0.633
0.7	0.6	110	0.659	0.634
0.6	0.6	110	0.68	0.658
0.5	0.6	110	0.678	0.648
0.4	0.6	110	0.64	0.655
0.3	0.6	110	0.71	0.669
0.2	0.6	110	0.645	0.666
0.1	0.6	110	0.62	0.649
0.9	0.5	110	0.68	0.630
0.8	0.5	110	0.68	0.635
0.7	0.5	110	0.7	0.676
0.6	0.5	110	0.657	0.646
0.5	0.5	110	0.658	0.636
0.4	0.5	110	0.66	0.667
0.3	0.5	110	0.66	0.664
0.2	0.5	110	0.669	0.665
0.1	0.5	110	0.67	0.655
0.9	0.3	110	0.67	0.652
0.8	0.3	110	0.67	0.669
0.7	0.3	110	0.67	0.693
0.6	0.3	110	0.678	0.693
0.5	0.3	110	0.68	0.658
0.4	0.3	110	0.68	0.684
0.3	0.3	110	0.68	0.711
0.2	0.3	110	0.681	0.672
0.1	0.3	110	0.684	0.662
0.9	0.25	110	0.69	0.662

0.8	0.25	110	0.69	0.693
0.7	0.25	110	0.69	0.724
0.6	0.25	110	0.693	0.719
0.5	0.25	110	0.7	0.682
0.4	0.25	110	0.7	0.711
0.3	0.25	110	0.71	0.684
0.2	0.25	110	0.71	0.674
0.1	0.25	110	0.71	0.700
0.9	0.15	110	0.712	0.684
0.8	0.15	110	0.715	0.726
0.7	0.15	110	0.715	0.700
0.6	0.15	110	0.72	0.701
0.5	0.15	110	0.72	0.716
0.4	0.15	110	0.72	0.689
0.3	0.15	110	0.72	0.685
0.2	0.15	110	0.72	0.692
0.1	0.15	110	0.72	0.683
0.9	0.6	150	0.72	0.738
0.8	0.6	150	0.72	0.757
0.7	0.6	150	0.724	0.683
0.6	0.6	150	0.725	0.689
0.5	0.6	150	0.725	0.731
0.4	0.6	150	0.725	0.757
0.3	0.6	150	0.727	0.718
0.2	0.6	150	0.729	0.719
0.1	0.6	150	0.73	0.693
0.9	0.5	150	0.73	0.712
0.8	0.5	150	0.73	0.749
0.7	0.5	150	0.73	0.711
0.6	0.5	150	0.735	0.693

0.5	0.5	150	0.74	0.706
0.4	0.5	150	0.74	0.749
0.3	0.5	150	0.745	0.721
0.2	0.5	150	0.748	0.734
0.1	0.5	150	0.75	0.743
0.9	0.3	150	0.755	0.750
0.8	0.3	150	0.755	0.769
0.7	0.3	150	0.756	0.742
0.6	0.3	150	0.757	0.763
0.5	0.3	150	0.76	0.744
0.4	0.3	150	0.76	0.734
0.3	0.3	150	0.76	0.734
0.2	0.3	150	0.76	0.763
0.1	0.3	150	0.76	0.782
0.9	0.25	150	0.76	0.779
0.8	0.25	150	0.7623	0.783
0.7	0.25	150	0.765	0.745
0.6	0.25	150	0.768	0.799
0.5	0.25	150	0.77	0.742
0.4	0.25	150	0.77	0.749
0.3	0.25	150	0.77	0.779
0.2	0.25	150	0.77	0.763
0.1	0.25	150	0.77	0.813
0.9	0.15	150	0.78	0.767
0.8	0.15	150	0.78	0.792
0.7	0.15	150	0.789	0.769
0.6	0.15	150	0.8	0.768
0.5	0.15	150	0.8	0.798
0.4	0.15	150	0.805	0.798
0.3	0.15	150	0.81	0.799

0.2	0.15	150	0.82	0.812
-----	------	-----	------	-------

**Design chart tables (Vibration analysis)**

Large particle volume fraction	Vibration frequency (50 Rad/s)				
	0.1	0.3	0.5	0.7	0.9
0.9	0.715	0.658	0.593	0.521	0.441
0.8	0.760	0.703	0.639	0.567	0.488
0.7	0.773	0.717	0.653	0.584	0.507
0.6	0.759	0.704	0.643	0.576	0.503
0.5	0.724	0.671	0.613	0.550	0.481
0.4	0.673	0.623	0.569	0.510	0.447
0.3	0.614	0.566	0.516	0.462	0.404
0.2	0.550	0.506	0.460	0.411	0.360
0.1	0.488	0.447	0.406	0.363	0.318

Large particle volume fraction	Vibration frequency (75 Rad/s)				
	0.1	0.3	0.5	0.7	0.9
0.9	0.759	0.698	0.631	0.557	0.477
0.8	0.808	0.747	0.679	0.605	0.525
0.7	0.822	0.761	0.695	0.623	0.544
0.6	0.807	0.749	0.685	0.615	0.539
0.5	0.771	0.715	0.654	0.587	0.516
0.4	0.720	0.666	0.608	0.547	0.481
0.3	0.659	0.608	0.555	0.498	0.438
0.2	0.596	0.548	0.499	0.447	0.394
0.1	0.536	0.492	0.447	0.401	0.354

Large particle volume fraction	Vibration frequency (100 Rad/s)				
	0.1	0.3	0.5	0.7	0.9
0.9	0.769	0.707	0.640	0.566	0.487
0.8	0.819	0.757	0.689	0.615	0.535
0.7	0.834	0.772	0.705	0.632	0.554
0.6	0.819	0.759	0.694	0.624	0.548
0.5	0.782	0.725	0.663	0.596	0.525
0.4	0.730	0.676	0.617	0.555	0.489
0.3	0.670	0.618	0.564	0.507	0.447
0.2	0.608	0.560	0.509	0.457	0.403
0.1	0.552	0.506	0.460	0.413	0.365

Large particle volume fraction	Vibration frequency (125 Rad/s)				
	0.1	0.3	0.5	0.7	0.9
0.9	0.745	0.685	0.620	0.549	0.472
0.8	0.795	0.734	0.668	0.596	0.519
0.7	0.809	0.749	0.684	0.613	0.536
0.6	0.794	0.736	0.672	0.604	0.531
0.5	0.757	0.701	0.641	0.576	0.507
0.4	0.706	0.653	0.596	0.536	0.472
0.3	0.647	0.597	0.544	0.488	0.430
0.2	0.587	0.540	0.491	0.441	0.388
0.1	0.534	0.489	0.444	0.399	0.352

Large particle volume fraction	Vibration frequency (150 Rad/s)				
	0.1	0.3	0.5	0.7	0.9
0.9	0.687	0.631	0.570	0.504	0.431
0.8	0.734	0.678	0.616	0.549	0.476
0.7	0.747	0.691	0.630	0.564	0.492



0.6	0.732	0.678	0.619	0.555	0.486
0.5	0.696	0.644	0.588	0.527	0.463
0.4	0.646	0.597	0.544	0.488	0.428
0.3	0.589	0.543	0.494	0.443	0.389
0.2	0.532	0.489	0.444	0.397	0.349
0.1	0.483	0.442	0.400	0.358	0.315

## Appendix B

### Packing density results with respect to particle shape

Shape factor	Large particle volume fraction								
	0.1	0.2	0.3	0.4	0.5	0.6	0.7	0.8	0.9
0.9	0.63	0.64	0.65	0.66	0.68	0.69	0.7	0.67	0.65
0.75	0.62	0.63	0.645	0.65	0.66	0.67	0.6826	0.65	0.63
0.45	0.615	0.625	0.63	0.643	0.649	0.655	0.668	0.645	0.623
0.3	0.61	0.615	0.62	0.63	0.645	0.65	0.65366	0.64	0.615
0.15	0.595	0.6	0.61	0.62	0.63	0.64	0.65	0.63	0.6

### Shape factor model correlation analysis

Shape Factor	Large particle volume fraction	Experimental packing density	Model predictions
0.9	0.1	0.630	0.626
	0.2	0.640	0.636
	0.3	0.650	0.650
	0.4	0.660	0.666
	0.5	0.680	0.680
	0.6	0.690	0.688
	0.7	0.700	0.688
	0.8	0.670	0.676
	0.9	0.650	0.650
0.75	0.1	0.620	0.619
	0.2	0.630	0.629

	0.3	0.645	0.643
	0.4	0.650	0.658
	0.5	0.660	0.671
	0.6	0.670	0.679
	0.7	0.683	0.678
	0.8	0.650	0.667
	0.9	0.630	0.641
0.45	0.1	0.615	0.607
	0.2	0.625	0.616
	0.3	0.630	0.628
	0.4	0.644	0.642
	0.5	0.650	0.653
	0.6	0.655	0.660
	0.7	0.668	0.660
	0.8	0.645	0.649
	0.9	0.624	0.624
0.3	0.1	0.610	0.601
	0.2	0.615	0.609
	0.3	0.620	0.621
	0.4	0.630	0.633
	0.5	0.645	0.645
	0.6	0.650	0.651
	0.7	0.654	0.650
	0.8	0.640	0.639
	0.9	0.615	0.615
0.15	0.1	0.595	0.595
	0.2	0.600	0.602
	0.3	0.610	0.613
	0.4	0.620	0.625
	0.5	0.630	0.636

	0.6	0.640	0.642
	0.7	0.650	0.641
	0.8	0.630	0.630
	0.9	0.600	0.601

## Appendix C

### Packing density results with respect to Surface texture (BPN)

BPN	Large particle volume fraction in a mixture								
	0	0.1	0.2	0.3	0.4	0.5	0.6	0.7	0.8
12	0.56	0.62	0.65	0.68	0.75	0.82	0.86	0.9	0.91
25	0.48	0.51	0.525	0.535	0.57	0.65	0.68	0.74	0.8
45	0.43	0.485	0.51	0.505	0.498	0.52	0.53	0.62	0.55
14	0.52	0.6	0.6	0.64	0.72	0.79	0.84	0.86	0.86
18	0.5	0.58	0.58	0.6	0.67	0.75	0.7	0.82	0.83
33	0.46	0.5	0.52	0.52	0.55	0.68	0.66	0.7	0.7
35	0.45	0.49	0.51	0.51	0.52	0.6	0.59	0.68	0.62
39	0.44	0.49	0.51	0.5	0.51	0.56	0.58	0.64	0.6
45	0.53	0.55	0.57	0.572	0.575	0.58	0.59	0.64	0.59

### Surface texture model correlation analysis

Surface Texture (BPN)	Volumetric fraction of large particles	Experimental packing density	Model Predictions
12	0	0.56	0.532
25	0	0.48	0.490
45	0	0.43	0.426
14	0	0.52	0.525
18	0	0.5	0.513
33	0	0.46	0.465
35	0	0.45	0.458
39	0	0.44	0.445
12	0.1	0.62	0.580
25	0.1	0.51	0.526
45	0.1	0.485	0.444
14	0.1	0.6	0.572
18	0.1	0.58	0.555
33	0.1	0.5	0.493
35	0.1	0.49	0.485
39	0.1	0.49	0.468
12	0.2	0.65	0.628
25	0.2	0.525	0.562
45	0.2	0.51	0.461
14	0.2	0.6	0.618
18	0.2	0.58	0.598
33	0.2	0.52	0.522
35	0.2	0.51	0.512
39	0.2	0.51	0.492
12	0.3	0.68	0.676
25	0.3	0.535	0.598
45	0.3	0.505	0.479
14	0.3	0.64	0.664

18	0.3	0.6	0.640
33	0.3	0.52	0.551
35	0.3	0.51	0.539
39	0.3	0.5	0.515
12	0.4	0.75	0.724
25	0.4	0.57	0.635
45	0.4	0.498	0.496
14	0.4	0.72	0.711
18	0.4	0.67	0.683
33	0.4	0.55	0.579
35	0.4	0.52	0.565
39	0.4	0.51	0.538
12	0.5	0.82	0.773
25	0.5	0.65	0.671
45	0.5	0.52	0.514
14	0.5	0.79	0.757
18	0.5	0.75	0.726
33	0.5	0.68	0.608
35	0.5	0.6	0.592
39	0.5	0.56	0.561
12	0.6	0.86	0.821
25	0.6	0.68	0.707
45	0.6	0.53	0.531
14	0.6	0.84	0.803
18	0.6	0.7	0.768
33	0.6	0.66	0.636
35	0.6	0.59	0.619
39	0.6	0.58	0.584
12	0.7	0.9	0.869
25	0.7	0.74	0.743

45	0.7	0.62	0.549
14	0.7	0.86	0.850
18	0.7	0.82	0.811
33	0.7	0.7	0.665
35	0.7	0.68	0.646
39	0.7	0.64	0.607
12	0.8	0.91	0.917
25	0.8	0.8	0.779
45	0.8	0.55	0.566
14	0.8	0.86	0.896
18	0.8	0.83	0.853
33	0.8	0.7	0.694
35	0.8	0.62	0.672
39	0.8	0.6	0.630



## Appendix D

### Modified 3-parameter model correlation analysis

Large particle volume fraction	Vibration	Surface Texture	Shape	Model	Real
1	50	10	1	0.58	0.57
0.9	50	10	1	0.62	0.61
0.8	50	10	1	0.65	0.64
0.7	50	10	1	0.65	0.64
0.6	50	10	1	0.65	0.64
0.5	50	10	1	0.64	0.63
0.4	50	10	1	0.64	0.63
0.3	50	10	1	0.63	0.62
0.2	50	10	1	0.62	0.61
0.1	50	10	1	0.61	0.60
0	50	10	1	0.60	0.59
1	60	10	1	0.58	0.57
0.9	60	10	1	0.62	0.61
0.8	60	10	1	0.66	0.65
0.7	60	10	1	0.67	0.65
0.6	60	10	1	0.66	0.65
0.5	60	10	1	0.66	0.65
0.4	60	10	1	0.65	0.64
0.3	60	10	1	0.64	0.63
0.2	60	10	1	0.63	0.62
0.1	60	10	1	0.61	0.61
0	60	10	1	0.60	0.59
1	70	10	1	0.58	0.57
0.9	70	10	1	0.62	0.61
0.8	70	10	1	0.66	0.65
0.7	70	10	1	0.69	0.67

0.6	70	10	1	0.68	0.67
0.5	70	10	1	0.67	0.66
0.4	70	10	1	0.66	0.65
0.3	70	10	1	0.65	0.64
0.2	70	10	1	0.63	0.63
0.1	70	10	1	0.62	0.61
0	70	10	1	0.60	0.59
1	80	10	1	0.58	0.57
0.9	80	10	1	0.62	0.61
0.8	80	10	1	0.66	0.65
0.7	80	10	1	0.69	0.69
0.6	80	10	1	0.71	0.70
0.5	80	10	1	0.70	0.68
0.4	80	10	1	0.68	0.67
0.3	80	10	1	0.66	0.65
0.2	80	10	1	0.64	0.64
0.1	80	10	1	0.62	0.62
0	80	10	1	0.60	0.59
1	90	10	1	0.59	0.58
0.9	90	10	1	0.63	0.62
0.8	90	10	1	0.67	0.66
0.7	90	10	1	0.71	0.70
0.6	90	10	1	0.74	0.73
0.5	90	10	1	0.73	0.72
0.4	90	10	1	0.71	0.70
0.3	90	10	1	0.69	0.68
0.2	90	10	1	0.66	0.65
0.1	90	10	1	0.64	0.63
0	90	10	1	0.61	0.60
1	100	10	1	0.59	0.58

0.9	100	10	1	0.63	0.62
0.8	100	10	1	0.67	0.66
0.7	100	10	1	0.71	0.70
0.6	100	10	1	0.74	0.73
0.5	100	10	1	0.75	0.74
0.4	100	10	1	0.73	0.72
0.3	100	10	1	0.70	0.69
0.2	100	10	1	0.67	0.66
0.1	100	10	1	0.64	0.63
0	100	10	1	0.61	0.60
1	110	10	1	0.60	0.59
0.9	110	10	1	0.64	0.64
0.8	110	10	1	0.68	0.68
0.7	110	10	1	0.72	0.71
0.6	110	10	1	0.75	0.74
0.5	110	10	1	0.77	0.75
0.4	110	10	1	0.75	0.74
0.3	110	10	1	0.72	0.71
0.2	110	10	1	0.69	0.68
0.1	110	10	1	0.65	0.65
0	110	10	1	0.62	0.61
1	120	10	1	0.60	0.59
0.9	120	10	1	0.64	0.64
0.8	120	10	1	0.68	0.68
0.7	120	10	1	0.72	0.71
0.6	120	10	1	0.75	0.74
0.5	120	10	1	0.77	0.75
0.4	120	10	1	0.75	0.74
0.3	120	10	1	0.72	0.71
0.2	120	10	1	0.69	0.68

0.1	120	10	1	0.65	0.65
0	120	10	1	0.62	0.61
1	130	10	1	0.60	0.59
0.9	130	10	1	0.64	0.64
0.8	130	10	1	0.68	0.68
0.7	130	10	1	0.72	0.71
0.6	130	10	1	0.75	0.74
0.5	130	10	1	0.76	0.74
0.4	130	10	1	0.73	0.72
0.3	130	10	1	0.71	0.70
0.2	130	10	1	0.68	0.67
0.1	130	10	1	0.65	0.64
0	130	10	1	0.62	0.61
1	140	10	1	0.60	0.59
0.9	140	10	1	0.64	0.64
0.8	140	10	1	0.68	0.68
0.7	140	10	1	0.72	0.71
0.6	140	10	1	0.74	0.72
0.5	140	10	1	0.72	0.71
0.4	140	10	1	0.71	0.70
0.3	140	10	1	0.69	0.68
0.2	140	10	1	0.67	0.66
0.1	140	10	1	0.64	0.64
0	140	10	1	0.62	0.61
1	150	10	1	0.60	0.59
0.9	150	10	1	0.64	0.64
0.8	150	10	1	0.68	0.68
0.7	150	10	1	0.70	0.69
0.6	150	10	1	0.70	0.69
0.5	150	10	1	0.69	0.68

0.4	150	10	1	0.68	0.67
0.3	150	10	1	0.67	0.66
0.2	150	10	1	0.65	0.64
0.1	150	10	1	0.64	0.63
0	150	10	1	0.62	0.61

Large particle volume fraction	Vibration	Surface Texture	Shape	Model	Real
1	50	20	1	0.58	0.56
0.9	50	20	1	0.62	0.60
0.8	50	20	1	0.64	0.62
0.7	50	20	1	0.64	0.62
0.6	50	20	1	0.64	0.62
0.5	50	20	1	0.64	0.62
0.4	50	20	1	0.63	0.61
0.3	50	20	1	0.63	0.61
0.2	50	20	1	0.62	0.60
0.1	50	20	1	0.61	0.59
0	50	20	1	0.60	0.58
1	60	20	1	0.58	0.56
0.9	60	20	1	0.62	0.60
0.8	60	20	1	0.66	0.64
0.7	60	20	1	0.66	0.64
0.6	60	20	1	0.66	0.64
0.5	60	20	1	0.65	0.63
0.4	60	20	1	0.64	0.62
0.3	60	20	1	0.63	0.62
0.2	60	20	1	0.62	0.61
0.1	60	20	1	0.61	0.60

0	60	20	1	0.60	0.58
1	70	20	1	0.58	0.56
0.9	70	20	1	0.62	0.60
0.8	70	20	1	0.66	0.64
0.7	70	20	1	0.68	0.66
0.6	70	20	1	0.68	0.66
0.5	70	20	1	0.67	0.65
0.4	70	20	1	0.66	0.64
0.3	70	20	1	0.65	0.63
0.2	70	20	1	0.63	0.61
0.1	70	20	1	0.62	0.60
0	70	20	1	0.60	0.58
1	80	20	1	0.58	0.56
0.9	80	20	1	0.62	0.60
0.8	80	20	1	0.66	0.64
0.7	80	20	1	0.69	0.68
0.6	80	20	1	0.70	0.68
0.5	80	20	1	0.69	0.67
0.4	80	20	1	0.68	0.66
0.3	80	20	1	0.66	0.64
0.2	80	20	1	0.64	0.62
0.1	80	20	1	0.62	0.60
0	80	20	1	0.60	0.58
1	90	20	1	0.59	0.57
0.9	90	20	1	0.63	0.61
0.8	90	20	1	0.67	0.65
0.7	90	20	1	0.71	0.69
0.6	90	20	1	0.74	0.72
0.5	90	20	1	0.72	0.70
0.4	90	20	1	0.71	0.69

0.3	90	20	1	0.68	0.67
0.2	90	20	1	0.66	0.64
0.1	90	20	1	0.64	0.62
0	90	20	1	0.61	0.59
1	100	20	1	0.59	0.57
0.9	100	20	1	0.63	0.61
0.8	100	20	1	0.67	0.65
0.7	100	20	1	0.71	0.69
0.6	100	20	1	0.74	0.72
0.5	100	20	1	0.75	0.73
0.4	100	20	1	0.72	0.70
0.3	100	20	1	0.70	0.68
0.2	100	20	1	0.67	0.65
0.1	100	20	1	0.64	0.62
0	100	20	1	0.61	0.59
1	110	20	1	0.60	0.58
0.9	110	20	1	0.64	0.63
0.8	110	20	1	0.68	0.67
0.7	110	20	1	0.72	0.70
0.6	110	20	1	0.75	0.74
0.5	110	20	1	0.77	0.75
0.4	110	20	1	0.74	0.72
0.3	110	20	1	0.71	0.70
0.2	110	20	1	0.68	0.67
0.1	110	20	1	0.65	0.64
0	110	20	1	0.62	0.60
1	120	20	1	0.60	0.58
0.9	120	20	1	0.64	0.63
0.8	120	20	1	0.68	0.67
0.7	120	20	1	0.72	0.70

0.6	120	20	1	0.75	0.74
0.5	120	20	1	0.77	0.75
0.4	120	20	1	0.74	0.72
0.3	120	20	1	0.71	0.70
0.2	120	20	1	0.68	0.67
0.1	120	20	1	0.65	0.64
0	120	20	1	0.62	0.60
1	130	20	1	0.60	0.58
0.9	130	20	1	0.64	0.63
0.8	130	20	1	0.68	0.67
0.7	130	20	1	0.72	0.70
0.6	130	20	1	0.75	0.74
0.5	130	20	1	0.75	0.73
0.4	130	20	1	0.73	0.71
0.3	130	20	1	0.70	0.68
0.2	130	20	1	0.68	0.66
0.1	130	20	1	0.65	0.63
0	130	20	1	0.62	0.60
1	140	20	1	0.60	0.58
0.9	140	20	1	0.64	0.63
0.8	140	20	1	0.68	0.67
0.7	140	20	1	0.72	0.70
0.6	140	20	1	0.73	0.71
0.5	140	20	1	0.72	0.70
0.4	140	20	1	0.70	0.68
0.3	140	20	1	0.68	0.67
0.2	140	20	1	0.66	0.65
0.1	140	20	1	0.64	0.63
0	140	20	1	0.62	0.60
1	150	20	1	0.60	0.58



0.9	150	20	1	0.64	0.63
0.8	150	20	1	0.68	0.67
0.7	150	20	1	0.69	0.67
0.6	150	20	1	0.69	0.67
0.5	150	20	1	0.68	0.66
0.4	150	20	1	0.67	0.66
0.3	150	20	1	0.66	0.65
0.2	150	20	1	0.65	0.63
0.1	150	20	1	0.64	0.62
0	150	20	1	0.62	0.60

Large particle volume fraction	Vibration	Surface Texture	Shape	Model	Real
1	50	30	1	0.580	0.557
0.9	50	30	1	0.619	0.595
0.8	50	30	1	0.636	0.586
0.7	50	30	1	0.637	0.595
0.6	50	30	1	0.636	0.600
0.5	50	30	1	0.633	0.614
0.4	50	30	1	0.629	0.624
0.3	50	30	1	0.623	0.605
0.2	50	30	1	0.616	0.595
0.1	50	30	1	0.608	0.586
0	50	30	1	0.597	0.576
1	60	30	1	0.580	0.557
0.9	60	30	1	0.619	0.595
0.8	60	30	1	0.652	0.624

0.7	60	30	1	0.653	0.624
0.6	60	30	1	0.651	0.624
0.5	60	30	1	0.646	0.624
0.4	60	30	1	0.640	0.614
0.3	60	30	1	0.631	0.605
0.2	60	30	1	0.622	0.605
0.1	60	30	1	0.611	0.595
0	60	30	1	0.597	0.576
1	70	30	1	0.580	0.557
0.9	70	30	1	0.619	0.595
0.8	70	30	1	0.658	0.634
0.7	70	30	1	0.673	0.643
0.6	70	30	1	0.670	0.643
0.5	70	30	1	0.663	0.643
0.4	70	30	1	0.654	0.634
0.3	70	30	1	0.642	0.624
0.2	70	30	1	0.629	0.605
0.1	70	30	1	0.615	0.595
0	70	30	1	0.597	0.576
1	80	30	1	0.580	0.566
0.9	80	30	1	0.619	0.605
0.8	80	30	1	0.658	0.643
0.7	80	30	1	0.695	0.682
0.6	80	30	1	0.695	0.682
0.5	80	30	1	0.685	0.672
0.4	80	30	1	0.672	0.653
0.3	80	30	1	0.656	0.643
0.2	80	30	1	0.638	0.624
0.1	80	30	1	0.620	0.605
0	80	30	1	0.597	0.586

1	90	30	1	0.590	0.566
0.9	90	30	1	0.630	0.605
0.8	90	30	1	0.669	0.643
0.7	90	30	1	0.707	0.682
0.6	90	30	1	0.732	0.701
0.5	90	30	1	0.719	0.691
0.4	90	30	1	0.701	0.672
0.3	90	30	1	0.681	0.653
0.2	90	30	1	0.658	0.634
0.1	90	30	1	0.634	0.614
0	90	30	1	0.607	0.586
1	100	30	1	0.590	0.576
0.9	100	30	1	0.630	0.624
0.8	100	30	1	0.669	0.662
0.7	100	30	1	0.707	0.691
0.6	100	30	1	0.738	0.730
0.5	100	30	1	0.741	0.720
0.4	100	30	1	0.720	0.701
0.3	100	30	1	0.694	0.682
0.2	100	30	1	0.667	0.653
0.1	100	30	1	0.638	0.624
0	100	30	1	0.607	0.595
1	110	30	1	0.600	0.576
0.9	110	30	1	0.640	0.624
0.8	110	30	1	0.681	0.662
0.7	110	30	1	0.718	0.691
0.6	110	30	1	0.750	0.730
0.5	110	30	1	0.763	0.730
0.4	110	30	1	0.739	0.710
0.3	110	30	1	0.711	0.682

0.2	110	30	1	0.681	0.662
0.1	110	30	1	0.651	0.634
0	110	30	1	0.617	0.595
1	120	30	1	0.600	0.576
0.9	120	30	1	0.640	0.624
0.8	120	30	1	0.681	0.662
0.7	120	30	1	0.718	0.691
0.6	120	30	1	0.750	0.730
0.5	120	30	1	0.762	0.730
0.4	120	30	1	0.738	0.710
0.3	120	30	1	0.710	0.682
0.2	120	30	1	0.681	0.653
0.1	120	30	1	0.650	0.624
0	120	30	1	0.617	0.595
1	130	30	1	0.600	0.576
0.9	130	30	1	0.640	0.624
0.8	130	30	1	0.681	0.662
0.7	130	30	1	0.718	0.691
0.6	130	30	1	0.750	0.730
0.5	130	30	1	0.743	0.710
0.4	130	30	1	0.723	0.691
0.3	130	30	1	0.699	0.672
0.2	130	30	1	0.674	0.653
0.1	130	30	1	0.647	0.624
0	130	30	1	0.617	0.595
1	140	30	1	0.600	0.576
0.9	140	30	1	0.640	0.624
0.8	140	30	1	0.681	0.662
0.7	140	30	1	0.718	0.691
0.6	140	30	1	0.723	0.691

0.5	140	30	1	0.712	0.682
0.4	140	30	1	0.698	0.672
0.3	140	30	1	0.681	0.653
0.2	140	30	1	0.662	0.643
0.1	140	30	1	0.641	0.624
0	140	30	1	0.617	0.595
1	150	30	1	0.600	0.576
0.9	150	30	1	0.640	0.624
0.8	150	30	1	0.681	0.662
0.7	150	30	1	0.689	0.662
0.6	150	30	1	0.686	0.662
0.5	150	30	1	0.680	0.653
0.4	150	30	1	0.671	0.643
0.3	150	30	1	0.660	0.634
0.2	150	30	1	0.648	0.624
0.1	150	30	1	0.634	0.614
0	150	30	1	0.617	0.595

Large particle volume fraction	Vibration	Surface Texture	Shape	3PM	Real
0	50	25	0.3	0.682	0.680
0.1	50	25	0.3	0.687	0.700
0.2	50	25	0.3	0.654	0.630
0.3	50	25	0.3	0.624	0.624
0.4	50	25	0.3	0.606	0.606
0.5	50	25	0.3	0.598	0.598
0.6	50	25	0.3	0.595	0.580
0.7	50	25	0.3	0.594	0.610
0.8	50	25	0.3	0.594	0.595

0.9	50	25	0.3	0.594	0.605
1	50	25	0.3	0.594	0.590
0	60	25	0.3	0.580	0.600
0.1	60	25	0.3	0.612	0.625
0.2	60	25	0.3	0.643	0.655
0.3	60	25	0.3	0.655	0.644
0.4	60	25	0.3	0.653	0.654
0.5	60	25	0.3	0.648	0.650
0.6	60	25	0.3	0.641	0.640
0.7	60	25	0.3	0.633	0.650
0.8	60	25	0.3	0.623	0.600
0.9	60	25	0.3	0.612	0.605
1	60	25	0.3	0.598	0.592
0	70	25	0.3	0.580	0.610
0.1	70	25	0.3	0.612	0.600
0.2	70	25	0.3	0.643	0.650
0.3	70	25	0.3	0.672	0.680
0.4	70	25	0.3	0.672	0.650
0.5	70	25	0.3	0.665	0.650
0.6	70	25	0.3	0.656	0.650
0.7	70	25	0.3	0.644	0.630
0.8	70	25	0.3	0.630	0.630
0.9	70	25	0.3	0.615	0.630
1	70	25	0.3	0.598	0.620
0	80	25	0.3	0.590	0.600
0.1	80	25	0.3	0.623	0.630
0.2	80	25	0.3	0.654	0.660
0.3	80	25	0.3	0.684	0.700
0.4	80	25	0.3	0.706	0.710
0.5	80	25	0.3	0.696	0.685

0.6	80	25	0.3	0.683	0.675
0.7	80	25	0.3	0.667	0.654
0.8	80	25	0.3	0.649	0.656
0.9	80	25	0.3	0.630	0.640
1	80	25	0.3	0.608	0.600
0	90	25	0.3	0.590	0.600
0.1	90	25	0.3	0.623	0.615
0.2	90	25	0.3	0.654	0.655
0.3	90	25	0.3	0.684	0.690
0.4	90	25	0.3	0.709	0.690
0.5	90	25	0.3	0.721	0.730
0.6	90	25	0.3	0.703	0.710
0.7	90	25	0.3	0.682	0.700
0.8	90	25	0.3	0.659	0.660
0.9	90	25	0.3	0.635	0.640
1	90	25	0.3	0.608	0.600
0	100	25	0.3	0.600	0.600
0.1	100	25	0.3	0.633	0.650
0.2	100	25	0.3	0.666	0.670
0.3	100	25	0.3	0.696	0.700
0.4	100	25	0.3	0.721	0.740
0.5	100	25	0.3	0.737	0.740
0.6	100	25	0.3	0.730	0.730
0.7	100	25	0.3	0.705	0.695
0.8	100	25	0.3	0.677	0.680
0.9	100	25	0.3	0.649	0.650
1	100	25	0.3	0.618	0.600
0	110	25	0.3	0.600	0.600
0.1	110	25	0.3	0.633	0.600
0.2	110	25	0.3	0.666	0.625

0.3	110	25	0.3	0.696	0.710
0.4	110	25	0.3	0.721	0.700
0.5	110	25	0.3	0.737	0.740
0.6	110	25	0.3	0.741	0.720
0.7	110	25	0.3	0.713	0.715
0.8	110	25	0.3	0.682	0.650
0.9	110	25	0.3	0.651	0.660
1	110	25	0.3	0.618	0.620
0	120	25	0.3	0.600	0.600
0.1	120	25	0.3	0.633	0.650
0.2	120	25	0.3	0.666	0.680
0.3	120	25	0.3	0.696	0.710
0.4	120	25	0.3	0.721	0.710
0.5	120	25	0.3	0.737	0.750
0.6	120	25	0.3	0.740	0.720
0.7	120	25	0.3	0.712	0.730
0.8	120	25	0.3	0.682	0.700
0.9	120	25	0.3	0.651	0.680
1	120	25	0.3	0.618	0.623
0	130	25	0.3	0.600	0.598
0.1	130	25	0.3	0.633	0.640
0.2	130	25	0.3	0.666	0.678
0.3	130	25	0.3	0.696	0.700
0.4	130	25	0.3	0.721	0.730
0.5	130	25	0.3	0.737	0.710
0.6	130	25	0.3	0.725	0.730
0.7	130	25	0.3	0.701	0.695
0.8	130	25	0.3	0.675	0.680
0.9	130	25	0.3	0.647	0.620
1	130	25	0.3	0.618	0.600



0	140	25	0.3	0.600	0.640
0.1	140	25	0.3	0.633	0.640
0.2	140	25	0.3	0.666	0.640
0.3	140	25	0.3	0.696	0.650
0.4	140	25	0.3	0.721	0.730
0.5	140	25	0.3	0.715	0.710
0.6	140	25	0.3	0.700	0.700
0.7	140	25	0.3	0.682	0.682
0.8	140	25	0.3	0.662	0.630
0.9	140	25	0.3	0.642	0.623
1	140	25	0.3	0.618	0.640
0	150	25	0.3	0.600	0.620
0.1	150	25	0.3	0.633	0.640
0.2	150	25	0.3	0.666	0.670
0.3	150	25	0.3	0.692	0.710
0.4	150	25	0.3	0.688	0.700
0.5	150	25	0.3	0.682	0.720
0.6	150	25	0.3	0.673	0.675
0.7	150	25	0.3	0.662	0.680
0.8	150	25	0.3	0.649	0.660
0.9	150	25	0.3	0.635	0.650
1	150	25	0.3	0.618	0.600

## Appendix E

### Mix design sample calculation

Combined aggregate proportion Quarry Dust: Sand: Coarse Aggregate= 42:28:30

Bulk Density of the proposed aggregate mix =  $2.02 \text{ g/cm}^3$

Total packing density of the mix = 0.8106

Voids content =  $1 - 0.8106 = 0.1894$

Paste content 10% in excess of voids =  $0.1894 + 0.1 * 0.1894$

= 0.20834

Volume of aggregates =  $1 - 0.20834$

=  $0.79166 \text{ cm}^3$

Total solid volume of aggregates =  $0.42/2.323 + 0.28/2.59 + 0.3/2.67$

=  $0.4013 \text{ cm}^3$

Weight of Q.D =  $0.79166/0.4013 \times 0.42 \times 1000$

=  $828.55 \text{ kg/m}^3$

Weight of sand =  $0.79166/0.4013 \times 0.28 \times 1000$

=  $552.36 \text{ kg/m}^3$

Weight of 12mm coarse aggregates =  $0.79166/0.4013 \times 0.3 \times 1000$

=  $591.82 \text{ kg/m}^3$

$$\text{Water Cement ratio} = 0.38$$

$$\text{Total Paste} = \text{Cement} + \text{water} = C/3.15 + 0.38C$$

$$= 0.6974C = 0.20834$$

$$\text{Cement content} = 0.20834 \times 1000 / 0.6974$$

$$= 298.73 \text{ kg/m}^3$$

$$\text{Water Content} = 0.38 \times 298.73 = 113.52 \text{ kg/m}^3$$